

Imperial College of Science, Technology and Medicine  
Department of Physics

# Magnetic Monopole Creation

Oliver Gould

Submitted in part fulfilment of the requirements for the degree of  
Doctor of Philosophy in Physics of Imperial College London and  
the Diploma of Imperial College, September 2017



## Declaration of Authorship

Unless otherwise referenced, the work presented in this thesis is my own, carried out under the supervision of Arttu Rajantie. Chapters 3, 4 and 5 are based on the following research papers:

- Oliver Gould and Arttu Rajantie, “Thermal Schwinger pair production at arbitrary coupling,” *Phys. Rev.* **D96** (2017) 076002, arXiv:1704.04801 [hep-th].
- Oliver Gould and Arttu Rajantie, “Magnetic monopole mass bounds from heavy ion collisions and neutron stars,” *Phys. Rev. Lett.* **119** (2017) 241601, arXiv:1705.07052 [hep-ph].
- Oliver Gould and Arttu Rajantie, “Worldline sphaleron for Schwinger pair production,” forthcoming.

The copyright of this thesis rests with the author and is made available under a Creative Commons Attribution Non-Commercial No Derivatives licence. Researchers are free to copy, distribute or transmit the thesis on the condition that they attribute it, that they do not use it for commercial purposes and that they do not alter, transform or build upon it. For any reuse or redistribution, researchers must make clear to others the licence terms of this work.



## Abstract

Elementary magnetic monopoles have never been experimentally observed but there are credible theoretical reasons to believe that they may nonetheless exist. This thesis gives partial answers to the questions: if magnetic monopoles do exist, can we create them? And if so, how?

Surprisingly little is known about the answers to these simple-sounding questions. The fundamental stumbling block is the strong coupling of magnetic monopoles. This prevents the usual arsenal of techniques from being used, which have proved so useful in understanding the creation of everything from electrons to Higgs particles to quarks.

I consider magnetic monopole creation in strong magnetic fields and at high temperatures. I show that the semiclassical approximation is valid, despite the strong coupling, and calculate the rate using the worldline formalism. The leading order results suggest that magnetic monopoles will be created amply above a certain threshold magnetic field strength and temperature. This is independent of many details of the particles, in particular their spin and whether they are elementary or composite.

Strong magnetic fields and high temperatures are present in neutron stars and in terrestrial heavy ion collisions. By comparison with known properties of neutron stars, and with a search for magnetic monopoles at CERN, I derive the strongest yet, model-independent bounds on the mass of any possible magnetic monopoles. However, investigating higher order corrections to my results, I encounter an instability in the equations which casts doubt on the validity of my approximations and hence the mass bounds.

In answer to my questions: if magnetic monopoles do exist, we may be able to create them in sufficiently high energy heavy ion collisions. However, more theoretical work is needed to decide upon this, both to overcome the issue of the instability and to understand the effects of the spacetime evolution of such collisions.



## Acknowledgements

I would like to thank my supervisor, Arttu Rajantie, for his dependable support and guidance and for all he has taught me about physics. I would also like to thank my fellow PhD students for innumerable discussions about physics, through which I learnt a great deal. In particular I would like to thank Giulia Ferlito, Ed Gillman, Mia Hughes, Ian Jubb and Alun Perkins for their enthusiastic help in understanding various difficult topics.

I would like to thank my family for their support throughout, and Lois, my partner, for helping with my computational work and, more generally, for sharing in all my efforts.





# Contents

<b>Declaration of Authorship</b>	<b>3</b>
<b>Abstract</b>	<b>5</b>
<b>Acknowledgements</b>	<b>7</b>
<b>Contents</b>	<b>9</b>
<b>List of Figures</b>	<b>13</b>
<b>Preface</b>	<b>15</b>
<b>1 Magnetic monopoles</b>	<b>17</b>
1.1 Introduction . . . . .	17
1.2 Dirac monopoles . . . . .	20
1.3 't Hooft-Polyakov monopoles . . . . .	23
1.4 Experimental searches . . . . .	27
<b>2 Few particle collisions</b>	<b>32</b>
2.1 Introduction . . . . .	32
2.2 Exponential suppression . . . . .	33
2.2.1 B+L violation . . . . .	33
2.2.2 Magnetic monopole pair creation . . . . .	35
2.3 Crossing symmetry . . . . .	38

2.4	Landau method . . . . .	43
2.5	Rubakov-Son-Tinyakov method . . . . .	46
2.5.1	Soliton pair creation . . . . .	52
<b>3</b>	<b>Thermal Schwinger pair creation</b>	<b>56</b>
3.1	Worldline expression . . . . .	57
3.1.1	Zero temperature rate . . . . .	57
3.1.2	Finite temperature rate . . . . .	60
3.1.3	Inclusive rate at fixed energy . . . . .	61
3.2	The dilute instanton gas . . . . .	62
3.3	Instantons . . . . .	70
3.3.1	Finite temperature rate . . . . .	70
3.3.2	Inclusive rate at fixed energy . . . . .	70
3.3.3	Regularisation . . . . .	71
3.3.4	Small $\kappa$ expansion . . . . .	73
3.3.5	Low temperature expansion . . . . .	83
3.3.6	High temperature . . . . .	84
3.4	Arbitrary temperature and $\kappa$ . . . . .	88
3.4.1	Finite temperature results . . . . .	90
3.4.2	Fixed energy results . . . . .	93
3.4.3	Numerical errors . . . . .	94
3.5	Summary . . . . .	96
<b>4</b>	<b>Magnetic monopole mass bounds</b>	<b>98</b>
4.1	Heavy ion collisions . . . . .	101
4.2	Neutron stars . . . . .	103
4.3	Summary . . . . .	107
<b>5</b>	<b>Thermal Schwinger sphaleron</b>	<b>108</b>
5.1	General approach . . . . .	110

5.2	The sphaleron and fluctuations about it . . . . .	112
5.3	Self-force instability . . . . .	115
5.4	The scalar prefactor for small $\kappa\tilde{T}$ . . . . .	117
5.5	The spinor prefactor for small $\kappa\tilde{T}$ . . . . .	121
5.6	Summary . . . . .	122
<b>6</b>	<b>Conclusion</b>	<b>124</b>
	<b>Appendix</b>	<b>126</b>
A.1	Induced Schwinger pair production at weak coupling . . . . .	126
A.2	Coherent states . . . . .	127
A.3	QED and SQED in weak external fields . . . . .	129
A.4	Worldline description of extended particles . . . . .	131
A.5	Worldline finite difference formulation . . . . .	133
A.6	Thermal Schwinger rate numerical data . . . . .	135
	<b>Bibliography</b>	<b>136</b>



# List of Figures

1.1	Map determining the existence of Dirac monopoles. . . . .	22
1.2	Map determining the existence of 't Hooft-Polyakov monopoles. . . . .	24
1.3	Hedgehog configuration. . . . .	26
1.4	Map showing the equivalence of Dirac and 't Hooft-Polyakov monopoles at large distances. . . . .	27
1.5	Summary of magnetic monopole flux bounds. . . . .	28
1.6	Summary of magnetic monopole cross section bounds. . . . .	30
2.1	Two processes related by crossing symmetry. . . . .	38
2.2	Complex time path of RST method. . . . .	50
2.3	Example solution to the lattice RST boundary value problem. . . . .	55
3.1	Feynman diagrams of quenched approximation. . . . .	63
3.2	The first three orders of the cluster expansion. . . . .	66
3.3	Sphere of influence of a point along a worldline. . . . .	73
3.4	Apparent intersection of worldlines. . . . .	75
3.5	Instanton solutions at small $\kappa$ . . . . .	80
3.6	Instability of high temperature instanton. . . . .	87
3.7	Examples of the three types of numerical solutions. . . . .	90
3.8	Contour plot of the action, $\tilde{S}(\kappa, \tilde{T})$ , as calculated numerically. . . . .	92
3.9	Plot of the action, $\tilde{S}(\kappa = 0.2, \tilde{T})$ , as calculated numerically and ana- lytically. . . . .	93

---

3.10	Contour plot of $\tilde{\Sigma}(\kappa, \tilde{\mathcal{E}})$ , the exponential suppression of the inclusive rate of Schwinger pair production at fixed energy, as calculated numerically. . . . .	94
3.11	Plot of extrapolation of data to remove cutoff, $a \rightarrow 0$ . . . . .	95
4.1	Summary of the lower bounds for the mass of magnetic monopoles . .	106
5.1	Worldline sphaleron. . . . .	109
5.2	Worldline instantons. . . . .	112
5.3	Plot of the first few eigenvalues showing the self-force instability. . . .	116
5.4	Plot of the logarithm of the sphaleron prefactor. . . . .	121

# Preface

I begin, in Chapter 1, with an introduction to magnetic monopoles, focusing on matters important to this thesis. I briefly review the history of thought on magnetic monopoles and give the main arguments for their existence. I then compare and contrast the two main types of magnetic monopoles: elementary and composite, or, rather, Dirac and 't Hooft-Polyakov. In the last section of the chapter, I discuss experimental searches for magnetic monopoles and their implications for possible physical theories of magnetic monopoles.

Chapter 2 reviews various approaches to calculating cross sections for magnetic monopole pair production from, what I call, *few particle collisions*, the most pertinent example being the proton-proton collisions currently happening at the Large Hadron Collider. I start by reviewing arguments which suggest that magnetic monopoles will never be produced in few particle collisions, noting that the matter remains unsettled. In the following sections I outline several approaches which could in principle substantiate these arguments, pointing out weaknesses and, in some cases, suggesting how these might be overcome.

Chapter 3, based on Ref. [1], contains the central theoretical calculation of the thesis, about which the rest hangs. It is the calculation of the rate of magnetic monopole production in strong magnetic fields and high temperatures. The calculation uses the worldline formalism and relies on a semiclassical approximation.

In Chapter 4, based on Ref. [2], I apply the results of the previous chapter to the creation of magnetic monopoles in two different physical circumstances: neutron stars and heavy ion collisions. From this I am able to show that if magnetic monopoles exist, they must be heavier than a certain lower bound.

Chapter 5, based on Ref. [3], builds on some of the work of Chapter 3. For a particular region of parameter space, I give an improved theoretical estimate for the rate of magnetic monopole production. This is important as it is the region of parameter space relevant for heavy ion collisions. In performing this calculation I encounter a subtle pathology of the approximations I make which reduces the validity of the approach to within a subspace of the full parameter space. This

raises doubts about the validity of the mass bounds derived in Chapter 4 and calls for more theoretical work to settle the matter.

In Chapter 6 I summarise the achievements of this thesis and suggest possible future directions of study.

Throughout I use the natural units common in high energy particle physics, where  $c = \hbar = k_B = \epsilon_0 = 1$ . I adopt the mostly minus signature for the spacetime metric,  $(+, -, -, -)$ . I use  $i, j, k, l, \dots$  to run over spatial directions;  $\mu, \nu, \rho, \sigma, \dots$  to run over spacetime indices and adopt the Einstein summation convention.



# Chapter 1

## Magnetic monopoles

### 1.1 Introduction

*Is it absurd to suppose the existence of bodily conductors of magnetism, of magnetic currents, of free magnetism?*

Pierre Curie

It has long been known that the two poles of a magnet cannot be separated. In 1269 Peregrinus showed that all fragments of lodestone are dipoles, with both a north and south pole [4]. However this has not stopped physicists thinking about the possibility that free magnetic (mono)poles might exist. Pierre Curie suggested their existence in 1894 [5], inspired by the otherwise perfect symmetry between electric and magnetic phenomena.

Without matter, classical electromagnetism is symmetric under an interchange of electric and magnetic fields. This is clear at a glance from Maxwell's equations without sources,

$$\partial_\mu F^{\mu\nu} = 0, \tag{1.1}$$

$$\partial_\mu \tilde{F}^{\mu\nu} = 0, \tag{1.2}$$

where  $\tilde{F}^{\mu\nu} := \frac{1}{2}\epsilon^{\mu\nu\rho\sigma} F_{\rho\sigma}$ . The equations are symmetric under the interchange of electric and magnetic fields, so-called electromagnetic duality,

$$\begin{aligned} F^{\mu\nu} &\rightarrow \tilde{F}^{\mu\nu}, \\ \tilde{F}^{\mu\nu} &\rightarrow -F^{\mu\nu}. \end{aligned} \tag{1.3}$$

The minus sign in the second equation is due to the Lorentzian signature of space-

time.

However the symmetry appears to be broken in nature, as we have only discovered a source for the electric field,  $j_E^\nu$ . In this case the right hand side of Eq. (1.1) is modified, but not that of Eq. (1.2). One can restore electromagnetic duality by the further addition of magnetic sources,  $j_M^\nu$ .

$$\begin{aligned}\partial_\mu F^{\mu\nu} &= j_E^\nu, \\ \partial_\mu \tilde{F}^{\mu\nu} &= j_M^\nu.\end{aligned}\tag{1.4}$$

The duality transformation now also involves the interchange of electric and magnetic sources,

$$\begin{aligned}j_E^\nu &\rightarrow j_M^\nu, \\ j_M^\nu &\rightarrow -j_E^\nu.\end{aligned}\tag{1.5}$$

So, if magnetic monopoles were to exist, nature would have an enhanced symmetry. From this observation it would be pleasing if they were to exist, though I need not attach much weight to this aesthetic argument.

In 1931 Dirac considered the possibility of including magnetic monopoles into a quantum mechanical description of matter [6]. He found that to do so, a consistency condition arises, following from the basic requirement that wave functions be single-valued functions. In the presence of a magnetic monopole with charge  $g$ , a wave function describing an electric particle with charge  $e$  will only be single-valued if  $e$  and  $g$  satisfy the Dirac quantisation condition,

$$eg = 2\pi n,\tag{1.6}$$

where  $n \in \mathbb{Z}$ . The same condition can be derived by imposing the quantisation of angular momentum. Note that the magnetic fine structure constant is then  $\alpha_M = 1/(4\alpha_E)$ , where  $\alpha_E$  is the electric fine structure constant. At low energies,  $\alpha_E \approx 1/137$  and hence  $\alpha_M \approx 34$ , meaning magnetic monopoles are necessarily strongly coupled.

The key importance of the Dirac quantisation condition is that it implies that electric charges come in integer multiples of one fundamental charge. This is, of course, what is observed and it is a remarkable empirical fact which is not explained in the Standard Model. All known particles have electric charges which are an integer multiple of one fundamental charge. For example, the experimental upper limit on the difference between the charge of the proton and (minus) that of the

electron is  $(0.8 \pm 0.8)10^{-21}e$  [7]. The converse, that electric charge quantisation implies the existence of magnetic monopoles has been conjectured by Polchinski [8]. However various extensions of the Standard Model which break the  $(B - L)$  symmetry explicitly may also explain charge quantisation via the requirement of anomaly cancellations [9, 10].

A complete, dynamical, quantum mechanical description of magnetic monopoles and their interactions with photons and electric charges was given somewhat later [11, 12, 13, 14, 15]. Due to topological issues, the theory is significantly more complicated than quantum electrodynamics (QED) in the absence of magnetic charges. Some formulations are non-local; others are not manifestly Lorentz invariant. However, the various apparently different constructions were shown to be equivalent [16] and the unifying theory is known as quantum electromagnetodynamics (QEMD). The theory is both Lorentz and gauge invariant [13, 14, 15, 17, 18]

An alternative approach to a quantum field theory for magnetic monopoles arises from considering the global structure of the QED gauge group [19, 20, 21]. There are two choices for the representation of the group  $U(1)$ : it can be either compact or non-compact. In the compact representation the gauge field strength is an angular variable, whereas in the non-compact representation its elements take values in  $\mathbb{R}$ . The differences between these two choices are not visible in perturbation theory but are manifest in a lattice regularisation. The compact choice leads to electric charge quantisation, whereas in the non-compact case electric charges can take any real number values. In accordance with the charge quantisation observed in nature, the natural choice is the compact one. However, in this case magnetic monopoles arise naturally. They do not need to be added by hand but are a set of field configurations which contribute to the path integral. The magnetic particles generically have masses of the order of the cut-off scale and hence decouple in the continuum limit. That is, unless one adds a mass counterterm to fine-tune the magnetic monopole mass to be small, just like for the Higgs boson.

In 1974 't Hooft [22] and Polyakov [23] showed that magnetic monopoles arise as localised, finite energy, classical solutions to the field equations of non-Abelian gauge theories with spontaneously broken symmetries. On scales of the order of the symmetry breaking scale, these magnetic monopoles appear as a coherent state of scalar and vector bosons particles. However, on distance scales much larger than this, they are virtually indistinguishable from the magnetic monopoles considered by Dirac and others [24, 25]. 't Hooft-Polyakov magnetic monopoles are a generic prediction of grand unified theories, those in which a semi-simple gauge group is spontaneously broken down to the low energy Standard Model gauge group [26].

Following the work of 't Hooft and Polyakov, magnetic monopoles have been investigated and developed by many authors, and have been found to act in a great wealth of physical phenomena. They have been shown to play a role in confinement in certain theories [20, 21, 27, 28]; they can lead to baryon number non-conservation [29, 30]; they may have electric as well as magnetic charges [31, 32]; their low energy scattering exhibits a rich structure [33, 34, 35] and the above-mentioned electromagnetic duality has been extended and developed [36, 28, 37]. However, for the most part, these topics will not be discussed here and I direct the interested reader to the many excellent reviews [38, 39, 40, 41, 42].

Magnetic monopoles also appear in gravitational theories. In Einstein gravity coupled to electromagnetism, there exist spherically symmetric black hole solutions, the Reissner-Nordström solutions, with magnetic as well as electric charge. There also exist instanton solutions which describe the pair production of such magnetic black holes [43, 44, 45]. Further, it has been argued that in a quantum theory of gravity, the existence of these instantons means that the existence of magnetic monopoles cannot be avoided [46]. In string theory or its parent theories, there are necessarily more than the four observable dimensions. If the extra dimensions are curled up into small compact spaces, there will exist what are called Kaluza-Klein magnetic monopoles [47, 48]. As before, though I have mentioned these topics for completeness, they will not be discussed further here.

In Secs. 1.2 and 1.3 I give theoretical overviews of Dirac and 't Hooft-Polyakov monopoles respectively. In Sec. 1.4 I discuss experimental searches for magnetic monopoles.

## 1.2 Dirac monopoles

In the presence of both electric and magnetic charges, neither the electric nor the magnetic fields are divergenceless. Though this does not lead to any real differences in describing the fields it does frustrate the usual description in terms of potentials,

$$F_{\mu\nu} = \partial_\mu A_\nu - \partial_\nu A_\mu. \quad (1.7)$$

This description was possible because of the Bianchi identity, Eq. (1.2). As this continues to hold outside magnetic sources, Eq. (1.7) can still be used there, locally. However, the presence of magnetic sources prevents a global definition of  $A_\mu$ , in terms of a set of globally defined functions.

The simplest example is that of a single, static magnetic monopole with mag-

netic charge  $g$ . This is the example Dirac originally considered [6] and it has become canonical [39, 49]. Using the Lorentz frame of the monopole, the electromagnetic field in this case is

$$\begin{aligned} F_{0i} &= 0, \\ F_{ij} &= \varepsilon_{ijk} \frac{gx^k}{4\pi|\mathbf{x}|^3}, \end{aligned} \quad (1.8)$$

where  $\varepsilon_{ijk}$  is the Levi-Civita symbol,  $x^\mu$  is a position vector, with origin at the magnetic monopole, and  $|\mathbf{x}|$  is its spatial magnitude. One cannot globally define a non-singular potential,  $A_\mu$ , which gives rise to this field [50, 51]. However, in the upper spatial hemisphere, one can choose,

$$A_\mu^+ dx^\mu = \frac{g}{4\pi r} \frac{(1 - \cos(\theta))}{\sin(\theta)} d\phi, \quad (1.9)$$

where  $(r, \theta, \phi)$  are the usual spherical polar coordinates. In the lower hemisphere, one can instead use

$$A_\mu^- dx^\mu = \frac{g}{4\pi r} \frac{(-1 - \cos(\theta))}{\sin(\theta)} d\phi. \quad (1.10)$$

Both of these equations are singular along a semi-infinite line extending from the monopole to infinity: Eq. (1.9) is singular along a line in the lower hemisphere and Eq. (1.10) is singular along a line in the upper hemisphere. In the region where they are both finite, they both lead to the same magnetic field, Eq. (1.8), and are related by the gauge transformation,

$$A_\mu^+ - A_\mu^- = \partial_\mu \left( \frac{g\phi}{2\pi} \right). \quad (1.11)$$

Under this gauge transformation, the wave function,  $\psi$ , of an electrically charged particle, with charge  $e$ , is transformed as

$$\psi \rightarrow \exp \left( -\frac{ieg\phi}{2\pi} \right) \psi. \quad (1.12)$$

Hence, for the wave function to be a single-valued function before and after the transformation, the charges  $e$  and  $g$  must satisfy the Dirac quantisation condition, Eq. (1.6). In this case the two gauge fields,  $A_\mu^+$  and  $A_\mu^-$ , are physically equivalent and can be consistently patched to define the gauge field of the magnetic monopole.

Comparing  $\phi = 0$  with  $\phi = 2\pi$  in Eq. (1.12) is equivalent to parallel transporting the charged particle around a circle centred on the monopole. The integer which arises in the Dirac quantisation condition is thus a winding number, it is the

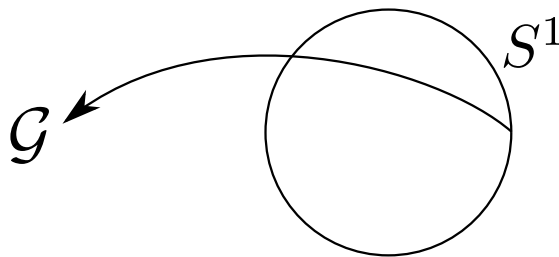


Figure 1.1: Map determining the existence of Dirac monopoles, from a circle to the gauge group.

number of times the phase of the wave function covers the complex unit circle as the charged particle encircles the magnetic monopole once. This winding number is independent of the distance,  $r$ , from the magnetic monopole and hence the magnetic charge must be contained in a single point. Further, being discrete the winding number cannot change in any continuous process, such as time evolution, and hence magnetic charge is conserved.

One can generalise this argument from the  $U(1)$  group of electromagnetism to more general groups,  $G$ , assuming a Coulomb phase. The result is that one must consider maps from the circle to  $G$  [52]. The generalisation of the winding number is given by homotopy theory. Maps which can be continuously deformed into each other are termed equivalent and the classification of such maps into equivalence classes is given by the first homotopy group,  $H_1(G)$ . If  $H_1(G)$  consists of just a single element then there are no Dirac monopoles in the theory. For electromagnetism  $H_1(U(1)) = \mathbb{Z}$  and hence there are an infinite number of different magnetic monopoles, labelled by a nonzero integer, zero labelling the absence of a magnetic monopole. For  $G = SU(2)$  one can show that  $H_1(SU(2)) = \mathbb{Z}_2$ . In this theory there is thus only one type of Dirac magnetic monopole.

So far the discussion of Dirac's magnetic monopoles has been kinematic. To add dynamical degrees of freedom for such a magnetic monopole requires adding a source field for it. This field can have any spin. Formulated without a cut-off, there will be an infinite self-energy and infinite charge renormalisation effects, which can be regularised and renormalised just as for an electric particle as long as there is an appropriate source field. In a theory containing both electric and magnetic particles, extra care is needed in taking care of the global properties of the gauge field. In principle there is no problem in doing so. The formalism is reviewed in Refs. [16, 53]. In practice however, very few calculations have been done in this formalism.

The magnetic monopoles considered in this section can be added to any gauge

theory containing electromagnetism. They can have any mass, any spin and any charge consistent with the Dirac quantisation condition. Although the quantisation of electric charge points to their existence, such magnetic monopoles are not strictly necessary.

### 1.3 't Hooft-Polyakov monopoles

In 1974 't Hooft and Polyakov found that magnetic monopoles necessarily arise in certain gauge theories [22, 23], without the addition of any explicit sources. The theories in question are spontaneously broken, non-Abelian gauge theories, with semi-simple gauge group, so called Grand Unified Theories (GUTs). The magnetic monopoles arise as solitons, as static, localised, finite-energy solutions of the classical equations of motion. As such they survive quantisation, giving poles in correlation functions just as elementary particles do, despite the absence of corresponding explicit fields in the Lagrangian [54, 55, 56].

For the spontaneous symmetry breaking of a GUT with gauge group  $\mathcal{G}$ , there must exist a scalar field charged under the gauge group, a so-called Higgs field [57, 58, 59]. The Higgs field takes a vacuum expectation value (vev) which breaks the gauge group  $\mathcal{G}$  down to a subgroup  $\mathcal{H}$ <sup>1</sup>. The scalar vev thus takes values in  $\mathcal{G}/\mathcal{H}$ , the vacuum manifold. For this GUT to describe nature, the gauge group must break down to the Standard Model gauge group,  $SU(3) \otimes SU(2) \otimes U(1)$ , before reaching the electroweak scale. There can, of course, be multiple symmetry breakings occurring at different scales.

Fermionic fields play no role in spontaneous symmetry breaking and so I will ignore them here. I consider a Georgi-Glashow type theory [26], with gauge group  $\mathcal{G}$  and Lagrangian

$$\mathcal{L} = -\frac{1}{4e^2} G_{\mu\nu}^a G^{a\mu\nu} + \frac{1}{2} D_\mu \phi^a D^\mu \phi^a - U(\phi^a). \quad (1.13)$$

The label  $a$  is an adjoint index, running over  $1, 2, \dots, \dim(\mathcal{G})$ . The field strength is the usual one,  $G_{\mu\nu}^a := \partial_\mu A_\nu^a - \partial_\nu A_\mu^a - e f_{abc} A_\mu^b A_\nu^c$ , where  $f_{abc}$  are the structure constants of the gauge group. The potential is invariant under  $\mathcal{G}$  but its minima are

---

<sup>1</sup>Of course, the usual picture of the Higgs field attaining a vev is naive. One can perform a gauge independent analysis [60], but I will use the more common language of the unitary gauge.

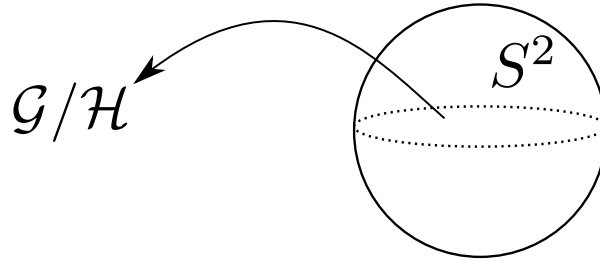


Figure 1.2: Map determining the existence of 't Hooft-Polyakov monopoles, from the sphere at spatial infinity to the vacuum manifold.

not, only being invariant under the smaller group  $\mathcal{H}$ . A typical example is given by

$$U(\phi^a) = \frac{\lambda}{4} (\phi^a \phi^a - v^2)^2. \quad (1.14)$$

Thus  $v$  is the classical vev and  $\lambda$  is the scalar field self-coupling.

One seeks finite energy, static field configurations. For such a field configuration to have finite energy, it must be that it tends to the vacuum manifold as the spatial distance  $|\mathbf{x}| \rightarrow \infty$ . For the example of Eq. (1.14) this is

$$\begin{aligned} G_{jk}^a &\rightarrow 0, \\ D_j \phi^a &\rightarrow 0, \\ \phi^a \phi^a &\rightarrow v^2, \end{aligned} \quad (1.15)$$

where the rate of approach must be such as to make the terms separately integrable. The condition on the magnitude of the scalar field defines a map from spatial infinity,  $S^2$ , to the vacuum manifold,  $\mathcal{G}/\mathcal{H}$ . Just as for the maps from the circle to the gauge group, which were relevant for Dirac magnetic monopoles, maps from  $S^2$  to  $\mathcal{G}/\mathcal{H}$  may be classified according to whether or not they are continuously deformable into each other. Maps which can be continuously deformed into each other are termed equivalent and the classification of such maps into equivalence classes is given by the second homotopy group of  $\mathcal{G}/\mathcal{H}$ , denoted  $\Pi_2(\mathcal{G}/\mathcal{H})$ . If the second homotopy group has only a single element then all maps from  $S^2$  to  $\mathcal{G}/\mathcal{H}$  can be continuously deformed into each other. If there are more than one elements, then there exist field configurations which cannot be continuously deformed to the vacuum.

Consider the canonical example,  $\mathcal{G} = SU(2)$ , with  $f_{abc} = \varepsilon_{abc}$ . In this case, for the Lagrangian of Eq. (1.13), the unbroken symmetry group is  $\mathcal{H} = U(1)$ . Then the second homotopy group is  $\Pi_2(SU(2)/U(1)) = \mathbb{Z}$ , the additive group of the integers. In each of these equivalence classes, i.e. for each integer, there should be a field



configuration which minimises the energy. This field configuration cannot decay as it is topologically protected: time evolution is a type of continuous deformation.

It only remains to explicitly construct such a field configuration. Being a minimum of the energy it should satisfy the field equations of motion. Such a solution was found independently by 't Hooft [22] and Polyakov [23] and takes the form

$$\begin{aligned}\phi^a(x) &= \frac{x^a}{e|\mathbf{x}|^2} (ev|\mathbf{x}| + H(ev|\mathbf{x}|)), \\ A_j^a(x) &= -\varepsilon_{ajk} \frac{x^k}{e|\mathbf{x}|^2} (1 - K(ev|\mathbf{x}|)), \\ A_0^a(x) &= 0.\end{aligned}\tag{1.16}$$

The functions  $H$  and  $K$  must satisfy [61]

$$\begin{aligned}\xi^2 \frac{d^2 K}{d\xi^2} &= K(H + \xi)^2 + K(K^2 - 1), \\ \xi^2 \frac{d^2 H}{d\xi^2} &= 2K^2(H + \xi) + \frac{\lambda}{e^2} (H + \xi) (H^2 + 2\xi H),\end{aligned}\tag{1.17}$$

where  $\xi := ev|\mathbf{x}| = M_W|\mathbf{x}|$  and appropriate boundary conditions are specified for finiteness of the energy. It can be rigorously shown that a solution to these equations exists [62] and it can be constructed numerically. It is everywhere smooth. In the limit  $\lambda \rightarrow 0$  it is known analytically [63, 64]. The functions  $H$  and  $K$  above are localised exponentially over a region of size  $O(1/M)$ , where  $M := \min(M_H, M_W)$ , the Compton wavelength of the lightest constituent particle. This is the monopole core.

In all cases the classical mass of the solution, which dominates over the quantum corrections when the theory is weakly coupled, is found to be of the order

$$m \sim \frac{4\pi}{e^2} M.\tag{1.18}$$

This is the same order of magnitude as the energy of the Coulomb magnetic field outside the monopole core [38],

$$\begin{aligned}\int \frac{1}{2} B_{Coulomb}^2 d^3x &= \int_{O(1/M)}^{\infty} \frac{1}{2e^2|x|^4} d^3x, \\ &= \frac{2\pi}{e^2} O(M),\end{aligned}\tag{1.19}$$

which also provides a lower bound on the mass in this theory as the energy density is everywhere positive. The core of the monopole adds to the energy of the config-

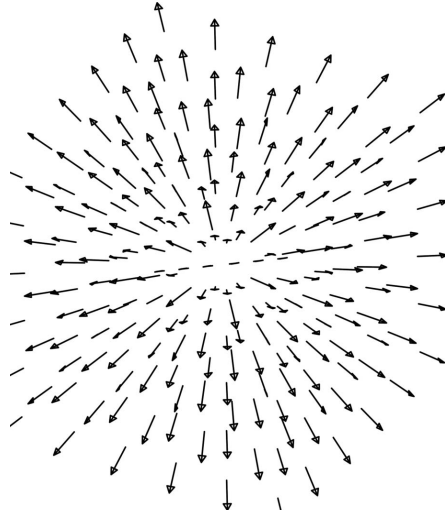


Figure 1.3: Scalar field configuration of the 't Hooft-Polyakov monopole, the so-called *hedgehog* (figure from [66]).

uration a contribution of the same magnitude. This can naturally be understood as coming from the rest mass of  $O(4\pi/e^2) := O(1/\alpha)$  particles. Likewise the large charge of the magnetic monopole, necessary for the Dirac quantisation condition to hold, can be understood as arising from the coherently combined charges of a large number of constituent charged particles,  $g = O(e/\alpha) = O(4\pi/e)$  [65]. Due to the large particle occupancy numbers, the quantum state of a magnetic monopole is well described by the coherent state of the classical solution.

This solution was called a *hedgehog* by Polyakov as the scalar field points outwards in all directions from the origin (see Fig. 1.3). The vector fields can be split into the Abelian photon part and the non-Abelian heavy vector boson part. The photon field is given by

$$F_{\mu\nu} := \frac{\phi^a}{\sqrt{\phi^b\phi^b}} G_{\mu\nu}^a - \frac{1}{e(\phi^d\phi^d)^{3/2}} \varepsilon_{abc} \phi^a (D_\mu\phi^b)(D_\nu\phi^c). \quad (1.20)$$

Outside a region of size  $O(1/M)$ , the monopole core, only the photon field is not exponentially suppressed. This region is a factor  $4\pi/e^2$  larger than the Compton wavelength of the monopole (see Eq. (1.18)). As  $M|\mathbf{x}| \rightarrow \infty$ , the photon field approaches the field of a magnetic monopole,

$$F_{ij} = \varepsilon_{ijk} \frac{x^k}{e|\mathbf{x}|^3} + O(e^{-M|\mathbf{x}|}). \quad (1.21)$$

The magnetic charge is thus  $4\pi/e$ , twice that required to satisfy the Dirac quantisation condition (this is because fields in the fundamental representation of  $SU(2)$

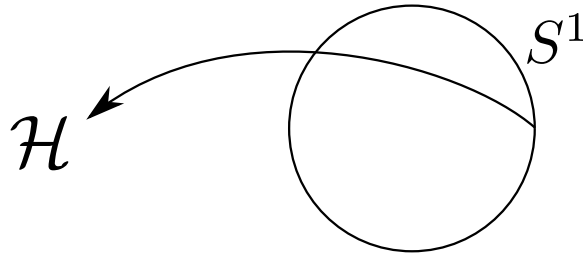


Figure 1.4: Map showing the equivalence of Dirac and 't Hooft-Polyakov monopoles at large distances, from a circle to the broken gauge group.

carry charge  $e/2$ ). More complicated quantisation conditions are possible in more complicated symmetry breaking schemes, when the magnetic monopole is charged under more than one gauge group. The magnetic charge of 't Hooft-Polyakov monopoles is topologically conserved, just as for Dirac magnetic monopoles.

Outside the monopole core the gauge group is broken and there appears a winding number,  $\Pi_1(U(1)) = \mathbb{Z}$ , exactly as for Dirac monopoles but with  $\mathcal{G}$  replaced by  $\mathcal{H}$ . On the other hand, the scalar field vanishes at the centre of the monopole, thus inside the monopole core the gauge group is unbroken. Inside the monopole the winding number is unwound: the field configuration is non-singular. This is possible because the first homotopy group of the full gauge group,  $\Pi_1(SU(2))$ , is trivial [38]. All maps from a circle to the full gauge group can be continuously deformed to the vacuum. The correspondence between Dirac and 't Hooft-Polyakov monopoles can also be seen from the following theorem [39],

$$\Pi_2(\mathcal{G}/H) = \Pi_1(\mathcal{H})/\Pi_1(\mathcal{G}). \quad (1.22)$$

The theory admits 't Hooft-Polyakov monopoles when the left hand side of this equation is nontrivial. The broken phase admits Dirac monopoles when  $\Pi_1(\mathcal{H})$  is nontrivial and these are non-singular when  $\Pi_1(\mathcal{G})$  is trivial. The equivalence of these two notions is demonstrated by the equality.

## 1.4 Experimental searches

So, there are compelling theoretical reasons to expect the existence of magnetic monopoles [6, 22, 23, 8]. As a consequence, there have been extensive searches for them [67, 68, 69], but so far with no positive results.

The experimental signatures of magnetic monopoles are clear and robust and

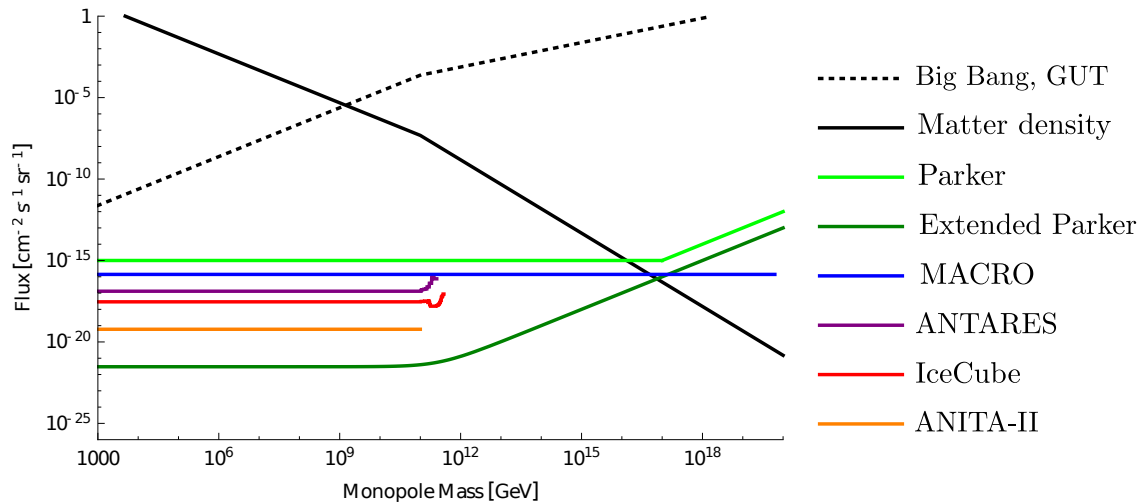


Figure 1.5: Summary of magnetic monopole flux bounds due to Arttu Rajantie (see also Ref. [69]), with data taken from Refs. [70, 71, 72, 73, 74, 75, 76, 77]. The dotted line gives the predicted density of GUT magnetic monopoles from a Big Bang cosmological history without inflation. The black line labelled “Matter density” corresponds to magnetic monopoles making up the entire observed matter density of the universe today.

many such signatures are independent of the particular underlying model. Due to the magnetic charge their interactions with electromagnetic fields are known and unlike those of any other particles. Magnetic charge is conserved and hence the lightest magnetic monopoles with given charge cannot decay. They are strongly interacting, due to the Dirac quantisation condition, and as a result are highly ionising. They can form bound states with magnetic dipole moments, such as those of nuclei. These experimental signatures are all generic, being independent of the internal structure of the magnetic monopoles.

There are also experimental signatures of magnetic monopoles which depend strongly on the internal structure of the magnetic monopole and hence on the particular underlying model. The core of ’t Hooft-Polyakov monopoles reveals the symmetry breaking pattern of the GUT from whence they come. This can be elucidated by scattering magnetic monopoles and Standard Model particles and may lead to such exotic behaviour as proton decay [29, 30].

For my purposes, magnetic monopole searches can be divided into two categories: those which search for existing magnetic monopoles [77] and those which try to create new magnetic monopoles, in colliders [78]. In the absence of a positive observation<sup>2</sup>, quite different information has been learnt from these two cat-

<sup>2</sup>There have been two apparent detections of a magnetic monopole [79, 80], though the absence of monopoles in larger follow-up experiments makes the reliability of the detections unconvincing.

egories of experiment [81]. Searches for existing magnetic monopoles can also be sub-categorised according to where the searches take place and attempts to create new magnetic monopoles can be sub-categorised according to which particles were collided and at what energies.

Non-observation in searches for existing magnetic monopoles allows one to derive bounds on the flux density of magnetic monopoles in the Universe today,  $\mathcal{F}$ , and on the magnetic monopole density. The current such bounds are rather stringent, implying that magnetic monopoles must be very rare. The strongest current bound on  $\mathcal{F}$  for lighter magnetic monopoles, the Extended Parker Bound, is derived from a dynamical consideration of the generation of today's galactic magnetic field [72],<sup>3</sup>

$$\mathcal{F} \lesssim \begin{cases} 3 \times 10^{-22} \text{cm}^{-2} \text{s}^{-1} \text{sr}^{-1} \left( \frac{B_0}{10^{-11} \text{G}} \right) & , m \lesssim 3 \times 10^{11} \text{GeV} \left( \frac{B_0}{10^{-11} \text{G}} \right) , \\ 1.2 \times 10^{-16} \left( \frac{m}{10^{17} \text{GeV}} \right) \text{cm}^{-2} \text{s}^{-1} \text{sr}^{-1} & , m \gtrsim 3 \times 10^{11} \text{GeV} \left( \frac{B_0}{10^{-11} \text{G}} \right) . \end{cases}$$

Here  $B_0$  is the magnitude of the magnetic field which seeded the growth of today's galactic magnetic field. As well as flux bounds derived from astrophysical and cosmological considerations, there have been several passive ground-based experiments searching for magnetic monopoles. These have directly constrained the flux of magnetic monopoles at the surface of the Earth. A summary of different flux bounds is given in Fig. 1.5.

From these bounds on the flux, one would like to derive constraints on the properties of possible magnetic monopoles. This requires comparison with theoretical predictions of the magnetic monopole flux which, in turn, depend on cosmological history. Inflation would have diluted away any pre-existing magnetic monopoles [83, 84, 85] but, during reheating, sufficiently light magnetic monopoles would have been produced thermally. One can derive a prediction for magnetic monopole flux today by calculating the time evolution of this initial density. Then by comparison with the experimental bounds on the flux, one can derive a bound on the ratio of the mass of any magnetic monopoles to the reheating temperature,  $m/T_{\text{RH}} \gtrsim 45$  [86, 87, 88]. Further, as the reheating temperature must be greater than the temperature of Big Bang nucleosynthesis (BBN),  $T_{\text{BBN}} \approx 10 \text{MeV}$ , the mass of any magnetic monopoles must satisfy

$$m \gtrsim 0.45 \text{GeV}. \quad (1.23)$$

This is considered a very weak bound, though to my knowledge it is the strongest reliable bound in the literature.

---

<sup>3</sup>In fact in Ref. [82] the authors derive an even stronger bound, also by a consideration of galactic magnetic fields, though this bound is more speculative.

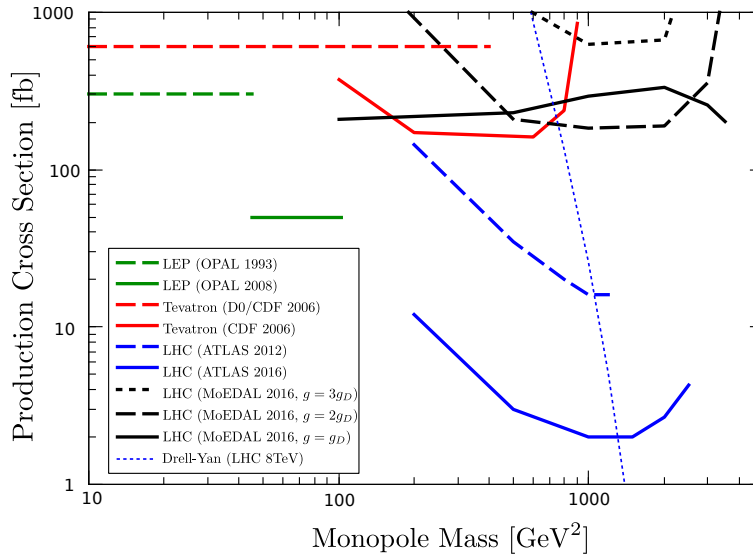


Figure 1.6: Summary of magnetic monopole cross section bounds due to Arttu Rajantie (see also Ref. [69]), with data taken from [78, 89, 90, 81]. The blue, dotted line labelled “Drell-Yan” is the tree-level cross section for pair production of magnetic monopoles. This is not a reliable estimate of the true cross section due to the large charge of magnetic monopoles.

From attempts to create magnetic monopoles in collider experiments, non-observation allows one to derive bounds on various cross sections for magnetic monopole production. Such bounds take the form

$$\sigma_{M\bar{M}}(s) \lesssim \sigma_{UB}(s), \quad (1.24)$$

where  $\sigma_{M\bar{M}}(s)$  is the cross section for pair production of magnetic monopoles in the given collision at centre of mass energy  $\sqrt{s}$  and  $\sigma_{UB}(s)$  is the experimental upper bound. Since the late 1970s, collider searches have focused on  $e\bar{e}$ ,  $p\bar{e}$ ,  $p\bar{p}$  and  $pp$  collisions [81]. A summary of the resulting cross section bounds is given in Fig. 1.6. There has also been a magnetic monopole search in heavy ion collisions [91].

As with the bounds on the flux, from these bounds on cross sections, one would like to derive constraints on the properties of possible monopoles. The tree-level Drell-Yan cross section has often been used to obtain indicative mass bounds [89, 90, 81]. However, this approach is not reliable because, if magnetic monopoles exist, they are strongly coupled and hence perturbation theory in the coupling constant fails.

As I will discuss in Chapter 2, it can be argued that the cross section for

---

magnetic monopole pair production in collider experiments (excluding in heavy ion collisions) is enormously exponentially suppressed. This would imply that, even if magnetic monopoles exist and are sufficiently light to be produced kinematically, one would not expect to produce them in such collider experiments.

# Chapter 2

## Few particle collisions

### 2.1 Introduction

The title of this chapter needs some explaining. By *few particle collisions*, I mean particle collisions for which the initial state contains a small number of particles, i.e. a small number of excitations above the vacuum in a Fock space representation or generalisation thereof. As such the initial state is far from the classical limit. For example  $e\bar{e}$ ,  $p\bar{e}$ ,  $p\bar{p}$  and  $pp$  collisions are all to be considered as few particle collisions. However, heavy ion collisions such as  $PbPb$  or  $AuAu$  collisions are not.

Magnetic monopoles, if they exist, may in principle be created as monopole-anti-monopole pairs, thus conserving magnetic charge. In this section I consider the question of whether or not magnetic monopoles may be created in few particle collisions. This question is closely related to several others which have been intensively studied and debated in the past decades. In particular whether or not few particle collisions can induce B+L violation [92, 93, 94, 95, 96, 97], or kink pair production [98, 99, 100, 101, 102], or vacuum decay [103].

In Sec. 2.2 I present several arguments in favour of the position that no, magnetic monopoles cannot be created in few particle collisions. However none of the arguments are altogether reliable and hence the matter cannot be said to be settled. In the following sections, Secs. 2.3, 2.4 and 2.5, I present three different approaches to answering the question here posed, discussing the hurdles still to be overcome. The content of this chapter is mostly available in the literature, though nowhere else is it collected together with a focus on magnetic monopoles.



## 2.2 Exponential suppression

In weakly coupled quantum field theories, the Feynman diagram expansion is most commonly the tool of choice. However, there are some phenomena which are beyond its purview. Magnetic monopoles are just such a phenomenon as they do not appear at any finite order in a Feynman diagram expansion. Their charge,  $g \propto 1/e$ , and, for 't Hooft-Polyakov monopoles, their mass,  $m \propto M/e^2$  (where  $M$  is the mass of a gauge boson), are both proportional to inverse powers of the small electric coupling,  $e$ . As such, their pair production cross sections should be smaller than any power of  $\alpha := e^2/(4\pi)$  as  $\alpha \rightarrow 0$ . There are infinitely many functional forms which obey this property but it has been conjectured that the relevant form for magnetic monopole production is [104]

$$\sigma \sim e^{-\frac{c}{\alpha}}, \quad (2.1)$$

for some  $c > 0$  and I use  $\sim$  to denote that the logarithms of the two sides agree to leading order in  $\alpha$ , i.e. that both sides are of the same order-of-magnitude.

### 2.2.1 B+L violation

This expectation is indeed borne out for some other non-perturbative phenomena, where explicit calculations have been performed. The canonical example, which has been the focus of decades of work, is B+L violating transitions in the Standard Model and in related gauge theories with a left-right asymmetry in the fermion sector. At low energies these are governed by a BPST-type instanton [105] and are exponentially suppressed by [92, 93]

$$\sigma_0 \sim e^{-\frac{4\pi}{\alpha}} \approx 10^{-154}, \quad (2.2)$$

where  $\sigma_0$  represents the cross section for the process,  $\alpha$  is now the Weak fine structure constant. The transition is a kind of quantum tunnelling and has an associated energy barrier, the sphaleron [94, 95], with height  $M_{sph} = O(M/\alpha)$ , where  $M$  is the mass of a gauge boson. The height of this energy barrier is parametrically the same as would be expected for magnetic monopole pair production, if this too were expressible as a tunnelling transition.

The exponential suppression in Eq. (2.2) is so incredibly small that B+L violating transitions will never be observed from low energy initial states. However, by

analogy with quantum tunnelling in simple, one-dimensional systems, one would expect that this suppression would be reduced for initial states with higher energy. In particular the question arises as to whether the exponential suppression would disappear altogether for over-barrier transitions, where the initial state has an energy greater than  $M_{sph}$ .

The answer to this question is not a simple yes or no. This is because in systems with many degrees of freedom there are, in general, many different ways to distribute a given amount of energy. At one extreme are, for example, high energy, few particle states in quantum field theory, where all the energy is concentrated in only a few degrees of freedom. At the other extreme are, for example, a thermal state or a semiclassical coherent state where the total energy is spread across a huge number of degrees of freedom. In general, such different states may have very different transition probabilities.

If one considers thermal states, as the temperature is raised from zero the exponential suppression is reduced due to the thermal fluctuations. At temperatures of the order of the barrier height, B+L violating transitions are unsuppressed [106, 107]. Likewise if one considers states with zero temperature but sufficiently high fermion density, one finds the states are absolutely unstable and B+L violating transitions are unsuppressed [108, 109]. A third example of an unsuppressed B+L violating process is for initial states containing particles with masses greater than  $M_{sph}$  [110, 111]. B+L violating transitions proceed via the decay of these particles.

The issue is more subtle when the energy of the initial state is concentrated in a small number of degrees of freedom, such as in few particle collisions. Perturbative corrections to Eq. (2.2) due to the presence of few particle collisions with energies much below the sphaleron mass have been shown to exponentially enhance the rate [112, 113]. The enhancement takes the form

$$\sigma_E \sim e^{-\frac{4\pi}{\alpha} F_{HG}\left(\frac{E}{M_{sph}}\right)}, \quad (2.3)$$

where  $\sigma_E$  is the cross section for the process with centre-of-mass energy  $E$  and  $F_{HG}$  is known as the Holy Grail Function. There is evidence that the function does not depend on any details of the initial state, except for the centre-of-mass energy [114, 115, 116, 117, 118]. For small argument,  $x := E/M_{sph} \ll 1$ , it has been calculated that

$$F_{HG}(x) = 1 - \frac{9}{8}x^{4/3} + \frac{9}{16}x^{6/3} + O(x^{8/3}), \quad (2.4)$$

as reviewed in Ref. [96]. This goes to zero when the argument is  $O(1)$ , leading to the suggestion that there may be no suppression for over-barrier transitions from few

particle collisions. However, at this point the perturbative calculation in  $E/M_{sph}$  is outside its region of validity.

Indeed a full non-perturbative calculation shows that  $F_{HG}(1) \approx 0.7$  and the exponential suppression is still significant at energies of at least  $30M_{sph}$  [97]. This nonperturbative calculation of the rate of B+L violations used a technique (based on a conjecture) introduced by Rubakov, Son and Tinyakov (RST) [119, 115, 120] (see Sec. 2.5) and extended by others [121, 122, 118]. The same technique has made possible calculations of other nonperturbative processes induced by few particle collisions. In particular the induced vacuum decay of scalar field theories [103, 99] and kink pair production [98, 100, 102]. It has also been explored in studies of low dimensional quantum mechanical systems [117]. In all these studies the rate has been found to be exponentially suppressed at and immediately above the barrier energy.

In fact, in some models it has been shown that the exponential suppression persists up to arbitrarily high energies. This suppression is determined by a limit of the RST method, for which the instanton lives on the real time axis [99, 101]. This real-time instanton describes the formation of the sphaleron from the few particle collision. One can intuitively understand the suppression by considering the improbability of the time-reversed process: the annihilation of a pair of 't Hooft-Polyakov monopoles, a coherent state of  $O(1/\alpha)$  particles, into a very small number of particles, each with very high energies,  $O(M/\alpha)$ .

### 2.2.2 Magnetic monopole pair creation

For magnetic monopole pair production from few particle collisions the corresponding nonperturbative calculations have not been done. However, attempts have been made to establish the exponential suppression of the cross section (Eq. (2.1)) from general considerations [123, 104, 65]. For the most part, the arguments can intuitively be understood as stemming from the observation that the initial few particle collision contains a small number of highly localised degrees of freedom whereas a magnetic monopole is a complicated, delocalised object. In particular, the arguments are based on:

- the apparent absence of magnetic monopoles in perturbation theory;
- perturbation theory to large orders;
- constraints from unitarity;
- phase space volume suppression;

- form factor suppression;
- and small wave function overlap.

The first of these arguments was given at the opening of Sec. 2.2. In the following, I outline the other arguments each in turn, most of which are only valid for 't Hooft-Polyakov monopoles.

't Hooft-Polyakov monopoles are semiclassical field configurations made up of a large number,  $O(1/\alpha)$ , of elementary bosons. At each order of perturbation theory, only  $O(1)$  elementary bosons can be produced. As a result, to create a pair of magnetic monopoles requires going to at least the  $O(1/\alpha)$ th order of perturbation theory. Such high order terms in the perturbative expansion contain correspondingly high powers of the coupling constant,  $\alpha$ , which can be expressed as an exponential suppression as in Eq. (2.1). The problem with this argument is that it treats the perturbative expansion too naively. It does not account for the fact that the Dyson perturbative series is only an asymptotic expansion, not a convergent one, and cannot so blithely be extrapolated to orders  $O(1/\alpha)$  [124, 125, 126, 127, 128, 129, 130, 131]. The factorially growing number of diagrams out-competes the powers of  $\alpha$  at such high orders.

Rigorous calculations of large-order perturbation theory have been carried out in various models in four dimensions, though as yet concrete results have relied on various simplifying properties of the theory such as superrenormalisability, supersymmetry [132] or containing only scalars [127, 128]. The assumption is that, although a given perturbative series may not converge, it may nevertheless give a representation of a well-defined function of the coupling,  $g$ , which can be found using summation techniques such as Borel summation. In particular, if the perturbative series is Borel summable, then one can derive uniform bounds on the remainder of the perturbative series at large orders (see for example Refs. [131]). In this way, large order information about the perturbative series of forward elastic scattering amplitudes can be used, via the Optical Theorem (a unitarity relation), to bound the contribution of non-perturbative phenomena, such as monopole pair production. However, in nonsupersymmetric theories containing magnetic monopoles, explicit expressions for the large orders of perturbation theory are not known, so this approach falls short for my purposes.

Another argument for exponential suppression can be given, which also exploits the large numbers of particles making up 't Hooft-Polyakov monopoles, if I assume that there is a fixed probability,  $p$ , for producing an elementary boson. Then the pair production of 't Hooft-Polyakov monopoles would be expected to be exponentially suppressed with coefficient  $c = O(-4\pi \log(p))$  (see Eq. (2.1)). This probabilistic

description however ignores quantum mechanical effects such as bosonic collective enhancement.

A 't Hooft-Polyakov monopole can be described as a coherent state of elementary bosonic fields. When compared to a random configuration of  $O(1/\alpha)$  elementary bosons, a magnetic monopole is very special. Thus, even if there is no suppression for the production of a large number of elementary bosons, one might still expect there to be a suppression of magnetic monopole pair production, essentially due to their comparatively low phase space volume. This is akin to the argument one would give for why, for example,  $Au\bar{A}u$  production is rare, even when there is sufficient energy. As pointed out in Ref. [133] the probability of producing any given classical field configuration is vanishingly small. But the transition need not exactly produce the classical 't Hooft-Polyakov monopole field configuration but only one sufficiently close to it. Thus in order to carry through this argument rigorously, one would need to introduce a suitable measure on the space of field configurations and then integrate over this measure.

The remaining arguments for exponential suppression rely on crossing symmetry, and will be discussed in Sec. 2.3. It is important to note that the physical electric charge, at a given energy scale, is a finite, nonzero number. Thus, even if magnetic monopole pair production is exponentially suppressed, it may still be experimentally observable if the suppression is not too large, i.e. if the coefficient  $c$  (see Eq. (2.1)) is not too large.

It has been argued in Ref. [65] not only that the exponential coefficient of the suppression,  $c$ , is greater than zero but that, for 't Hooft-Polyakov monopoles, it is given by  $c = 4$  for all collision energies. As  $4/\alpha \approx 548 \gg 1$ , this would effectively rule out the production of 't Hooft-Polyakov magnetic monopoles in few particle collisions. Note that this suggestion goes against what has been learned from B+L violation, where the few particle collision provides an exponential enhancement of the cross section. One would thus expect the coefficient  $c$  to be a function of the centre-of-mass energy of the few particle collision, and hence there should exist a Monopole Holy Grail Function,

$$\sigma \sim e^{-\frac{1}{\alpha} F_{MHG}\left(\frac{E}{2m}\right)}. \quad (2.5)$$

As was the case for B+L violation, to this order, the cross section would be expected to be independent of the all details of the initial state except for its centre of mass energy. The rest of this chapter focuses on the possible methods one could use to calculate this function.

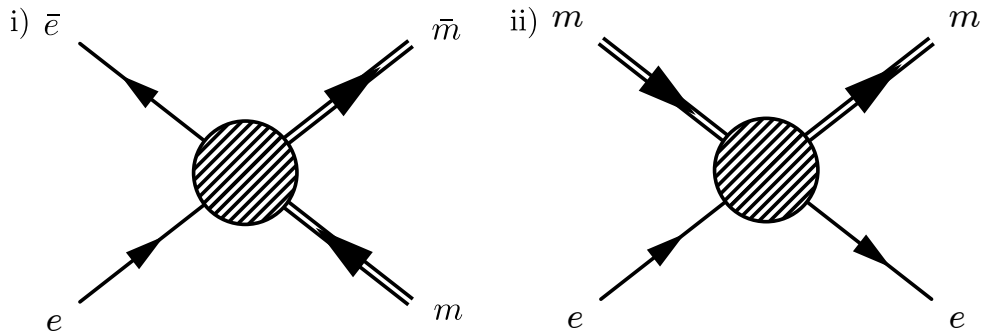


Figure 2.1: Two processes related by crossing symmetry: (i) magnetic monopole pair production from electron-positron annihilation and (ii) electron-magnetic monopole elastic scattering.

### 2.3 Crossing symmetry

Cross symmetry relates the amplitudes for two different processes. The symmetry holds order by order in perturbation theory and has been shown to hold for soliton scattering in the Sine-Gordon theory [134, 135]. An example of two processes related by crossing symmetry is: (a) muon-antimuon pair production from electron-positron annihilation and (b) electron-muon scattering. For my purposes, a more relevant example would be (i) magnetic monopole pair production from electron-positron annihilation and (ii) electron-magnetic monopole scattering (see Fig. 2.1). However, unlike processes (a) and (b), processes (i) and (ii) are not naively crossing symmetric, as pointed out in Refs. [136, 137]. For example, for scalar electric and magnetic particles with charges satisfying  $eg = 2\pi$ , the amplitude for process (ii) contains an extra spin, the angular momentum of the electromagnetic field, which is not present in process (i). Hence, the two amplitudes will transform differently under Lorentz transformations and the usual crossing relations must fail. Despite this, in this section I will assume that some suitable generalisation of crossing symmetry is obeyed by the amplitudes for processes (i) and (ii), and that the subtleties can be “factored out”.<sup>1</sup> These processes can be written as,

$$\begin{aligned} \text{(i)} \quad & e(p_1) + \bar{e}(p_2) \rightarrow \bar{m}(p_3) + m(p_4), \\ \text{(ii)} \quad & e(q_1) + m(q_2) \rightarrow e(q_3) + m(q_4), \end{aligned}$$

where here  $e$  denotes electron,  $m$  denotes magnetic monopole and the  $ps$  and  $qs$  are the momenta. Other processes involving quarks, say, instead of electrons could

<sup>1</sup>Alternatively one could replace the electrons and positrons with electrically neutral particles for which this issue would not arise.

equally well have been considered. Note that here I consider specific, exclusive processes, whereas the Monopole Holy Grail Function (Eq. (2.5)) is defined in terms of the inclusive cross section for magnetic monopole creation.

I adopt the standard nomenclature based on the Mandelstam variables [138, 139],

$$\begin{aligned} s_p &:= (p_1 + p_2)^2, & t_p &:= (p_1 - p_3)^2, & u_p &:= (p_1 - p_4)^2, \\ s_p + t_p + u_p &= 2m^2 + 2M^2, \end{aligned} \quad (2.6)$$

where here  $m$  is the monopole mass and  $M$  is the electron mass. I define Mandelstam variables,  $\{s_q, t_q, u_q\}$ , for the process (ii) analogously.

Crossing symmetry relates the amplitudes for the two channels thuswise,

$$\mathcal{A}_{(i)}(p_1, p_2, p_3, p_4) = \mathcal{A}_{(ii)}(q_1 = p_1, q_2 = -p_3, q_3 = -p_2, q_4 = p_4), \quad (2.7)$$

where I have defined the amplitude as the matrix element of the  $\hat{T}$  matrix, related to the  $\hat{S}$  matrix by  $\hat{S} = \mathbf{1} + i\hat{T}$ . To write this relation somewhat more simply, I factor off the momentum-conserving delta function,

$$\mathcal{A}_{(i)}(p_1, p_2, p_3, p_4) = (2\pi)^4 \delta^{(4)}(p_1 + p_2 - p_3 - p_4) \mathcal{F}(s_p, t_p). \quad (2.8)$$

The same function,  $\mathcal{F}$ , determines the amplitude for the process (ii) but with  $\{s_p, t_p, u_p\}$  switched with  $\{t_q, s_q, u_q\}$ ,

$$\mathcal{A}_{(ii)}(q_1, q_2, q_3, q_4) = (2\pi)^4 \delta^{(4)}(q_1 + q_2 - q_3 - q_4) \mathcal{F}(t_q, s_q). \quad (2.9)$$

In order to exceed the kinematic threshold for magnetic monopole pair production, it must be that  $s_q = t_p \geq 4m^2$ . There is also a condition on the Mandelstam variables which is required for the scattering angles to be real [138, 140].

The usefulness of crossing symmetry is that, though it may not be possible to directly calculate the amplitude for process (i), one might instead calculate the amplitude for process (ii) then find that for process (i) by crossing. In the following I discuss the prospects of carrying out this calculation.

For Dirac monopoles, the amplitude for the elastic scattering process, (ii), has been calculated in two different kinematic regimes: at zero monopole velocity [141, 142] and in the high energy, eikonal approximation [143, 144]. The amplitude at zero monopole velocity cannot be crossed to the pair production process as the approximation requires that the monopole mass,  $m$ , be much larger than all other energy scales. The amplitude for charged particle-magnetic monopole scattering in

the eikonal approximation is

$$\mathcal{F}(t_q, s_q) \approx 2eg \frac{s_q}{t_q} e^{i\chi}, \quad (2.10)$$

where  $t_q < 0$  is required for the scattering angles be real [138, 140] and  $-t_q, m, M \ll s_q$  is required for the approximation to be valid. The phase factor,  $\chi$ , is gauge dependent and cancels out in the cross section. The cross section is thus

$$\frac{d\sigma_{(ii)}}{dt_q} \approx \frac{(eg)^2}{4\pi t_q^2}. \quad (2.11)$$

Crossing Eq. (2.10) gives

$$\mathcal{F}(s_p, t_p) \approx 2eg \frac{t_p}{s_p} e^{i\chi'}, \quad (2.12)$$

where again the phase factor,  $\chi'$ , will cancel out in the cross section. Now we require  $s_p > 4m^2$  for the amplitude to be above threshold and  $s_p, m, M \ll |t_p|$  for the eikonal approximation to be valid. However in this case the scattering angles are complex and hence unphysical. A necessary and sufficient condition for the scattering angles to be real in process (i) is [140]

$$s_p t_p u_p > s_p (m^2 - M^2)^2. \quad (2.13)$$

Now if  $t_p \gg s_p$  then  $t_p \approx -u_p$  and the left hand side is negative and the inequality cannot hold. Thus Eq. (2.10) can not be crossed to give any information about monopole pair production.

For 't Hooft-Polyakov monopoles, the amplitude for the elastic scattering process, (ii), has been calculated for small monopole velocities. The standard approach, as with other solitons, is to perform a semiclassical expansion of the fields about the classical solution. This can be done in a canonical or path integral framework [145, 146, 23, 147, 148, 54, 55, 56, 149, 150, 151]. In the canonical framework the expansion takes the form,

$$\hat{\varphi}^a(x) = \varphi_{cl}^a(x) + \hat{\phi}^a(x), \quad (2.14)$$

where  $\hat{\varphi}^a(x)$  denotes all the fields in the theory, as  $a$  runs over an appropriate range. The c-number functions  $\varphi_{cl}^a(x)$  are the classical soliton field configuration and the operators  $\hat{\phi}^a(x)$  are the fluctuations about it. An expansion in powers of the fluctuations amounts to an expansion in the small, electric coupling constant. To leading order, the results of this expansion are simply the classical results. This



expansion has been used to calculate the magnetic monopole mass to next-to-leading order [152, 153].

For small monopole velocities and to leading order in the semiclassical expansion, the amplitude of process (ii) is determined by the form factor of some relevant intermediate operator, such as the photon field operator,

$$\begin{aligned} \langle \mathbf{q}_4 | \hat{F}^{\mu\nu}(\mathbf{x}) | \mathbf{q}_2 \rangle &\approx \langle \mathbf{q}_4 | F_{cl}^{\mu\nu}(\mathbf{x}) | \mathbf{q}_2 \rangle, \\ &\approx \sqrt{4q_2^0 q_2'^0} \int d^3 X e^{i(\mathbf{q}_4 - \mathbf{q}_2) \cdot \mathbf{X}} F_{cl}^{\mu\nu}(\mathbf{x} - \mathbf{X}), \end{aligned} \quad (2.15)$$

where  $|\mathbf{q}\rangle$  denotes a magnetic monopole state with spatial momentum  $\mathbf{q}$  and I have normalised the states following the convention of Peskin and Schröder [154]. The field  $\hat{F}^{\mu\nu}(\mathbf{x})$  is the photon field, given by, for example, the Abelian projection in Ref. [22]. I have expanded the photon field as in Eq. (2.14) in the first line.

From Eq. (2.15), one can calculate the amplitude for process (ii) only when the monopole velocities are small, or when  $t_q \ll m^2$ . Upon crossing  $t_q \rightarrow s_p$  and hence the approximation of small monopole velocities ensures that one cannot use the result to deduce anything about magnetic monopole pair production above threshold,  $s_p > 4m^2$ . It might be hoped that the non-relativistic result can be uniquely extended to the full relativistic one. If for example, I were to simply make the replacement  $\mathbf{p} \cdot \mathbf{x} \rightarrow -p \cdot x$ , then from the photon form factor one would find that magnetic monopole pair production is *not* exponentially suppressed as in Eq. (2.1). Had I chosen, instead of the photon field in Eq. (2.15), a massive vector or scalar boson field, the same replacement  $\mathbf{p} \cdot \mathbf{x} \rightarrow -p \cdot x$  would result in an amplitude which *is* exponentially suppressed as in Eq. (2.1) [155]. However, in either case, this simple replacement is not unique. One can construct an infinite number of different functions of the Lorentz invariants which reduce to the same the non-relativistic limit.

A more sophisticated semiclassical calculation of amplitudes of processes analogous to (ii) was carried out by Papageorgakis and Royston [156] for a wide class of scalar theories with solitons. Importantly the approximation of small soliton velocities was relaxed. They did however make the simplifying assumption, following Ref. [33], that the scattering process does not significantly deform the solitons (in directions which are not zero-modes). Intuitively, this means that the process considered is an exclusive one, for the scattering of solitons in their ground state, however the correctness of the assumption has not been demonstrated (see, for comparison, Ref.

[157]). After crossing symmetry they find

$$|\mathcal{F}(s_p, t_p)| \leq e^{-\frac{2R_S}{R_C} \sqrt{\frac{t_p}{t_p - 4M_{\text{cl}}^2}}}, \quad (2.16)$$

where  $M_{\text{cl}}$  is the classical mass of the soliton,  $R_C = 1/M_{\text{cl}}$  is its Compton wavelength and  $R_S$  is the soliton size. The ratio  $\frac{R_S}{R_C}$  is parametrically large for kinks at weak coupling as well as for magnetic monopoles, for which it is  $O(1/\alpha)$ . However, as it stands, this is not the end of the story as the inclusive cross section for soliton pair production will be larger and may be unsuppressed. The calculation of the inclusive process requires including soliton excited states and the production of extra perturbative particles. Further, for application to solitonic magnetic monopoles one must include radiation effects.

The question arises as to whether one can go beyond the semiclassical approximation to the calculation of the amplitude for process (ii). The Euclidean amplitude can be calculated on the lattice by using twisted boundary conditions [158, 159]. An analytic continuation is required to relate this to the amplitude for process (i) in Minkowski space. Attempts have been made at this general problem, with some success, though errors due to the analytic continuation are difficult to quantify [160, 161, 162].

The appearance of the ratio,  $\frac{R_S}{R_C}$ , in the exponent of Eq. (2.16) might lead one to think that no such exponential suppression would occur for a Dirac monopole, which has a pointlike magnetic charge. However, Goebel has argued that photon-magnetic monopole interactions are effectively delocalised on the scale of the classical radius, or Thompson scattering length, of the monopole,  $r_{cl} = g^2/(4\pi m)$  [123]. The scattering length,  $f(E)$ , for a photon of energy  $E$  on a magnetic monopole can be calculated exactly at zero energy [163, 164]. It is given by

$$f(0) = -\frac{g^2}{4\pi m} = -r_{cl}. \quad (2.17)$$

Combining this result with the Kramers-Krönig Relations [165, 166, 167] and the Optical Theorem, one can derive a generalisation of the Thomas-Reich-Kuhn sum rule [168, 123]. From this Goebel argues that the magnetic charge of an elementary monopole should be delocalised over a region of the size of the classical radius. If this is indeed the case, then  $\frac{R_S}{R_C} = O(1/\alpha)$  for both Dirac and 't Hooft-Polyakov monopoles.

## 2.4 Landau method

The calculation of the amplitude for monopole-electron scattering, process (ii), for a large monopole velocity change would give the amplitude for monopole pair production after crossing. As a warm up, I consider the overlap of the in and out states. I assume that a magnetic monopole can be effectively described by a large number,  $O(1/\alpha)$ , of weakly coupled particles. I may then express its wave function in a Fock space representation of these weakly coupled particles and the interactions between particles should be analysable in a mean field approximation. Due to the difference in speeds of the in and out monopoles, the constituent particles will be in different states in the two monopoles. Hence the overlap of their states will be less than 1. The overlap of the two monopole states is essentially equal to the product of the overlaps of the  $O(1/\alpha)$  states of the constituent particles. Hence its magnitude is exponentially suppressed as in Eq. (2.1). The two states are thus called *strongly different*.

Now, rather than simply the overlap of the two states, I wish to calculate the scattering amplitude for process (ii). This is determined by the matrix element,

$$\langle \mathbf{q}_4 | \hat{F}^{\mu\nu}(\mathbf{x}) | \mathbf{q}_1 \rangle, \quad (2.18)$$

for  $|\mathbf{q}_4 - \mathbf{q}_1| = O(m)$ . If the particles making up the monopoles are sufficiently weakly coupled then the operator inside the matrix element will not affect the above argument and the matrix element will be exponentially suppressed as in Eq. (2.1). However, given that  $\alpha$  is not infinitesimal but finite, the interactions between the many weakly coupled particles may invalidate this argument. Further, it is crucially important to know the coefficient,  $c$ , in the exponential suppression, as it may be small.

An analogous problem arises in one-dimensional quantum mechanics, the calculation of the matrix element of some operator between two *strongly different* states, i.e. states with exponentially suppressed overlap. A general, semiclassical solution to this problem has been proposed by Landau in Refs. [169, 170, 171, 172].

Consider initial and final states with significantly different energies,  $E_1$  and  $E_2$  respectively. One expresses the wave functions of the states in terms of their semiclassical approximations in the coordinate basis. Then, one separates the terms in these wave functions according to their exponential behaviour on the argument,  $q$ . One can then analytically continue the argument of the wave functions into various regions of the complex plane such that each term is exponentially small. To find

the transition amplitude, one uses the saddle point approximation. This amounts to finding a path obeying the equations of motion from the initial state to a complex, or singular transition point,  $q_*$ , and then on to the final state. The transition state is necessarily complex or singular because the in and out states have different energies and hence there is no real, non-singular path satisfying the equations of motion which can join them. The Landau formula for the matrix element is

$$\langle \psi_2 | \hat{f} | \psi_1 \rangle \sim \exp \left\{ -Im \left[ \int_{q_1}^{q_*} p(q; E_1) dq + \int_{q_*}^{q_2} p(q; E_2) dq \right] \right\}, \quad (2.19)$$

where  $p(q, E_1)$  is the classical expression for the momentum as a function of the total energy and coordinate,  $q$ ;  $q_1$  is any classically allowed point of the system with energy  $E_1$  and  $q_2$  is the same for energy  $E_2$ . The transition point,  $q_*$ , is a (complex and singular) stationary point of the exponent. If there is more than one stationary point,  $q_*$  is chosen such that the exponent in Eq. (2.19) is negative and the smallest in magnitude. It is interesting to note that the result does not depend on the details of the operator, to this order. Its presence simply provides the energy to transition between the states.

This technique has been extended to field theoretic contexts in Refs. [173, 174, 175, 176, 177, 178, 179, 180, 181, 182]. However a rigorous and quantitative calculation using the Landau method requires a careful analysis of WKB estimates of the wave function in different regions of the complex plane, in particular of the Stokes and anti-Stokes lines of these solutions. This has been carried out for the quantum mechanical quartic oscillator in Ref. [183]. For field theories the Landau technique has primarily been used either when the theory admits an effective description in terms of one degree of freedom or to extract qualitative behaviours of amplitudes.

In Ref. [177], Voloshin used the Landau formula, Eq. (2.19), to calculate the rate of vacuum bubble nucleation induced by a virtual, high energy particle. In the thin wall limit, the dynamics of the bubbles can be effectively described in terms of a single degree of freedom, the radial size of the bubble. This enabled Voloshin to directly apply the Landau formula to this field theoretic problem. One starts from the relativistic Hamiltonian,  $\mathcal{H}$ , for the bubble radius  $r$ ,

$$(\mathcal{H} + \eta r^3)^2 - \mathbf{P}^2 = (\mu r^2)^2, \quad (2.20)$$

where  $\eta$  is proportional to the energy difference between the two vacua,  $\mathbf{P}$  is the spatial momentum of the bubble walls and  $\mu$  is proportional to the surface energy of the bubble.

The Landau formula can then be applied to the matrix element

$$|\langle B(E)|\phi(E)|0\rangle| \sim \exp \left\{ -Im \left[ \int_0^{r^*} \sqrt{(\mu r^2)^2 - (\eta r^3)^2} dr + \int_{r^*}^{r(E)} \sqrt{(\mu r^2)^2 - (\eta r^3 + E)^2} dr \right] \right\}, \quad (2.21)$$

where  $|B(E)\rangle$  refers to the state with a bubble in it, with energy  $E$ ;  $\phi(E)$  is the field operator which creates a virtual particle with energy  $E$ ;  $r(E)$  is the classical turning point for a state with energy  $E$  and  $r^*$  is the transition point. This matrix element gives the required induced bubble nucleation rate, which is found to be exponentially suppressed with exponent  $O(\mu^4/\eta^3)$  for all energies.

A key step in the above is finding the transition point,  $r^*$ . Demanding equation (2.21) is stationary with respect to  $r^*$  gives

$$\sqrt{(\mu r^{*2})^2 - (\eta r^{*3})^2} - \sqrt{(\mu r^{*2})^2 - (\eta r^{*3} + E)^2} = 0, \quad (2.22)$$

which has solutions given by the cubic root,  $(-E/(2\eta))^{1/3}$ . One must choose the solution such that the exponent in Eq. (2.21) is negative and the smallest in magnitude.

To apply this method to the calculation of the matrix element, Eq. (2.18), or to that of the crossed process, I need first the relativistic Hamiltonian for the system. But, due to the finiteness of the speed of light and to the long range of electromagnetic forces, no such local Hamiltonian exists which depends solely on the degrees of freedom of the charged particles (whether electric or magnetic). It has long been known that for small particle velocities,  $v \ll 1$ , one can write down an approximate Hamiltonian, accurate to  $O(v^2)$  [184, 185]. Beyond this order, radiation effects appear which are essentially non-local in character. Alternatively, one can write down a local Hamiltonian in the *test particle* approximation, when the field due to the charged particles is negligible. This is essentially a weak coupling approximation and hence is not expected to be applicable to magnetic monopoles. Nevertheless, for illustration I discuss such an approach in App. A.1 and show a simple tunnelling calculation in the presence of an external field.

I do not pursue the Landau method further. Instead, I consider a powerful field-theoretic method developed by Rubakov, Son, Tinyakov and others, many of whom had actively worked on applying the Landau method to field theory.

## 2.5 Rubakov-Son-Tinyakov method

The method of Rubakov, Son and Tinyakov (RST) [119, 115, 120] was designed in order to calculate the cross section for  $(B + L)$  violation due to high energy, few particle collisions, eventually achieved in Ref. [97]. As mentioned in Sec. 2.2.1, it is a general method for the calculation of the cross section, or rate, of instanton processes induced by few particle collisions. It was adapted to calculate the pair production of solitons in Refs. [98, 100, 102, 101].

I denote the small semiclassical parameter by  $\alpha$  and assume that the action,  $S[\phi^a; \alpha]$ , depending on fields,  $\phi^a$ , satisfies the property

$$S[\phi^a; \alpha] = \frac{1}{\alpha} S[\alpha^{\sigma_a} \phi^a; 1], \quad (2.23)$$

for some set of numbers  $\sigma_a$ . In particular, many bosonic actions in four dimensions satisfy this property, such as renormalisable scalar theories; renormalisable Abelian and non-Abelian gauge theories and coupled combinations thereof. This includes theories containing composite monopoles such as the Georgi-Glashow theory [26] and the bosonic sector of the electroweak theory, which is relevant for  $(B + L)$  violation.

For  $(B+L)$  violation at energies low compared with the sphaleron energy,  $M_{sph}$ , corrections to the zero energy cross section can be calculated perturbatively. The leading order corrections exponentiate and the naively extrapolated cross section appears to be unsuppressed at energies of the order of  $M_{sph}$  [112, 113]. Higher order corrections however are significant at this point. They can be naturally divided into three groups: soft-soft, hard-soft and hard-hard [116, 96]. The soft-soft corrections are due to the final state. They are determined by tree-level diagrams about the zero energy instanton, and their contribution can be calculated with semiclassical methods [186, 187]. On the other hand, the hard-soft and hard-hard corrections depend on the initial state and are determined by loop diagrams about the zero energy instanton. Despite this, their contribution to the cross section has been argued to exponentiate [188, 189, 190, 191]. Hence, as noted in Sec. 2.2.1, the cross section takes the form

$$\sigma_E \sim e^{-\frac{4\pi}{\alpha} F_{HG} \left( \frac{E}{M_{sph}} \right)}.$$

This exponential form suggests a semiclassical procedure for the calculation of  $F_{HG}$ , however the presence of loop diagrams means that the usual semiclassical approach fails. This is because the initial state is far from semiclassical: it contains a small

number of particles (such as two), with a high energy.

The key step in the RST method is to replace the few particle initial state with a sufficiently similar semiclassical state. One requires that the overlap between the true initial state and the replacement state is not exponentially small in the semiclassical parameter. Then, the rate can be calculated semiclassically to exponential accuracy (i.e. the logarithm can be calculated to leading order) in the small semiclassical parameter, the result being independent of all details of the initial state other than its energy. For a true initial state with particle number  $O(1)$ , it has been argued that a valid such replacement state is one with the same energy and with number of particles,  $N$ , satisfying  $1 \ll N \ll 1/\alpha$  [114, 115, 116, 117, 118]. Though this state is not itself semiclassical, it may be described as the limit of a set of semiclassical states.

For a state to be semiclassical, it must have a parametrically large energy,  $E = \epsilon/\alpha$ , and particle number,  $N = \nu/\alpha$ , where  $\epsilon$  and  $\nu$  are independent of  $\alpha$ . To leading order, the semiclassical approximation is given by the double-scaling limit:

$$\begin{aligned} \alpha &\rightarrow 0, \\ E, N &\rightarrow \infty, \\ \epsilon, \nu &= \text{const.} \end{aligned} \tag{2.24}$$

In the approach to this limit, the cross section for instanton transitions from a semiclassical state with energy  $E$  and particle number  $N$  takes the form

$$\sigma(E, N) \sim e^{-\frac{4\pi}{\alpha} F(\epsilon, \nu)}. \tag{2.25}$$

The RST method starts with the semiclassical calculation of this function,  $F(\epsilon, \nu)$ . The Holy Grail function is then argued to be given by the limit,

$$\lim_{\nu \rightarrow 0} F(\epsilon, \nu) = F_{HG} \left( \frac{E}{M_{sph}} \right). \tag{2.26}$$

Singular behaviour of the  $\nu \rightarrow 0$  limit could mar this.

In practice, rather than considering a particular initial state, for which extraneous details would complicate the calculation, it is preferable to sum over all states with a given energy and particle number. One defines the following cross section,

$$\sigma(E, N) := \sum_{i, f} |\langle f | \hat{S} \hat{P}_n \hat{P}_E | i \rangle|^2, \tag{2.27}$$

where  $|i\rangle$  and  $|f\rangle$  are the initial and final states respectively and  $\hat{P}_n$  and  $\hat{P}_E$  are projection operators onto the space of states with particle number  $N$  and energy  $E$  respectively. For  $(B + L)$  violation, one sums over all initial states in the trivial vacuum sector and all final states in the one-instanton sector. Note that the cross section calculated in this way should be larger than the desired cross section,  $\sigma_E$ ,

$$F(\epsilon, \nu) < F_{HG} \left( \frac{E}{M_{sph}} \right). \quad (2.28)$$

This is because the semiclassical approximation to  $\sigma(E, N)$  is dominated by the field configuration giving the most probable instanton transition for given energy,  $E$ , and particle number,  $N$ . Further, the sum over field configurations includes those consisting of a few particle collision and a large number of spectator particles, and hence includes the field configuration dominating  $\sigma_E$  as a special case.

For definiteness, and for simplicity, I consider a real scalar field theory with action

$$S[\phi; \alpha] = \frac{1}{\alpha} S[\sqrt{\alpha}\phi; 1]. \quad (2.29)$$

Within the path integral, one can then change variables to integrating over  $\varphi := \sqrt{\alpha}\phi$  and relabel  $\varphi \rightarrow \phi$ .

To express Eq. (2.27) less formally it is convenient to adopt the coherent state representation outlined in App. A.2. The coherent state path integral is well suited to describe initial and final boundary conditions. The projection operators also take a simple form. The discussion here follows Refs. [115, 119, 120] closely. In the coherent state representation, Eq. (2.27) becomes

$$\sigma(E, N) = \int d\eta d\xi e^{-iN\eta - iE\xi + W(\eta, \xi)}, \quad (2.30)$$

where  $W$  has the path integral representation

$$e^W := \int \mathcal{D}a_{\mathbf{p}}^* \mathcal{D}a_{\mathbf{p}} \mathcal{D}b_{\mathbf{p}}^* \mathcal{D}b_{\mathbf{p}} \mathcal{D}\phi \mathcal{D}\phi' e^Q, \quad (2.31)$$

in terms of  $Q$ , which has the form

$$Q := - \int \mathbf{d}\mathbf{p} a_{\mathbf{p}} a_{\mathbf{p}}^* e^{-i\eta - i\omega_{\mathbf{p}}\xi} - \int \mathbf{d}\mathbf{p} b_{\mathbf{p}} b_{\mathbf{p}}^* \\ + B_i(a, \phi_i) + B_f(b^*, \phi_f) + B_i^*(a^*, \phi_i) + B_f^*(b, \phi_f) + iS[\phi; \alpha] - iS[\phi'; \alpha], \quad (2.32)$$

where the  $B_{i/f}$  are boundary terms defined in App. A.2. In Eqs. (2.30), (2.31) and (2.32), the integrations over  $a_{\mathbf{p}}$ ,  $a_{\mathbf{p}}^*$ ,  $b_{\mathbf{p}}$  and  $b_{\mathbf{p}}^*$  are Gaussian and hence can be carried



out exactly, resulting in

$$\begin{aligned}
e^W &= \int \mathcal{D}\phi \mathcal{D}\phi' \left( \prod_{\mathbf{p}} \delta(\tilde{\phi}_f(\mathbf{p}) - \tilde{\phi}'_f(\mathbf{p})) \right) \\
&\exp \left\{ -\frac{1}{2} \int \tilde{\mathbf{d}}\mathbf{p} \frac{\omega_{\mathbf{p}}}{1 - \gamma_{\mathbf{p}}^2} \left[ (1 + \gamma_{\mathbf{p}}^2) [\tilde{\phi}_i(\mathbf{p})\tilde{\phi}_i(-\mathbf{p}) + \tilde{\phi}'_i(\mathbf{p})\tilde{\phi}'_i(-\mathbf{p})] \right. \right. \\
&\quad \left. \left. - 4\gamma_{\mathbf{p}} \tilde{\phi}_i(\mathbf{p})\tilde{\phi}'_i(-\mathbf{p}) \right] + iS[\phi; \alpha] - iS[\phi'; \alpha] \right\}, \tag{2.33}
\end{aligned}$$

where I have defined

$$\gamma_{\mathbf{p}} := e^{i\eta + i\omega_{\mathbf{p}}\xi}. \tag{2.34}$$

Now using the scalings of Eq. (2.24) and (2.29) results in the whole exponent of the integrand of Eq. (2.30) being proportional to  $1/\alpha$ . This is key and, for  $\alpha \ll 1$ , the exponent is consequently large, allowing one to evaluate the path integral in the stationary phase, or semiclassical, approximation. Evaluating the path integral in this approximation requires finding the relevant stationary point of the exponent, which amounts to solving the classical equations of motion,

$$\begin{aligned}
\frac{\delta S[\phi, 1]}{\delta \phi(x)} &= 0, \\
\frac{\delta S[\phi', 1]}{\delta \phi'(x)} &= 0, \tag{2.35}
\end{aligned}$$

with boundary conditions,

$$\begin{aligned}
i\dot{\tilde{\phi}}_i(\mathbf{p}) + \omega_{\mathbf{p}}\tilde{\phi}_i(\mathbf{p}) &= \gamma_{\mathbf{p}} \left[ i\dot{\tilde{\phi}}'_i(\mathbf{p}) + \omega_{\mathbf{p}}\tilde{\phi}'_i(\mathbf{p}) \right], \\
-i\dot{\tilde{\phi}}_i(\mathbf{p}) + \omega_{\mathbf{p}}\tilde{\phi}_i(\mathbf{p}) &= \frac{1}{\gamma_{\mathbf{p}}} \left[ -i\dot{\tilde{\phi}}'_i(\mathbf{p}) + \omega_{\mathbf{p}}\tilde{\phi}'_i(\mathbf{p}) \right], \\
\phi(T_f, \mathbf{x}) &= \phi(T_f, \mathbf{x}), \\
\dot{\phi}(T_f, \mathbf{x}) &= \dot{\phi}(T_f, \mathbf{x}). \tag{2.36}
\end{aligned}$$

There are also the saddle point equations for the integrations over  $\eta$  and  $\xi$  in Eq. (2.30). They amount to

$$\begin{aligned}
\epsilon &= \int \tilde{\mathbf{d}}\mathbf{p} \frac{2\omega_{\mathbf{p}}^2\gamma_{\mathbf{p}}}{(1 - \gamma_{\mathbf{p}}^2)^2} [\phi_i(\mathbf{p}) - \gamma_{\mathbf{p}}\phi'_i(\mathbf{p})] [\phi'_i(-\mathbf{p}) - \gamma_{\mathbf{p}}\phi_i(-\mathbf{p})], \\
\nu &= \int \tilde{\mathbf{d}}\mathbf{p} \frac{2\omega_{\mathbf{p}}\gamma_{\mathbf{p}}}{(1 - \gamma_{\mathbf{p}}^2)^2} [\phi_i(\mathbf{p}) - \gamma_{\mathbf{p}}\phi'_i(\mathbf{p})] [\phi'_i(-\mathbf{p}) - \gamma_{\mathbf{p}}\phi_i(-\mathbf{p})]. \tag{2.37}
\end{aligned}$$

The equations can be simplified somewhat. First, I note that the boundary condi-

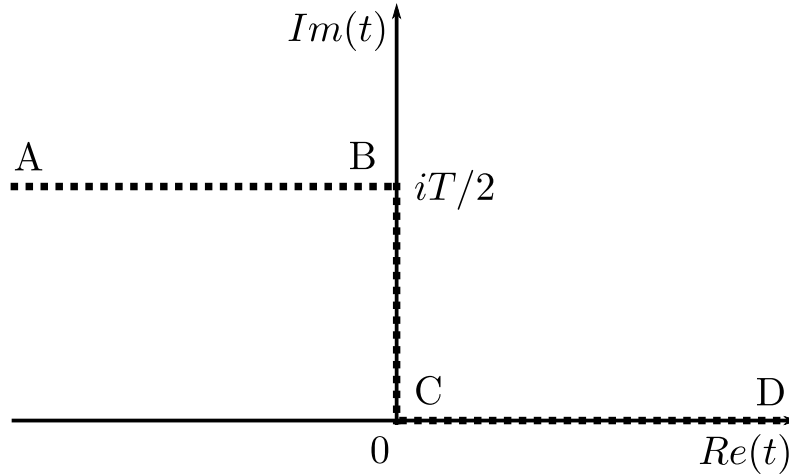


Figure 2.2: Complex time path of RST method, shown as dotted line. The initial and final times, A and D respectively, are to be understood as having asymptotically large real parts.

tions at  $t = T_f$  imply that  $\phi(x) = \phi'(x)$  everywhere, hence there is only one field to solve for. Next, any real part of the parameter  $\xi$  can be set to zero by using time translation invariance. Hence I may take  $T := \xi/i$ , with  $T$  purely real. Likewise, I define  $\theta := \eta/i$ . Based on perturbation theory at  $\epsilon \ll 1$ , it is expected that  $\theta$  can also be taken purely real [115, 120].

Explicit dependence on  $T$  can be removed by deforming the time path into the complex plane as in Fig. 2.2. This may seem baroque but is important for the numerical solution of the equations of motion as it bypasses exponentially small and large quantities.

The final simplification of Eqs. (2.36) and (2.37) can be achieved by expressing the field in terms of its positive and negative frequency modes,

$$\phi(x) = \int \frac{d\mathbf{p}}{\sqrt{2E_{\mathbf{p}}}} (f_{\mathbf{p}} e^{-ip \cdot x} + g_{\mathbf{p}}^\dagger e^{ip \cdot x}). \quad (2.38)$$

As a result, the simplified boundary value problem is

$$\begin{aligned} \frac{\delta S[\phi, 1]}{\delta \phi(x)} &= 0, \\ \text{Im} \phi(T_f, \mathbf{x}) &= \text{Im} \dot{\phi}(T_f, \mathbf{x}) = 0, \\ f_{\mathbf{p}} &= \gamma g_{\mathbf{p}}, \end{aligned} \quad (2.39)$$

where  $f_{\mathbf{p}}$  and  $g_{\mathbf{p}}$  are the frequency components at the initial time A in Fig. 2.2. I have also defined  $\gamma := e^{-\theta}$ . The boundary conditions are to be applied asymptotically, as  $T_i - iT/2 \rightarrow -\infty$  and  $T_f \rightarrow +\infty$ . The energy and particle number of the

solution are now,

$$\begin{aligned}\epsilon &= \int \bar{d}\mathbf{p} \omega_{\mathbf{p}} f_{\mathbf{p}} g_{\mathbf{p}}^*, \\ \nu &= \int \bar{d}\mathbf{p} f_{\mathbf{p}} g_{\mathbf{p}}^*.\end{aligned}\tag{2.40}$$

After solution of the boundary value problem, evaluation of the exponent of Eq. (2.30) on-shell gives the exponential suppression,

$$\begin{aligned}\sigma(E, N) &\sim \exp \left\{ -\frac{1}{\alpha} F(\epsilon, \nu) \right\}, \\ F(\epsilon, \nu) &= -\nu\theta - \epsilon T - 2\text{Re}(iS[\phi, 1]) \\ &\quad + \frac{1-\gamma}{1+\gamma} \int \bar{d}\mathbf{p} \omega_{\mathbf{p}} \text{Re}\phi_i(\mathbf{p}) \text{Re}\phi_i(-\mathbf{p}) \\ &\quad - \frac{1+\gamma}{1-\gamma} \int \bar{d}\mathbf{p} \omega_{\mathbf{p}} \text{Im}\phi_i(\mathbf{p}) \text{Im}\phi_i(-\mathbf{p}).\end{aligned}\tag{2.41}$$

The boundary value problem consists of an initial Minkowskian (AB) evolution, followed by a Euclidean (BC) evolution and then another Minkowskian evolution (CD). This can be interpreted as a classical field configuration evolving up until a time, B, when it tunnels, reaching C and then undergoing real time evolution again. For  $\theta \neq 0$  the field is generically complex on the entire time contour (except at  $T_f$ ). As the classical field is real, the existence of an imaginary part shows the quantum mechanical nature of the process.

The solution to the boundary value problem is a saddle point of the exponent. If there exist more than one solution, that with smallest exponential suppression dominates the path integral. As this solution describes tunnelling, the spectrum of fluctuations about the solution is expected, on general grounds, to have a single negative mode, a finite number of zero modes and an infinite tower of positive modes [192].

Eq. (2.39) is a non-linear partial differential equation and boundary value problem, with non-local initial conditions. It is partially hyperbolic and partially elliptic<sup>2</sup>. For these reasons its solution is extremely non-trivial. For some theories, progress has been made in analytically solving the boundary value problem for small  $\epsilon$  (see, e.g. [115, 120, 193]). However, for general  $\epsilon$ , the most promising approaches have been numerical (see, e.g. [194, 103, 97]), for which the problem is well suited. The continuum problem is approximated by a discrete analogue on a finite lattice,

---

<sup>2</sup>For such an equation, the existence of solutions is a subtle matter (Toby Wiseman, private correspondence).

replacing derivatives with finite differences. The resulting discrete problem is a set of non-linear, coupled algebraic equations which can be solved using the Newton-Raphson method. That is, one linearises the problem about an initial guess, solves the linear problem and then uses that solution as input for a second iteration. If the initial guess is good enough, the iterations will converge on the true solution. Apart from on the initial time slice, the second derivative matrix has a sparse structure, for which there are well developed numerical methods [195, 196].

The initial guess is crucial in solving the problem using the Newton-Raphson method. If the solution is known for a particular value of  $\epsilon$  and  $\nu$  (or  $T$  and  $\theta$ ), one can use this known solution as an input guess at nearby points in the  $(\epsilon, \nu)$  plane (or the  $(T, \theta)$  plane). Iterating this procedure, one can step out from the initial known solution to find all solutions which are continuously connected to it. A bifurcation of solutions can thwart this method.

With the solution to the semiclassical problem given by Eq. (2.41), one must investigate the  $\nu \rightarrow 0$  limit. If  $F(\epsilon, \nu)$  has a smooth limit, then the limit is equal to the Holy Grail Function, the exponential suppression of the tunnelling rate from a few particle collision.

### 2.5.1 Soliton pair creation

The RST method, as originally formulated, describes a method to calculate the cross section for semiclassical tunnelling processes induced by a high energy few particle collision. Unfortunately, this does not include magnetic monopole pair production, or any other soliton pair production. This is because there is no potential barrier separating the initial and final states, which one can understand by noting that there is no barrier to monopole-antimonopole annihilation, the reverse process (studied numerically in Ref. [197]).

In this context, a method to convert the process of monopole pair production into a tunnelling problem was introduced in Refs. [100, 102, 101]. One turns on an external magnetic field,  $B$ , in which case the process of monopole pair production can be viewed as the decay of a false vacuum (without magnetic monopoles) into a lower energy state containing a separated monopole pair. This is a tunnelling process, the magnetic analogue of Schwinger pair production [198, 199, 200, 201, 25]. For kinks and other solitons, one can likewise turn on an external field which couples to the topological current of the solitons [202].

The presence of non-zero particle number and energy in the initial state enhances the rate of the Schwinger process, increasingly so at higher multiplicities and

energies. In fact, when the initial energy is above the kinematic threshold,  $E > 2m$ , a finite rate of pair production may survive even as the external magnetic field goes to zero,  $B \rightarrow 0$ . This is therefore the rate of pair production in the absence of the external field. Though the process at  $B = 0$  is not a tunnelling process, that for  $B$  arbitrarily small and non-zero is a tunnelling process and hence the desired result can be obtained by considering the limit  $B \rightarrow 0$ .

This approach was adopted in Refs. [100, 102, 101] to calculate the rate of kink pair production in a particular 1+1 dimensional scalar theory. Their results showed that  $F(\epsilon, \nu)$  decreases with energy, reaches a (positive) minimum at finite energy and stays constant for higher energies. These properties are inherited by the extrapolated Kink Holy Grail function,  $F_{KHG}(E/(2m_k))$  (where  $m_k$  is the kink mass), and hence kink pair production from few particle collisions is exponentially suppressed at all energies. Quantitatively they find,

$$\lim_{\frac{E}{2m_k} \rightarrow \infty} \frac{F_{KHG}\left(\frac{E}{2m_k}\right)}{F_{KHG}(1)} \approx 0.8. \quad (2.42)$$

However, in these papers, a specific non-polynomial scalar potential was chosen in order to avoid a key problem: the presence of long-lived, quasi-periodic nonlinear excitations. Such excitations, dubbed oscillons, were discovered in this context in Refs. [149, 203], for the 1+1 dimensional theory with Lagrangian,

$$\mathcal{L} = \frac{1}{\alpha} \left[ \frac{1}{2} (\partial_\mu \phi)^2 - \frac{1}{4} (\phi^2 - 1)^2 \right]. \quad (2.43)$$

This theory has a  $\mathbb{Z}_2$  symmetry breaking. The perturbative particles about either of the minima have mass  $M = \sqrt{2}$ .

The stability of oscillons has been argued to be due to the approximate conservation of an adiabatic charge [204], in turn related to an approximate  $U(1)$  symmetry, which becomes exact in the nonrelativistic regime [205]. In the theory defined by Eq. (2.43), using a multiple-scale analysis [206], the oscillon solution can be found as a series expansion in  $\gamma = \sqrt{(M/\omega)^2 - 1}$ , where  $\omega$  is their frequency of oscillation. In Ref. [207, 208] it was shown numerically that the lifetime of oscillons in this theory is over  $10^8$  oscillations. Oscillons have also been found in scalar field theories in other dimensions [209, 210, 211]; in the Abelian Higgs model [212, 213, 214]; in an  $SU(2)$  gauge theory [215] and in the electroweak theory [216]. They appear to be an almost generic phenomenon in nonlinear field theories and, crucially, similar long-lived, nonlinear excitations have been discovered in numerical investigations of 't Hooft-Polyakov monopoles [217, 218, 219, 159].

Oscillons pose a serious problem for the RST method. This is because the initial and final boundary conditions are to be applied at asymptotically large times, after all nonlinear excitations have died off. If the boundary conditions are imposed at a time,  $T_i$ , when the nonlinear excitations are still significant, the results will depend sensitively on  $T_i$ . Hence, the time extent of the lattice must be larger than the lifetime of the oscillon, which may require unfeasibly large lattices.

As an exploratory study, before attempting to calculate the Monopole Holy Grail function (Eq. (2.5))<sup>3</sup>, I attempted the simpler calculation of the Kink Holy Grail function for the theory given by Eq. (2.43). The calculation is very similar to that of Refs. [100, 102, 101], which I followed closely. I was chiefly interested in the effect of the oscillons on the calculation.

To measure the presence of nonlinear excitations on a given time slice I compared the total energy,  $\epsilon_{total}$  with the linearised energy,  $\epsilon$ . For the theory given by Eq. (2.43), with  $\varphi = 1 + \phi$ , these are

$$\begin{aligned}\epsilon &= \int d\mathbf{x} \left( \frac{1}{2} \dot{\varphi}^2 + \frac{1}{2} \varphi'^2 + \frac{M^2}{2} \varphi^2 \right), \\ \epsilon_{total} &= \epsilon + \int d\mathbf{x} \left( \varphi^3 + \frac{1}{4} \varphi^4 \right),\end{aligned}\tag{2.44}$$

to zeroth order in the external field. When all nonlinear excitations have died off, these two expressions should agree, so that  $\delta := |\epsilon/\epsilon_{total} - 1| \ll 1$ .

Using the Newton-Raphson method, the key computationally challenging step of the calculation is the solution of the linear matrix equation. The matrix has dimension equal to the number of lattice points (excepting zero modes). Using serial processing, I was limited to lattices of size  $O(10^2) \times O(10^2)$ . Long lived nonlinear excitations were indeed present in my calculations on the AB part of the time contour (see Fig. 2.2). This led to an  $O(1)$  dependence of  $\epsilon$  and  $\nu$  on the initial time,  $T_i$ , when the boundary conditions were applied. Using the maximum feasible lattice size I was able to observe about 30 periods of the nonlinear oscillation, though my measure of nonlinearity,  $\delta$ , was still of  $O(1)$  at  $T_i$ .

A similar problem has been observed in the literature for above threshold calculations using the RST method [121, 122, 118]. In this case the solution to the boundary value problem stays very near the nonlinear sphaleron configuration for long times on the CD part of the time contour (see Fig. 2.2). In this case the

---

<sup>3</sup>Note that, a numerical study of classical monopole pair creation was carried out in Ref. [220].

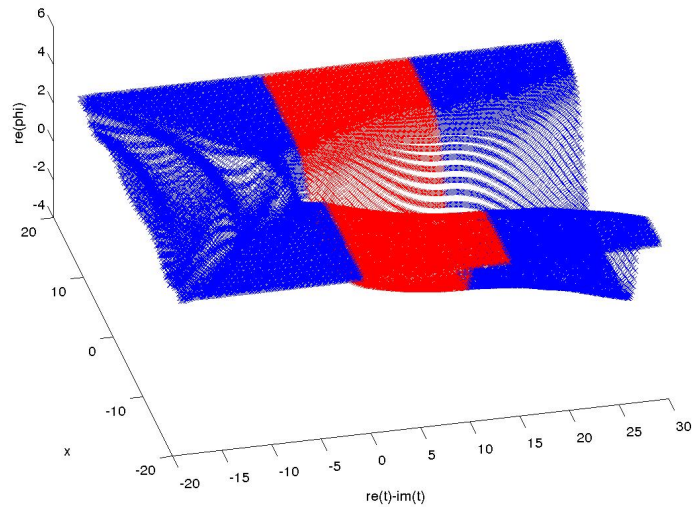


Figure 2.3: Example solution to the lattice RST boundary value problem with Lagrangian given by Eq. (2.43). From left to right: the initial blue region is the evolution of the initial wave packet; the red region corresponds to the tunnelling and the final blue region to the two kinks accelerating apart. However, nonlinear excitations were still present in the initial time slice implying finite size errors of  $O(1)$ .

problem was solved by adding a regulating term to the action,

$$\mathcal{L} \rightarrow \mathcal{L} + i\lambda f(\phi, x), \quad (2.45)$$

where  $f(\phi, x)$  is chosen such that it is only nonzero near the sphaleron configuration, hence causing the long lived sphaleron configuration to decay more quickly, while affecting the dynamics as little as possible. With the addition of the regulating term, one can find a solution to the boundary value problem which is independent of the precise final time. This gives a corresponding suppression exponent,  $F(\epsilon, \nu, \lambda)$ . One then varies the parameter  $\lambda$  and extrapolates to  $\lim_{\lambda \rightarrow 0} F(\epsilon, \nu, \lambda) = F(\epsilon, \nu)$ . A similar approach may be feasible to destabilise the oscillon.

# Chapter 3

## Thermal Schwinger pair creation

In the presence of an electric field, empty space is unstable to the production of electron-positron pairs, called Schwinger pair production [198, 199, 200, 201]. The usual perturbative vacuum is not the true vacuum, the lowest energy state, and hence it decays. At finite temperature, the energy available from the thermal bath enhances the rate of decay.

If there exist magnetic monopoles, by electromagnetic duality, in the presence of a magnetic field empty space would be unstable to the production of magnetic monopole-antimonopole pairs. This is the magnetic dual of Schwinger pair production, as first considered at zero temperature by Affleck, Manton and Alvarez [25, 221]. The key difference to the usual electric Schwinger pair production is the strong coupling of magnetic monopoles.

One can study magnetic monopole Schwinger pair production via its electromagnetic dual if one does not consider electric and magnetic charges simultaneously. In this case the duality amounts simply to a relabelling of electric degrees of freedom and charges as magnetic. I will, in the bulk of the chapter, refer to pair production of particles with charge  $g$  in an external field  $E$ , whether electric or magnetic. The mass of the charged particles is denoted by  $m$ . As my calculation reduces to a semiclassical one, it only relies on the classical electromagnetic duality.

In this chapter I calculate the rate of Schwinger pair production from a thermal bath, making no assumptions about the strength of the coupling. I do though restrict myself to weak external fields. The results are argued to be valid for the full range from zero to infinite coupling [221, 222] (see, however, [223, 224, 225]). They are also independent of many properties of the charged particles, in particular their spin (see Appendix A.3) and whether they are electric or magnetic. For magnetic monopoles, the results are valid for both Dirac and 't Hooft-Polyakov monopoles (see Appendix A.4). This is because, in the physical regime I consider, any structure of the particles



is invisible, as in Refs. [226, 24, 227].

The calculation is also of relevance to Schwinger pair production of atomic nuclei, especially those with charges  $Ze \gtrsim 1$  ( $Z \gtrsim 3$ ) where the usual weak coupling approaches break down, and to pair production of quarks in QCD, in the Abelian dominance approximation [228, 229, 230, 231, 232]. Further it gives an all-orders correction to the known weak coupling results. This will be of interest to current and future experimental studies of Schwinger pair production (see for example [233] for a discussion), as well as to multiloop and asymptotic analyses of the QED perturbation series [223, 224, 225].

In Sec. 3.1 I set up the calculation using the worldline formalism, deriving an expression for the thermal Schwinger rate at arbitrary coupling. In Sec. 3.2 I explain a key approximation that I make, the dilute instanton gas approximation. In Sec. 3.3 I derive analytic results in various limits and in Sec. 3.4 I extend beyond these limits via numerical calculations. I also discuss the general form of the rate in terms of a phase diagram. In Sec. 3.5 I conclude and suggest further work.

## 3.1 Worldline expression

### 3.1.1 Zero temperature rate

Physically, I consider at an initial time a state, such as a thermal state. I choose the state such that, in the absence of an external field, there are no net production or annihilation rates. If I then adiabatically turn on an external field, the initial state becomes unstable to a net production of charged particles. I wish to calculate this rate.

I denote by  $|\Omega\rangle$  the zero temperature state in the absence of the external field, the so-called false vacuum. The probability of the decay of this state is given by

$$P = 1 - |\langle\Omega|\hat{S}|\Omega\rangle|^2 = 1 - e^{-\mathcal{V}\Gamma}, \quad (3.1)$$

where  $\hat{S}$  is the S-matrix including the external field and  $\mathcal{V}$  is the volume of spacetime. As both the false vacuum state and the external field are homogeneous, the quantity of interest is the probability per unit spacetime volume, or the rate per unit volume,  $\Gamma$ . The rate of pair production is given by twice the imaginary part of the energy

density of the initial state.

$$\begin{aligned}\Gamma &= \frac{2}{\mathcal{V}} \text{Im}(-i \log \langle \Omega | \hat{S} | \Omega \rangle) \\ &= 2\text{Im}(\mathcal{E}),\end{aligned}\tag{3.2}$$

where  $\mathcal{E}$  is the energy density of the false vacuum. Note that for this to make sense I should do the calculation in a finite volume and take the volume to infinity at the end.

I can analytically continue Eq. (3.2) to Euclidean time, as the energy density can equally well be calculated in Euclidean time. It then becomes [202]

$$\Gamma = \frac{2}{\mathcal{V}} \text{Im}(-\log \langle \Omega | \hat{S}_E | \Omega \rangle),\tag{3.3}$$

where  $\hat{S}_E$  refers to the ‘‘S-matrix’’ corresponding to Euclidean time evolution. The generalisation of this result to nonzero temperatures can then easily be made. Using the Matsubara formalism, finite temperatures simply correspond to finite Euclidean time extents and periodic boundary conditions [234].

I consider quantum electrodynamics (QED) and scalar quantum electrodynamics (SQED) in 4D flat spacetime. In the worldline formalism these two theories are related, the only difference being the presence of a spin factor in the QED worldline path integral. In Appendix A.3 I show that the spin factor does not turn up in the leading approximation for weak external fields. As I will make this approximation below, I restrict my attention to SQED, the final results also being valid for QED. SQED is the model of a photon,  $A_\mu$ , interacting with a massive charged scalar particle,  $\phi$ , with charge  $g$ . The introduction of the external field,  $A_\mu^{\text{ext}}$ , is achieved by shifting the gauge field,  $A_\mu \rightarrow A_\mu + A_\mu^{\text{ext}}$ , in the covariant derivative of  $\phi$ . The Euclidean Lagrangian is then

$$\mathcal{L}_{\text{SQED}} := \frac{1}{4} F^{\mu\nu} F_{\mu\nu} + D_\mu \phi (D^\mu \phi)^* + m^2 \phi \phi^*,\tag{3.4}$$

where  $F_{\mu\nu} = \partial_\mu A_\nu - \partial_\nu A_\mu$  is the field strength;  $D_\mu = \partial_\mu + igA_\mu^{\text{ext}} + igA_\mu$  is the covariant derivative and  $m$  is the mass of the charged particle. I assume the scalar self-coupling, i.e.  $\lambda(\phi\phi^*)^2/4$ , is sufficiently small that I may ignore it, at least in the range of energies considered<sup>1</sup>. Note that for QED no such term would arise.

I write the false vacuum transition amplitude as a path integral and note that

---

<sup>1</sup>Of course photon loops will generate this term. However, the term is a pointlike interaction between scalar loops (given no external legs) and, in the dilute instanton approximation that I will make, such loops are subdominant and are neglected.

I may integrate out the charged particle, as it enters quadratically.

$$\begin{aligned}
\langle \Omega | \hat{S}_E | \Omega \rangle &= \int \mathcal{D}A_\mu \mathcal{D}\phi e^{-\int_x \mathcal{L}_{\text{SQED}}} \\
&= \int \mathcal{D}A_\mu \det(-D^2 + m^2)^{-1} e^{-\int_x \frac{1}{4} F^{\mu\nu} F_{\mu\nu}} \\
&= \int \mathcal{D}A_\mu e^{-\text{Tr} \log(-D^2 + m^2) - \int_x \frac{1}{4} F^{\mu\nu} F_{\mu\nu}}, \tag{3.5}
\end{aligned}$$

where  $\int_x := \int d^4x$  and the functional integrations are normalised such that the amplitude is 1 for zero external field. The normalisation drops out once I take the imaginary part of the logarithm to find the rate, as in Eq. (3.3).

I can now use Schwinger's trick (i.e. Frullani's integral) to express the logarithm as a proper time integral [201]

$$\log(A) = - \int_0^\infty \frac{ds}{s} (e^{-As} - e^{-s}), \tag{3.6}$$

and drop the second term as it is field independent and will not contribute an imaginary part. The UV divergences of the theory will then turn up as divergences at small  $s$  which can be renormalised using the heat kernel expansion. Introducing the proper time integral leads to the expression  $\text{Tr}(e^{-(D^2+m^2)s})$ , which I express as a path integral over closed worldlines, [235, 236, 237, 238, 239]

$$\text{Tr}(e^{-(D^2+m^2)s}) = \int \mathcal{D}x^\mu e^{-S_0[x^\mu, A_\mu^{\text{ext}} + A_\mu; s]}, \tag{3.7}$$

where the action is given by

$$S_0[x^\mu, a_\mu; s] := m^2 s + \frac{1}{4} \int_0^s d\tau \dot{x}^\mu \dot{x}_\mu - ig \oint a_\mu dx^\mu, \tag{3.8}$$

and  $\dot{x}^\mu := dx^\mu/d\tau$ . This is the worldline path integral for a charged scalar particle with the reparameterisation invariance fixed such that the einbein (also-called the vierbein or tetrad by analogy to 4 dimensions) is equal to 2 (see for example Chapter 1 of Ref. [240]). The false vacuum transition amplitude is now

$$\begin{aligned}
\Gamma &= -\frac{2}{\mathcal{V}} \text{Im} \log \int \mathcal{D}A_\mu e^{-\int_x \frac{1}{4} F^{\mu\nu} F_{\mu\nu}} \left\{ 1 + \right. \\
&\quad \left. \sum_{n=1}^{\infty} \frac{1}{n!} \left( \prod_{j=1}^n \int_0^\infty \frac{ds_j}{s_j} \int \mathcal{D}x_j^\mu e^{-S_0[x_j^\mu, A_\mu^{\text{ext}} + A_\mu; s_j]} \right) \right\}. \tag{3.9}
\end{aligned}$$

At each order in  $n$  the integration over the photon is now Gaussian and can be

done exactly, resulting in an effective nonlocal worldline action. If I denote the free photon propagator by  $G_{\mu\nu}(x_j, x_k)$ , I can write this as

$$\Gamma = -\frac{2}{\mathcal{V}} \text{Im} \log \left\{ 1 + \sum_{n=1}^{\infty} \frac{1}{n!} \left( \prod_{j=1}^n \int_0^{\infty} \frac{ds_j}{s_j} \int \mathcal{D}x_j^\mu \right) e^{-\sum_{k=1}^n (S_0[x_k^\mu, A_\mu^{\text{ext}}; s_k] - \frac{g^2}{2} \sum_{l=1}^n \oint dx_k^\mu dx_l^\nu G_{\mu\nu}(x_k, x_l))} \right\}. \quad (3.10)$$

Integrating out the photon has left me with a nonlocal, long-range interaction. At this point I have made no approximations regarding the strength of the external field, or of the coupling. The relatively simple exponential form of Eq. (3.10) only obtains for Abelian gauge fields (see for example [241]).

At weak coupling,  $g^2 \ll 1$ , the nonlocal interaction term in Eq. (3.10) can be dropped at leading order. In this case the sum exponentiates, leaving only one path integration which can be carried out exactly, leading to Schwinger's result [201]

$$\Gamma_{\text{Schwinger}} = \frac{g^2 E^2}{8\pi^3} \sum_{n=0}^{\infty} \frac{(-1)^{n+1}}{n^2} e^{-\frac{\pi m^2}{gE} n}. \quad (3.11)$$

In this chapter I consider arbitrary coupling,  $g$ , for which the nonlocal interaction cannot be dropped.

### 3.1.2 Finite temperature rate

The derivation thus far has been at zero temperature. At finite temperature,  $T = 1/\beta$ , I make the following replacements

$$\begin{aligned} \langle \Omega | \hat{S}_E | \Omega \rangle &\rightarrow \mathcal{N}^{-1} \text{Tr} e^{-\hat{H}\beta}, \\ \mathcal{V} &\rightarrow \mathcal{V}_T, \end{aligned}$$

where  $\hat{H}$  is the Hamiltonian of the system in the presence of the external field and the normalisation,  $\mathcal{N}^{-1}$ , ensures the amplitude is 1 in the absence of the external field (see [242] for a physical discussion of thermal Schwinger pair creation). In the second line  $\mathcal{V}_T$  is equal to the spatial volume,  $V$ , multiplied by the inverse temperature  $\beta^2$ .

---

<sup>2</sup>Eq. (3.12) for the thermal rate has been advocated by Linde [243, 244]. An analysis by Langer shows that a different expression for  $\mathcal{V}_T$  should be used, with the inverse temperature replaced by the decay time of an intermediate state [245, 246, 107]. Though, as I only work to exponential accuracy (i.e. the leading order of the logarithm) in this chapter, the difference does not affect my

The rate is then given by

$$\Gamma_T = \frac{2}{\mathcal{V}_T} \text{Im} \left\{ -\log \left( \text{Tr} e^{-\hat{H}\beta} \right) \right\}. \quad (3.12)$$

This transition to finite temperature can be made straightforwardly using the Matsubara formalism, i.e. by enforcing periodicity in the Euclidean time coordinate,  $x^4(\tau) = x^4(\tau) + \beta$ , and including interactions between the periodic copies.

Including interactions between periodic copies is equivalent to replacing the photon propagator,  $G_{\mu\nu}(x_j, x_k)$ , by its thermal cousin,  $G_{\mu\nu}(x_j, x_k; T)$ . In a general  $R_\xi$  gauge the  $\xi$  dependent term drops out when integrated around a closed loop leaving just a term proportional to  $\delta_{\mu\nu}$ . This gauge independent part is

$$\begin{aligned} G_{\mu\nu}(x_j, x_k; T) &:= \sum_{n=-\infty}^{\infty} G(x_j, x_k + \frac{n}{T}e_4) \delta_{\mu\nu} \\ &= \sum_{n=-\infty}^{\infty} \frac{-\delta_{\mu\nu}}{4\pi^2(x_j - x_k - \frac{n}{T}e_4)^2} \\ &= \frac{T \sinh(2\pi T r_{jk}) \delta_{\mu\nu}}{4\pi r_{jk} (\cos(2\pi T t_{jk}) - \cosh(2\pi T r_{jk}))}, \end{aligned} \quad (3.13)$$

where  $e_4$  is the unit vector in the Euclidean time direction and I have defined  $t_{jk} := x_j^4 - x_k^4$  and  $r_{jk} := \sqrt{(x_j^1 - x_k^1)^2 + (x_j^2 - x_k^2)^2 + (x_j^3 - x_k^3)^2}$ . This is the Matsubara thermal Green's function in position space.

To generalise Eq. (3.10), and get an expression for the rate at finite temperature, one need only replace the zero temperature Green's function with that of Eq. (3.13), and impose periodic boundary conditions in the Euclidean time direction, with period  $1/T$ . The aim of this chapter is to calculate this thermal rate.

### 3.1.3 Inclusive rate at fixed energy

I will also consider inclusive tunnelling rates at a fixed energy  $\mathcal{E}$ , i.e. rates from a microcanonical ensemble. The microcanonical density operator projects onto the subspace of states with energy,  $\mathcal{E}$ . In this case one makes the replacements

$$\begin{aligned} \langle \Omega | \hat{S}_E | \Omega \rangle &\rightarrow \mathcal{N}^{-1} \text{Tr} \left( \delta(\mathcal{E} - \hat{H}) \right), \\ \mathcal{V} &\rightarrow \mathcal{V}_\mathcal{E}, \end{aligned}$$

where the normalisation again ensures the amplitude is 1 in the absence of the external field. In the second line  $\mathcal{V}_\mathcal{E}$  is equal to the spatial volume,  $V$ , multiplied by some time scale, which is expected to be  $O(1/\mathcal{E})$  on dimensional grounds. The exact form of  $\mathcal{V}_\mathcal{E}$  will not concern me in this chapter as my final results are only to exponential accuracy. The delta function of the Hamiltonian is defined by the following integral,

$$\delta(\mathcal{E} - \hat{H}) = \lim_{B \rightarrow \infty} \int_{-iB}^{iB} \frac{d\beta}{2\pi i} e^{(\mathcal{E} - \hat{H})\beta}, \quad (3.14)$$

an inverse Laplace transform of the Boltzmann factor. The rate,  $\Gamma_\mathcal{E}$ , is then given by

$$\Gamma_\mathcal{E} = \frac{2}{\mathcal{V}_\mathcal{E}} \text{Im} \left\{ -\log \left( \text{Tr} \delta(\mathcal{E} - \hat{H}) \right) \right\}, \quad (3.15)$$

The thermal density matrix is related to the microcanonical one by a sum over Boltzmann weights, or a Laplace transform,

$$e^{-\hat{H}\beta} = \int_0^\infty d\mathcal{E} e^{-\mathcal{E}\beta} \delta(\mathcal{E} - \hat{H}). \quad (3.16)$$

These rates and their relationship to thermal tunnelling rates have been discussed by various authors [246, 247, 248, 119, 115]. For sufficiently slow rates one can expand the logarithms in Eqs. (3.12) and (3.15) to derive the following approximate relation,

$$\Gamma_T \sim \int_0^\infty d\mathcal{E} e^{-\mathcal{E}\beta} \Gamma_\mathcal{E}, \quad (3.17)$$

where I have ignored the ratio  $\mathcal{V}_\mathcal{E}/\mathcal{V}_T$  as I will only use the relation to exponential accuracy.

## 3.2 The dilute instanton gas

I wish to consider Schwinger pair production in QED and SQED for arbitrary coupling,  $g$ . This requires going beyond perturbation theory in  $g$ . For a sufficiently weak external field, as I will show, an alternative set of approximations are valid and allow me to proceed. These are the semiclassical and dilute instanton gas approximations.

Although Feynman diagrams will not be utilised in this calculation, they can illuminate the structure of the approximations I will make. The rate, Eq. (3.10), contains only connected Feynman diagrams, due to the logarithm. The constituents of the contributing diagrams are internal charged particles lines; external photon

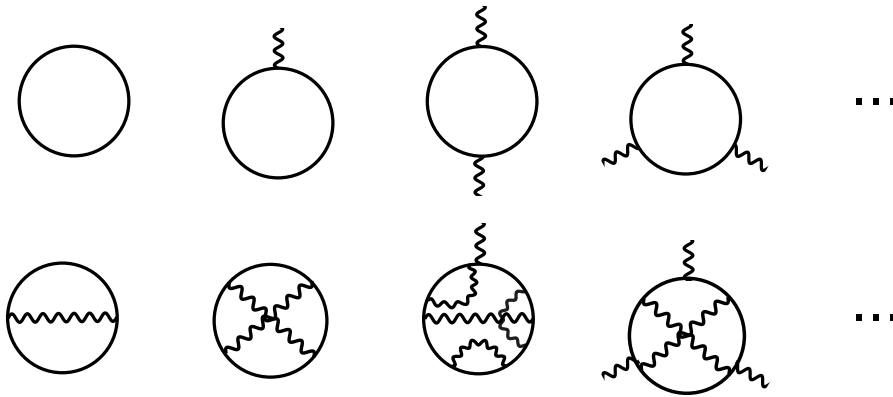


Figure 3.1: External photon legs denote couplings to the fixed external field whilst internal photon lines denote dynamical virtual photons. The Schwinger formula, Eq. (3.11), valid at weak coupling, accounts for the infinite set of diagrams represented in the first row. The quenched approximation also includes all diagrams which include any number of internal photon lines, with any topology. Some examples are shown in the second line. Note that in SQED there are also four-point interactions involving two photons and two charged particles (not shown here though included in quenched approximation). In all the diagrams there is only one charged particle loop. Figure taken from Ref. [1].

lines, for  $A_\mu^{\text{ext}}$ ; internal, dynamical photon lines, for  $A_\mu$ , and vertices joining two charged particle lines and one or two photon lines.

At weak coupling,  $g \ll 1$ , to leading order all dependence on the dynamical photon can be dropped. The path integrations in Eq. (3.10) are then uncoupled and the sum exponentiates. The Feynman diagrams which contribute to this all contain one charged particle loop and an arbitrary number of external photon lines. These are the diagrams in the first row of Fig. 3.1. The sum of these diagrams at zero temperature is Schwinger's original result, Eq. (3.11). At finite temperature the rate has been calculated in Refs. [249, 250, 251, 252]. The inclusion of a single dynamical photon line (i.e. two loops) was calculated first by Ritus at zero temperature [253, 254, 222, 255] and by Gies at finite but low temperature [256]. In these calculations the approximation of weak external fields has not been made.

At stronger coupling one must include the extra infinitely many diagrams containing arbitrary numbers of internal, dynamical photon lines as well as arbitrary numbers of charged particle loops. However, as I will argue, for a sufficiently weak external field, diagrams with a large number of charged particle loops will be suppressed and hence a loop expansion in charged particle loops is possible. At each order one must sum the infinite set of diagrams containing a fixed, finite number of charged particle loops and an arbitrary number of both external and dynamical pho-

ton lines. To first order this is the quenched approximation, which in this context was argued to be valid (at zero temperature) in the Refs. [25] and [221] (see also [257]). Fig. 3.1 shows some examples of diagrams which contribute in the quenched approximation.

Following Refs. [25] and [221], I consider the situation where the external field is weak and sufficiently slowly varying to be considered constant. I choose the external field to point in the 3 direction,  $F_{\mu\nu} = -i(\delta_{\mu 3}\delta_{\nu 4} - \delta_{\nu 3}\delta_{\mu 4})E$  (the factor of  $-i$  is present due to the Wick rotation and the fact that  $E$  is the value of the Minkowskian field). As long as the worldline  $x^\mu(\tau)$  forms the boundary of some surface within the space, I can use Stokes's theorem to reexpress the interaction with the external field,

$$\begin{aligned} -ig \oint A_\mu^{ext} dx^\mu &= -\frac{ig}{2} \int \int F_{\mu\nu} dx^\mu \wedge dx^\nu \\ &= -gE \oint x_3 dx^4, \end{aligned} \quad (3.18)$$

which is simply the area enclosed by the worldline, projected onto the 3-4 plane and multiplied by  $-gE$ . Now, I am in a position to set up the weak field approximation to Eq. (3.10), which will amount to a semiclassical approximation. To see this it will be useful for me to rescale the  $\tau$  in the integrand of  $S_0$ , the parameters  $s_j$  and the fields  $x_j^\mu(\tau)$ . I rescale them according to

$$\begin{aligned} \tau &\rightarrow \tau/s_j, \\ s_j &\rightarrow s_j/gE, \\ x_j^\mu &\rightarrow x_j^\mu m/gE, \end{aligned} \quad (3.19)$$

making all three dimensionless. The inverse temperature must be scaled in the same way as  $x_j^\mu(\tau)$ . I define the scaled temperature  $\tilde{T} := mT/gE$  and  $\tilde{\beta} := 1/\tilde{T}$ .

The full rate at finite temperature becomes 3, upon rescaling,

$$\Gamma_T = -\frac{2}{\mathcal{V}_T} \text{Im} \log \left[ 1 + \sum_{n=1}^{\infty} \frac{1}{n!} \prod_{j=1}^n \left( \int_0^\infty \frac{ds_j}{s_j} \int \mathcal{D}x_j^\mu e^{-\frac{1}{\epsilon} \tilde{S}[x_j; s_j; \kappa; \tilde{T}]} e^{\frac{\kappa}{\epsilon} \sum_{k < j} \oint dx_j^\mu dx_k^\nu G_{\mu\nu}(x_j, x_k; \tilde{T})} \right) \right], \quad (3.20)$$

where  $\epsilon := gE/m^2$  and  $\kappa := g^3 E/m^2$ . The parameter  $\epsilon$  is the potential energy that would be gained by a charged particle in moving a Compton wavelength in the direction of the external field, expressed as a fraction of the rest mass of the particle.



I also have defined,  $\tilde{S}$ , the scaled action as

$$\begin{aligned} \tilde{S}[x; s; \kappa, \tilde{T}] &:= s + \frac{1}{4s} \int_0^1 d\tau \dot{x}^\mu \dot{x}_\mu - \int_0^1 d\tau x_3 \dot{x}^4 \\ &- \frac{\kappa}{2} \int_0^1 d\tau \int_0^1 d\tau' \dot{x}^\mu(\tau) \dot{x}^\nu(\tau') G_{\mu\nu}(x(\tau), x(\tau'); \tilde{T}). \end{aligned} \quad (3.21)$$

Everything inside the logarithm is now separately dimensionless. Note that Eq. (3.20) is exact. I have as yet made no approximations regarding the strength of the external field or the coupling.

The parameters  $m$ ,  $g$ ,  $E$  and  $T$  only arise in equations (3.20) and (3.21) in three combinations: in the overall prefactor of the exponent,  $1/\epsilon$ , as  $\kappa$  and as  $\tilde{T}$ . For a sufficiently weak external field,  $\epsilon \ll 1$ , the path integral is calculable in the saddle-point, or semiclassical, approximation. This is the condition that the charged particle gains a small amount of energy compared with its rest mass, in moving a Compton wavelength along the external field. This condition is independent of the value of the coupling,  $g$ . The worldline configurations which dominate the path integral are then those which satisfy the classical equations of motion. Of these, those which give a nonzero imaginary part are those which are saddle points of the action with an odd number of negative modes in the spectrum of fluctuations about the solution. The solutions relevant to tunnelling have just one negative eigenvalue and are called bounces or instantons.

Note that the requirement that  $\epsilon \ll 1$ , which leads to semiclassicality, entails that

$$\begin{aligned} \kappa &\ll g^2, \\ \tilde{T} &\gg \frac{T}{m}. \end{aligned} \quad (3.22)$$

Semiclassicality also requires that  $\kappa \leq O(1)$ , which translates to the requirement that  $g$  is not parametrically larger than  $1/\epsilon$ , a very weak constraint on  $g$ . I will also require  $T \ll m$  for semiclassicality, which implies that  $\tilde{T} \ll 1/\epsilon$ , a very weak constraint. As a result, I will only calculate to leading order in  $\epsilon$  but to all orders in  $\kappa$  and  $\tilde{T}$ .

To proceed in calculating the rate, Eq. (3.20), I perform a cluster expansion, as introduced by Ursell [258] and Mayer [259]. I define the two-particle function  $f_{kl}$ , for  $k \neq l$ , by

$$f_{kl} = \exp \left\{ \frac{\kappa}{\epsilon} \oint \oint dx_k^\mu dx_l^\nu G_{\mu\nu}(x_k, x_l; \tilde{T}) \right\} - 1. \quad (3.23)$$

The cluster expansion to Eq. (3.20) is then found by expanding in powers of  $f_{kl}$  and

$$\Gamma_T = \bullet + \bullet\text{---}\bullet + 3 \bullet\text{---}\bullet\text{---}\bullet + \begin{array}{c} \bullet \\ \diagup \quad \diagdown \\ \bullet\text{---}\bullet \end{array} + \dots$$

Figure 3.2: The first three orders of the cluster expansion of the rate. Each circle symbolises a closed worldline. The lines joining them are interactions given by the two-particle function of Eq. (3.23). These diagrams are expressed algebraically in equations (3.24) and (3.25). Figure taken from Ref. [1].

grouping connected terms into so-called clusters. Only connected terms contribute to  $\Gamma_T$ . The expansion can be written as

$$\Gamma_T = \sum_{n=1}^{\infty} \Gamma_T^{(n)}, \quad (3.24)$$

where  $\Gamma_T^{(n)}$  is the contribution to  $\Gamma_T$  from clusters of  $n$  worldlines. The terms in the expansion can be mapped to connected graphs of increasing complexity, such as in Fig. 3.2 (these are textbook results, see for example Ref. [260]). The  $\Gamma_T^{(n)}$  are proportional to the imaginary parts of what might conventionally be called cluster integrals (commonly denoted  $b_n$ ) for the ensemble of charged particle worldlines, and so for brevity I will refer to them as cluster integrals.

The first three are given by

$$\begin{aligned} \Gamma_T^{(1)} &= -\frac{2}{1!\mathcal{V}_T} \text{Im} \int_0^\infty \frac{ds_1}{s_1} \int \mathcal{D}x_1^\mu e^{-\frac{1}{\epsilon} \tilde{S}[x_1; s_1; \kappa, \tilde{T}]}, \\ \Gamma_T^{(2)} &= -\frac{2}{2!\mathcal{V}_T} \text{Im} \prod_{j=1}^2 \left( \int_0^\infty \frac{ds_j}{s_j} \int \mathcal{D}x_j^\mu e^{-\frac{1}{\epsilon} \tilde{S}[x_j; s_j; \kappa, \tilde{T}]} \right) f_{12}, \\ \Gamma_T^{(3)} &= -\frac{2}{3!\mathcal{V}_T} \text{Im} \prod_{j=1}^3 \left( \int_0^\infty \frac{ds_j}{s_j} \int \mathcal{D}x_j^\mu e^{-\frac{1}{\epsilon} \tilde{S}[x_j; s_j; \kappa, \tilde{T}]} \right) \\ &\quad \left\{ 3f_{12}f_{13} + f_{12}f_{13}f_{23} \right\}. \end{aligned} \quad (3.25)$$

Eq. (3.24) is still formally exact but, importantly, is now expressed in a form that I can directly approximate. I follow Refs. [20, 261, 262, 263, 264, 265, 266] in performing a dilute instanton gas approximation. Essentially I will assume that the leading order behaviour of  $\Gamma_T$  is captured by the lowest nonzero term in the cluster expansion. This is a self-consistent approximation: within the approximation the higher order cluster integrals are exponentially suppressed with respect to the leading term.

First, suppose that there exists an instanton for  $\Gamma_T^{(1)}$ , so that  $\Gamma_T^{(1)} \neq 0$ . The

path integral is invariant under translations  $x^\mu(\tau) \rightarrow x^\mu(\tau) + a^\mu$ . The instanton solution for  $\Gamma_T^{(1)}$  will necessarily break the translation symmetry and hence fluctuations around the instanton will contain (at least) four zero modes. Integration over these can be done using the collective coordinate method (see for example [21]), resulting in an integral over the position of the instanton.

The higher order cluster integrals give the contributions due to interactions between instantons. The interactions die off as the inverse of the fourth of the distance between the instantons. Hence, approximate multi-instanton solutions can be constructed by combinations of single instantons a large distance apart. The contribution of these approximate saddle points can be found using the method of constrained instantons [263, 267]. The integrations over the collective coordinates and constraints of these approximate instantons will take the form of cluster integrals for a gas of classical point particles (rather than worldlines), with dipole interactions (as the worldlines are closed and hence have zero net charge). In this way, the infinite number of degrees of freedom of each particle worldline are reduced to the four degrees of freedom of a point in spacetime.

From this perspective, the rate,  $\Gamma_T$ , can be interpreted as the pressure of the instanton gas. Standard statistical mechanical relations then give the density of instantons,  $n_{\text{inst}}$ , as

$$n_{\text{inst}} = \sum_{n=1}^{\infty} n \Gamma_T^{(n)}. \quad (3.26)$$

Combining equations (3.24) and (3.26), the rate,  $\Gamma_T$ , can be written as an expansion in powers of the density

$$\Gamma_T = n_{\text{inst}} + B_2 n_{\text{inst}}^2 + B_3 n_{\text{inst}}^3 + O(n_{\text{inst}}^4). \quad (3.27)$$

This is the virial expansion and the coefficients,  $B_n$ , are the virial coefficients. For  $n \geq 3$  they are given by the irreducible graphs in the cluster expansion, those which cannot be cut into two pieces by cutting one line, and  $B_2 n_{\text{inst}}^2 = -\Gamma_T^{(2)}$ . At weak coupling, this virial expansion has been introduced previously in Refs. [222, 255].

To leading order in the cluster expansion the instanton density will be given simply by  $\Gamma_T^{(1)}$ . The average separation between instantons is then  $(\Gamma_T^{(1)})^{-1/4}$ . The density of instantons can be considered small if this distance is much larger than the maximum size of the instantons,  $R$ .

There is however a subtlety due to the long-range interactions of the instantons which was also found in the dilute instanton gas expansion of QCD [261, 262]. The contribution to the action due to the interaction between a pair of dipoles in four dimensions a distance  $|x|$  apart, decreases as  $1/|x|^4$ . This is such that, at zero

temperature, its integral over the volume of spacetime diverges proportionally to  $\log(\mathcal{V}_T)$ . As a result there is such a divergence in the second virial coefficient,  $B_2$ , and in all *reducible* diagrams, defined to be those diagrams that can be split into two disconnected parts by cutting a single line. On the other hand, at nonzero temperature, there is no logarithmic divergence due to the finite extent of the Euclidean time direction. As the thermodynamic limit, in which the spatial volume is taken to infinity, should be taken before the limit of zero temperature, this divergence in fact never arises.

Hence, at finite temperature, for sufficiently small, nonzero  $\Gamma_T^{(1)}$ , I expect

$$\Gamma_T = \Gamma_T^{(1)} \left( 1 + O(\Gamma_T^{(1)} L^4) \right), \quad (3.28)$$

where  $L = \text{Max}(R, \beta)$ . This leading order approximation is equivalent to the quenched approximation. The semiclassical approximation of  $\Gamma_T^{(1)}$  gives  $\Gamma_T^{(1)} L^4 \sim e^{-\tilde{S}(\kappa, \tilde{T})/\epsilon}$ , where I have written  $\tilde{S}(\kappa, \tilde{T})$  for the value of the scaled action,  $\tilde{S}[x; s; \kappa, \tilde{T}]$ , evaluated at the saddle point.

On the other hand, if there does not exist an instanton solution consisting of a single worldline, then  $\Gamma_T^{(1)} = 0$ . In this case I must repeat the above arguments for the first nonzero cluster integral,  $\Gamma_T^{(n_0)}$ , say. In that case the particles of the instanton gas would consist of groups of  $n_0$  worldlines and Eq. (3.28) would be replaced by

$$\Gamma_T = \Gamma_T^{(n_0)} \left( 1 + O(\Gamma_T^{(n_0)} L^4) \right). \quad (3.29)$$

In this chapter, I consider only the leading order term in the dilute instanton gas approximation,  $\Gamma_T^{(n_0)}$ . Further, I only calculate the exponential suppression of the leading term. This is equivalent to saying that I calculate the logarithm of the rate to leading order in the small parameter  $\epsilon$ . When  $n_0 = 1$ , this is

$$\log(\Gamma_T) = -\frac{\tilde{S}(\kappa, \tilde{T})}{\epsilon} + O(\log(\epsilon)). \quad (3.30)$$

In semiclassically evaluating the terms  $\Gamma_T^{(n)}$ , the saddle point of the  $s_j$  integrations can be easily found. For  $\Gamma_T^{(1)}$ , I find

$$\Gamma_T^{(1)} = -\frac{2m^4\epsilon^4}{\mathcal{V}_{\tilde{T}}} \sqrt{2\pi\epsilon} \int \mathcal{D}x^\mu \left( \int_0^1 d\tau \dot{x}^\mu \dot{x}_\mu \right)^{-\frac{1}{4}} e^{-\frac{1}{\epsilon} \tilde{S}[x; \kappa, \tilde{T}]} \quad (3.31)$$

where  $\tilde{\mathcal{V}}_{\tilde{T}} := \mathcal{V}_T m^4 \epsilon^4$  is the (dimensionless) scaled volume and I have defined  $\tilde{S}[x; \kappa, \tilde{T}]$

to be the scaled action evaluated at the saddle point of the  $s$  integration,

$$\tilde{S}[x; \kappa, \tilde{T}] := L[x] - A[x] + \kappa V[x; \tilde{T}], \quad (3.32)$$

written in this way to emphasise its geometric nature. The constituent terms are the kinetic term, which is equal to the length of the worldline on-shell, and which I will loosely refer to as the (parameterisation fixed) length of the worldline

$$L[x] := \sqrt{\int_0^1 d\tau \dot{x}^\mu \dot{x}_\mu}, \quad (3.33)$$

the area projected onto the 3-4 plane

$$A[x] := \int d\tau x_3 \dot{x}^4, \quad (3.34)$$

and the self-interaction term

$$V[x; \tilde{T}] := \frac{1}{2} \int_0^1 \int_0^1 d\tau d\tau' \dot{x}^\mu(\tau) \dot{x}^\nu(\tau') G_{\mu\nu}(x(\tau), x(\tau'); \tilde{T}). \quad (3.35)$$

The first term,  $L[x]$ , is the only nongeometric term, in the sense that it depends on the coordinates along the worldline. It is however equal to the length of the worldline when evaluated on shell. Note that the action is invariant under  $\tau \rightarrow \tau + c$ , where  $c$  is a constant. The corresponding conserved charge is  $\dot{x}^2(\tau)$ .

In some cases there may be no instanton solution consisting of a single worldline (explicit examples arise at high temperatures, Sec. 3.3). As I have argued, in these cases one should next look for instanton solutions consisting of two and then more worldlines. The (scaled) action for  $n_0$  worldlines could be thought of as that for a single discontinuous worldline (where one does not take derivatives across the discontinuities), except that the kinetic term, Eq. (3.33), does not appear to be additive. However, the kinetic term is, in fact, additive if each of the disconnected worldlines have the same (parameterisation fixed) length,

$$n_0 \sqrt{\int_0^1 d\tau \dot{x}_1^\mu \dot{x}_{1\mu}} = \sqrt{\int_0^{1/n_0} d\tau \dot{x}_1^\mu \dot{x}_{1\mu} + \cdots + \int_{(n_0-1)/n_0}^1 d\tau \dot{x}_{n_0}^\mu \dot{x}_{n_0\mu}}. \quad (3.36)$$

For the instanton solutions relevant in this chapter, this allows me to always talk about a single (possibly discontinuous) worldline and to always use the action in Eq. (3.32).

## 3.3 Instantons

### 3.3.1 Finite temperature rate

The problem of finding the rate of pair production due to a weak external field at given  $g$ ,  $E$ ,  $m$  and  $T$  is now reduced to a problem which depends only on two parameters,  $\kappa$  and  $\tilde{T}$ . The general solution amounts to finding the saddle point of  $\tilde{S}[x; \kappa, \tilde{T}]$  with one negative mode, and the fluctuations about it.

Integrations over fluctuations in the negative mode, via an analytic continuation, give the all important factor of  $i$  [268, 245, 269, 270]. There are also zero modes due to translation invariance. Integration over these degrees of freedom requires first introducing a constraint which fixes the translation invariance and then integrating over that constraint. I choose to fix the centre of mass of the worldline to be at the origin,  $\bar{x}^\mu = 0$ . Integration over the constraint then gives a factor  $\tilde{\mathcal{V}}_T = m^4 \epsilon^4 \mathcal{V}_{\tilde{T}}$ , cancelling the  $1/\tilde{\mathcal{V}}_{\tilde{T}}$  in Eq. (3.31). The remaining integrations over positive mode fluctuations give a subleading prefactor.

To calculate the logarithm of the rate to leading order in  $\epsilon$ , I need only find the instanton solution and calculate its action,  $\tilde{S}(\kappa, \tilde{T})$ . Even this is a difficult enough problem, made so by the nonlocal photon interaction in (3.32). In the following I consider the equations of motion analytically in certain limits:  $\kappa \ll 1$ ,  $\tilde{T} \ll 1$  and large  $\tilde{T}$ . Then for arbitrary  $\kappa$  and  $\tilde{T}$  I use numerical methods.

### 3.3.2 Inclusive rate at fixed energy

From  $\tilde{S}(\kappa, \tilde{T})$ , I can calculate the inclusive rate at fixed energy. In the semiclassical approximation, Eq. (3.17) shows that the two rates are related by a Laplace transform and hence the exponents of the rates are related via a Legendre transform. In the thermodynamic language  $\tilde{S}(\kappa, \tilde{T})$  is the free energy divided by the temperature. The (scaled) energy of the solution  $\tilde{\mathcal{E}}$  is

$$\tilde{\mathcal{E}} = \frac{\partial \tilde{S}}{\partial \tilde{\beta}}, \quad (3.37)$$

corresponding to a physical energy  $\mathcal{E} = m\tilde{\mathcal{E}}$ . By further scaling the worldlines by  $x \rightarrow x/\tilde{\beta}$ , taking the derivative with respect to  $\tilde{\beta}$ , and then reversing the scaling, I find the following useful result

$$\tilde{\beta}\tilde{\mathcal{E}} = L[x] - 2A[x], \quad (3.38)$$

which holds on shell. Note that everything in this equation is separately dimensionless. The exponential suppression of the rate of pair production at fixed energy is

$$\begin{aligned} \Sigma &= \frac{1}{\epsilon}(\tilde{S} - \tilde{\mathcal{E}}\tilde{\beta}) \\ &= \frac{1}{\epsilon}\tilde{\Sigma}(\kappa, \tilde{\mathcal{E}}). \end{aligned} \quad (3.39)$$

### 3.3.3 Regularisation

As I have mentioned the interaction term,  $V$ , diverges at zero distance. For smooth worldlines, this is the long known self-energy divergence of electromagnetism. Its appearance in the worldline formulation of QED has been studied by many authors (see for example [237, 241, 271, 272]). The divergence, being due to the strong interactions between nearby sections of a worldline, is proportional to its length.

I first consider a well-known regularisation scheme due to Polyakov [237]. At zero temperature this amounts to replacing the interaction term,  $V[x; 0]$ , with

$$\begin{aligned} V_{\text{Polyakov}}[x; 0] &:= \frac{1}{8\pi^2} \int_0^1 \int_0^1 d\tau d\tau' \frac{\dot{x}^\mu(\tau)\dot{x}_\mu(\tau')}{(x(\tau) - x(\tau'))^2 + a^2} \\ &\quad - \frac{1}{8\pi^2} \frac{\pi}{a} \int_0^1 \sqrt{\dot{x}^2(\tau)} d\tau. \end{aligned} \quad (3.40)$$

The second term in (3.40), proportional to the length of the worldline, is a counterterm which absorbs the short distance divergence of the first term. It is almost of the same form as the term  $L[x]$  in the action (Eq. (3.33)), except without the reparameterisation fixing. On shell the two terms are equal, hence I can see it as a mass counterterm.

This self-energy divergence has been shown to be the only divergence for smooth loops with no intersections [241]. Worldlines with discontinuous first derivatives (cusps) and intersections may arise when there are delta function interactions in the action or when a ratio of scales is taken to zero. Such worldlines also generate

logarithmic divergences<sup>3</sup>.

Unfortunately the regularisation scheme of Eq. (3.40) leads to problems when trying to formulate the equations of motion which prevent me taking the limit  $a \rightarrow 0$  in my numerical calculations. This is because, for sufficiently small  $a$ , the counterterm gives a negative bare mass. To bypass this problem I adopt an alternative regularisation in my numerical calculations for which the bare mass and the renormalised masses are equal,

$$V_R[x; 0] := \frac{1}{8\pi^2} \int_0^1 \int_0^1 d\tau d\tau' \frac{\dot{x}^\mu(\tau) \dot{x}_\mu(\tau')}{(x(\tau) - x(\tau'))^2 + a^2} - \frac{1}{8\pi^2} \frac{\sqrt{\pi}}{a^2} \int_0^1 \int_0^1 d\tau d\tau' \dot{x}^\mu(\tau) \dot{x}_\mu(\tau') e^{-(x(\tau) - x(\tau'))^2/a^2}. \quad (3.41)$$

Equations (3.40) and (3.41) agree as  $a \rightarrow 0$  as can be seen by recognising the Gaussian representation of the delta function. At finite temperature I must include the infinite sum of interactions with the periodic copies. If the periodic copies are disconnected and a finite distance apart, there is no ultraviolet divergence from their interaction and the unregularised interaction may be used. However, if the periodic copies are connected, the interaction between them must be regularised.

As well as the mass, there is, of course, charge renormalisation. Physically this is due to charged particle-antiparticle pairs popping into and out of existence and screening the bare charge. Thus the dilute instanton gas approximation, which only takes into account a small number of charged particle loops, does not take into account these effects. In the worldline formalism such short-lived virtual pairs are represented by small, closed worldlines. Though there are many such possible fluctuations, any given one will have an action of order  $\epsilon^0$  and hence will not arise in the stationary phase approximation I have made. Including these fluctuations should result in the final rates depending on the renormalised charge as argued for in Ref. [221].

For the small worldlines of the short-lived virtual pairs to simply renormalise the charge, there must be a separation of scales between them and the larger worldlines which constitute the saddle point. I can make a simple estimate for the scale of the virtual pairs by equating the rest mass to the Coulomb attraction. This equality reads  $2m = g^2/(4\pi r)$  and gives the distance between charges as  $r = g^2/(8\pi m)$ . In my dimensionless units, this translates to a distance  $\kappa/(8\pi)$ , which must be smaller than any scale present in the instanton for the charge renormalisation effects to be

---

<sup>3</sup>These logarithmic divergences can be interpreted as due to bremsstrahlung radiation. They give the anomalous dimension for Wilson loops, and hence for the propagator of the charged particles.



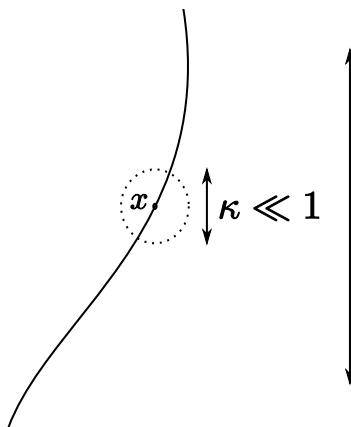


Figure 3.3: Sphere of influence of the point  $x$ , of size  $O(\kappa)$ , compared to the curvature of the worldline on a scale  $O(1)$ . Figure taken from Ref. [1].

independent. This essentially amounts to

$$\frac{\kappa}{8\pi} \ll \text{Min} \left( 1, \frac{1}{\tilde{T}} \right). \quad (3.42)$$

In this and the following chapter I optimistically consider  $\kappa$  to take values up to and including  $O(1)$ . In Chapter 5, in considering the corrections to the leading order result, I critically examine the necessary condition on  $\kappa$ . The modification of the photon-charged particle interaction at distances below  $g^2/(8\pi m)$  has been discussed in Refs. [123, 273], with regard to magnetic monopoles.

### 3.3.4 Small $\kappa$ expansion

#### A singular perturbation problem

Throughout this chapter, I make the approximation that the external field is weak, i.e. that  $0 < \epsilon \ll 1$ . The parameter  $\kappa := g^2\epsilon$  is proportional to  $\epsilon$ . Hence, for not too large couplings, it will also be that  $0 < \kappa \ll 1$ . This is the case I will consider in this section. Parametrically large couplings, such that  $\kappa = O(1)$ , will be considered in Secs. 3.3.5, 3.3.6 and 3.4.

For sufficiently small  $\kappa$ , one would naively expect that I could simply set  $\kappa = 0$  in the scaled action  $\tilde{S}[x^\mu; \kappa, \tilde{T}]$ , so dropping the interaction term. The problem is that the interaction term diverges at short distance and hence cannot be ignored for arbitrarily small but positive  $\kappa$ . This signals that for small  $\kappa$  I am dealing with a singular perturbation problem related to the existence of widely separated scales (see for example [206]).

I seek *distinguished limits* of the action  $\tilde{S}[x; \kappa, \tilde{T}]$ , and its corresponding equations of motion, by considering the scalings  $x = \kappa^\alpha y$  and  $\tilde{T} = \kappa^{-\alpha} \Theta$ . The aim is to find scalings such that there is a balance between two terms in the action and that the leading order equations of motion give nontrivial solutions. After the scaling the action is

$$\tilde{S}[x; \kappa, \tilde{T}] = \kappa^\alpha L[y] - \kappa^{2\alpha} A[y] + \kappa V[y, y'; \Theta]. \quad (3.43)$$

There are three distinguished limits:  $\alpha = 0, 1/2, 1$ . The first, the  $\alpha = 0$  scaling, corresponds to scales  $x = O(1)$ , which I will refer to as the infrared (IR) problem. The last, the  $\alpha = 1$  scaling, corresponds to shorter scales  $x = O(\kappa)$ , which I will refer to as the ultraviolet (UV) problem. The intermediate scaling,  $\alpha = 1/2$ , corresponds to scales  $x = O(\kappa^{1/2})$ , which I will refer to as the matching problem.

For small  $\kappa$ , an approximate solution to the equations of motion valid on all scales can be found by solving the leading order equations of motion in these three distinguished limits and matching them smoothly together. The simplest of the three problems is the matching problem,  $\alpha = 1/2$ . The leading approximation amounts to simply keeping the length term

$$\tilde{S}(\kappa \ll 1, \tilde{T}) \approx \kappa^{1/2} L[y]. \quad (3.44)$$

The area and interaction terms are equally subdominant on these scales, both being of order  $\kappa$ . Solutions to the minimisation of the length term are simply straight lines. Hence the IR and UV solutions must be matched with straight lines. The matching is done at some scale  $\lambda = O(\kappa^{1/2})$  which acts as a UV cutoff for the IR problem and as an IR cutoff for the UV problem. The final solution should be independent of the specific choice of  $\lambda$ .

The IR problem, the  $\alpha = 0$  scaling, in the leading approximation amounts to simply dropping the interaction term, i.e. to

$$\tilde{S}(\kappa \ll 1, \tilde{T}) \approx L[y] - A[y]. \quad (3.45)$$

In terms of a Feynman diagram language, this approximation takes into account all external field photon exchanges but no virtual photon exchanges. This is the top row of Fig. 3.1, a one-loop approximation. Making this action stationary is the old problem of maximising the area of a field given a fixed length of fencing. The solution at zero temperature is a circle of radius 1 in the 3-4 plane. At finite temperature the solution can be found using the method of images.

The UV problem, the  $\alpha = 1$  scaling, in the leading approximation amounts to

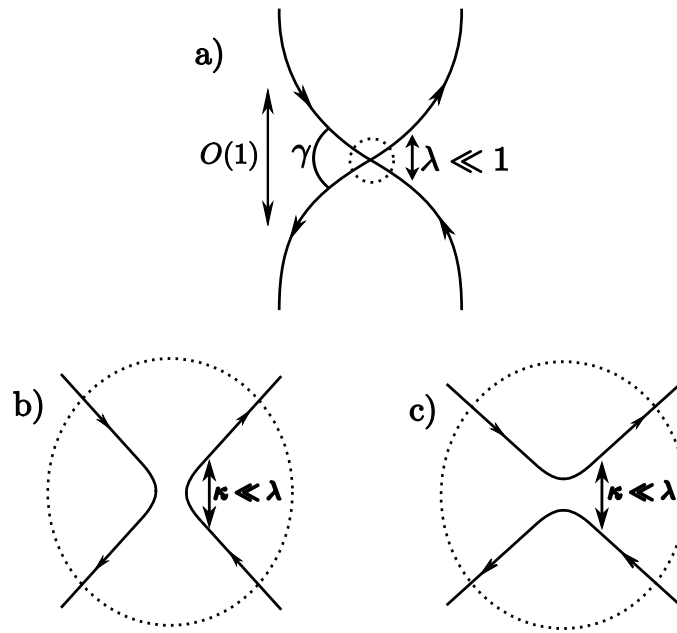


Figure 3.4: On scales  $x = O(1)$  there may appear an intersection, as in a). This must be resolved on shorter scales,  $x = O(\kappa)$ , as b) or c). Due to the fact that the problem can be specified completely in the plane, I expect that these are the only possibilities. The long and short distance pictures are matched at some scale  $\lambda = O(\kappa^{1/2})$ . Figure taken from Ref. [1].

dropping the area term, i.e. to

$$\tilde{S}(\kappa \ll 1, \tilde{T}) \approx \kappa(L[y] + V[y, y'; \Theta]). \quad (3.46)$$

This equation determines the dynamics at scales  $y = \kappa^{-1}x = O(1)$ . In terms of Feynman diagrams this approximation takes into account all virtual photon loops but no external photon lines.

Eq. (3.46) is the action of a massive charged particle, in the absence of an external field. Hence I can immediately find one solution, that of a straight line, the particle sitting still (or 4D rotations thereof). To find a solution to the full equations of motion, valid at all scales I can stitch this straight line solution together with a solution of Eq. (3.45). This is possible if for every point  $x$  on the worldline, I can draw a ball of size  $\lambda$  within which the worldline appears straight as  $\kappa \rightarrow 0$ . As solutions to (3.45) are independent of  $\kappa$ , this will always be possible as long as the worldline has everywhere finite curvature and does not self-intersect. Otherwise, in the region of a cusp or self-intersection, the straight line solution to Eq. (3.46) cannot be used.

Such cusps or self-intersections are not permissible when all the parameters of

the theory are finite as they give new divergences which depend on the angle at the nonanalytic point,  $\gamma$  in Fig. 3.4. Due to this the divergences cannot be absorbed as counterterms in the field theory. However, if a ratio of scales in the problem goes to zero, as when  $\kappa \rightarrow 0$ , such apparent cusps or self-intersections can appear at larger scales,  $O(1)$  and  $O(\kappa^{1/2})$  in my case. On the smallest scale,  $O(\kappa)$  in my case, these apparent nonanalytic points can be resolved as in Fig. 3.3. The separation of scales in processes which involve a large momentum transfer, such as deep inelastic scattering, gives divergences for the same reason [274, 275].

For apparent nonanalytic points to be resolved on scales  $O(\kappa)$ , there must exist solutions of (3.46) which have the topology (in the plane) of b) and c) in Fig. 3.3. Note that these two possibilities are related by a rotation by  $\pi/2$ . Hence all points of self-intersection can be resolved if solutions with the topology of b) can be found for all angles  $\pi/2 < \gamma \leq \pi$ . These solutions must be stitched together with the IR solutions at some scale  $\lambda$ . Thus I must impose boundary conditions at  $\lambda$  such that the solutions can be smoothly matched.

The existence of such solutions can be made plausible by noting that for  $\pi/2 < \gamma \leq \pi$  the scalar product between the tangent vectors on the left and right hand sides of b) is negative and hence the interaction term is repulsive. The magnitude of the repulsion increases without bound as the worldlines approach each other, suggesting that the worldlines should approach to some minimum distance,  $|y - y'| = O(1)$ . The minimum distance is a function of the incoming angle  $\gamma$  and is independent of  $\kappa$ , as long as  $\gamma$  and  $\pi - \gamma$  are both  $O(1)$ . Naively one might expect that the scaled action  $L[y] + V[y, y']$  would then be  $O(1)$  and hence the contribution to the  $\tilde{S} = \kappa(L[y] + V[y, y'; \Theta]) = O(\kappa)$ . However the following argument shows that this is not the case.

The matching of the IR and UV solutions is carried out at the scale  $\lambda$ . Due to the long-range of the interaction, the UV scaled action,  $L[y] + V[y, y'; \Theta]$ , will get large as  $\log(\lambda/\kappa)$ . This is the infrared divergence of the interaction of two long straight worldlines which are not parallel. Upon matching the IR and UV solutions all dependence on  $\lambda$  must drop out. However I will be left with a contribution to the action of the order  $\kappa \log(\kappa)$ . Note that this matching argument would still hold if the short distance physics was modified at distances  $O(\kappa)$  by virtual charged particle loops.

Overall I find that for solutions with apparent cusps or intersections

$$\tilde{S}(\kappa, \tilde{T}) = c(\tilde{T}) + d(\tilde{T})\kappa \log(\kappa) + O(\kappa), \quad (3.47)$$

for some  $c(\tilde{T})$  and  $d(\tilde{T})$ . For solutions without cusps or intersections the  $\kappa \log(\kappa)$

term is absent, i.e.  $d(\tilde{T}) = 0$ .

### Small $\kappa$ results

At zero temperature the solution to the IR problem is a circle of radius 1 in the 3 – 4 plane. At every point,  $x$ , on the circle, a small ball of radius  $\lambda = O(\kappa^{1/2})$  can be drawn within which the worldline looks approximately straight. Hence, the circle of radius 1 solves the equations of motion at all scales. The resulting action is

$$\tilde{S}(\kappa, 0) = \pi - \frac{\kappa}{4}. \quad (3.48)$$

This result was first derived in [25, 221]. Due to the symmetry of the problem this result is in fact exact for arbitrary  $\kappa$  and hence applies even for parametrically strong coupling. The prefactor is given by the determinant of fluctuations about this solution. This has been computed at leading order in  $\kappa$ . There is one negative mode, corresponding to changing the radius of the circle, there are five zero modes and all the rest are positive. Including the prefactor, the rate is given by

$$\Gamma \approx (2s + 1) \frac{m^4 \epsilon^2}{8\pi^3} e^{-\frac{1}{\epsilon}(\pi - \frac{\kappa}{4})}, \quad (3.49)$$

where  $s$  is the spin of the charged particle. At  $\kappa = 0$  this reduces to Schwinger's result for weak external fields (Eq. (3.11)).

At finite temperatures,  $\tilde{T}$ , and small  $\kappa$ , the leading order solution to the IR problem is given by an infinite sequence of circles of radius 1 separated by a distance  $\tilde{\beta}$  along the Euclidean time axis (see Fig. 3.5 (b)). For temperatures such that  $\tilde{T} < 1/2$ , these circles do not overlap and, for sufficiently small  $\kappa$ , I am able to draw a small ball of radius  $O(\kappa^{1/2})$  within which there is a single worldline which looks approximately straight. Hence for such temperatures, the sequence of circles solves the equations of motion at all scales and, to lowest order in  $\kappa$ , the rate is the same as at zero temperature. This means that, at one-loop order, I find no corrections to the zero temperature rate for  $\tilde{T} < 1/2$ .

Corrections to this can be calculated using perturbation theory, for small  $\kappa$ . I write the full action and its solution as expansions in  $\kappa$ ,

$$\begin{aligned} \tilde{S}[x] &= \tilde{S}_0[x] + \kappa \Delta \tilde{S}[x], \\ x^\mu(\tau) &= x_0^\mu(\tau) + \kappa x_1^\mu(\tau) + \kappa^2 x_2^\mu(\tau) + \dots \end{aligned} \quad (3.50)$$

where  $\tilde{S}_0[x] = L[x] - A[x]$  and  $\Delta \tilde{S}[x] = V[x]$ . First order perturbation theory requires me to simply evaluate  $\Delta \tilde{S}[x_0]$ . I split this up into interactions between

pairs of loops,

$$\kappa\Delta\tilde{S}[x_0] = \kappa \sum_{n=-\infty}^{\infty} \Delta\tilde{S}_n[x_0], \quad (3.51)$$

where I have defined  $\Delta\tilde{S}_n[x_0]$  to be the interaction between the loop at the origin and that centred at Euclidean time  $n/\tilde{T}$ ,

$$\kappa\Delta\tilde{S}_n[x_0] = \frac{\kappa}{8\pi^2} \oint \oint \frac{dx dx'}{(x - x' - \frac{n}{\tilde{T}}e_4)^2}. \quad (3.52)$$

The  $x$  denotes the positions on the circle at the origin with respect to the origin. The  $x'$  denotes the positions on the circle centred at Euclidean time  $n/\tilde{T}$  with respect to its centre. The  $e_4$  is a unit vector in the Euclidean time direction. The result of the integration, for  $n \neq 0$ , is

$$\kappa\Delta\tilde{S}_n[x_0] = -\frac{\kappa}{4} \frac{\left(\sqrt{\frac{1}{4} - \left(\frac{\tilde{T}}{n}\right)^2} - \frac{1}{2}\right)^2}{\sqrt{\frac{1}{4} - \left(\frac{\tilde{T}}{n}\right)^2}}. \quad (3.53)$$

This was first derived in Ref. [276]. For  $n = 0$ , the integral is  $-\kappa/4$  after regularisation and is the zero temperature correction in Eq. (3.48). The full first order correction is given by the sum, (3.51). It is negative for  $\tilde{T} \geq 0$ ; hence it increases the rate of pair production. It also diverges to  $-\infty$  as  $\tilde{T} \rightarrow 1/2$ , i.e. where the zero temperature instantons touch. However, following the discussion of Sec. 3.3.4, the separation of scales breaks down when neighbouring circles are only a distance  $O(\kappa^{1/2})$  apart, when  $1/2 - \tilde{T} = O(\kappa^{1/2})$ .

Unlike the zero temperature result, there are corrections at second order in  $\kappa$  due to the warping of the shape of the circles. To calculate these, I must solve

$$\int_0^1 \left( \frac{\delta^2 \tilde{S}_0}{\delta x^\mu(\tau) \delta x^\nu(\tau')} \Big|_{x_0} x_1^\nu(\tau') \right) d\tau' + \frac{\delta \Delta \tilde{S}}{\delta x^\mu(\tau)} \Big|_{x_0} = 0. \quad (3.54)$$

The solution should lie in the 3–4 plane, due to the symmetry of the problem, and must be closed. Hence, I may express it as

$$x_1^\mu(\tau) = \epsilon(\tau)(0, 0, \cos(2\pi\tau), \sin(2\pi\tau)). \quad (3.55)$$

In terms of  $\epsilon(\tau)$ , the terms in the action at second order in  $\kappa$  are

$$\begin{aligned} & \frac{\kappa^2}{2} \left( \int_0^1 \frac{\dot{\epsilon}^2}{2\pi} d\tau - 2\pi \bar{\epsilon}^2 \right) \\ & - \frac{\kappa^2 \tilde{T}^4}{2\pi} \int_0^1 \left( 4\zeta(4) + 24\tilde{T}^2 \zeta(6)(1 - \cos(4\pi\tau)) \right) \epsilon(\tau) d\tau, \end{aligned} \quad (3.56)$$

where  $\bar{\epsilon}^2$  denotes the square of the average of  $\epsilon(\tau)$  (not the average of the square) and  $\zeta$  denotes the Riemann zeta function<sup>4</sup>. From Eq. (3.56) I find the equations of motion for  $\epsilon(\tau)$ , the solution of which can be found straightforwardly via a Fourier series expansion. The two arbitrary parameters in the general solution are fixed by satisfying the constraint,  $\bar{x}^\mu = 0$ , which I am using to fix translation invariance. The solution is given by

$$\kappa\epsilon(\tau) = -\frac{\kappa\tilde{T}^4}{2\pi} \left\{ 4\zeta(4) + 24\zeta(6)\tilde{T}^2 + 6\zeta(6)\tilde{T}^2 \cos(4\pi\tau) \right\}. \quad (3.57)$$

The constant terms reduce the radius of the circle and the term proportional to  $\cos(4\pi\tau)$  makes the circle prolate (stretched in the  $x^4$  direction). Substituting this solution into Eq. (3.56) and putting it together with the zeroth and first order terms I arrive at

$$\begin{aligned} \tilde{S}(\kappa, \tilde{T}) &= \pi - \frac{\kappa}{4} \left\{ 1 + 2 \sum_{n=1}^{\infty} \frac{\left( \sqrt{\frac{1}{4} - \left(\frac{\tilde{T}}{n}\right)^2} - \frac{1}{2} \right)^2}{\sqrt{\frac{1}{4} - \left(\frac{\tilde{T}}{n}\right)^2}} \right\} \\ &+ \frac{\kappa^2}{\pi} (4\zeta(4)^2 \tilde{T}^8 + 48\zeta(4)\zeta(6)\tilde{T}^{10} + 126\zeta(6)^2 \tilde{T}^{12}) + O(\kappa^3). \end{aligned} \quad (3.58)$$

For the corresponding inclusive rate at fixed energy I consider the Legendre transform of this sum. The energy is, from Eq. (3.37),

$$\tilde{\mathcal{E}} = -\tilde{T}^2 \frac{\partial \tilde{S}(\kappa, \tilde{T})}{\partial \tilde{T}}. \quad (3.59)$$

The leading term on the right hand side takes the form of  $\kappa$  multiplying a function of  $\tilde{T}$ . A consideration of this function implies that if I wish to consider energies much larger than  $\kappa$ , the corresponding temperature must be very close to  $1/2$ . This is the region of parameter space where the circular worldlines almost touch, the minimum distance  $d \ll 1$ . The UV problem in this case is nonrelativistic, with  $y^3$  being the

---

<sup>4</sup>Note that had the kinetic term been the actual length, rather than its reparameterisation fixed form, the only difference would be the replacement of  $\bar{\epsilon}^2$  with  $\int_0^1 \epsilon(\tau)^2 d\tau$ .

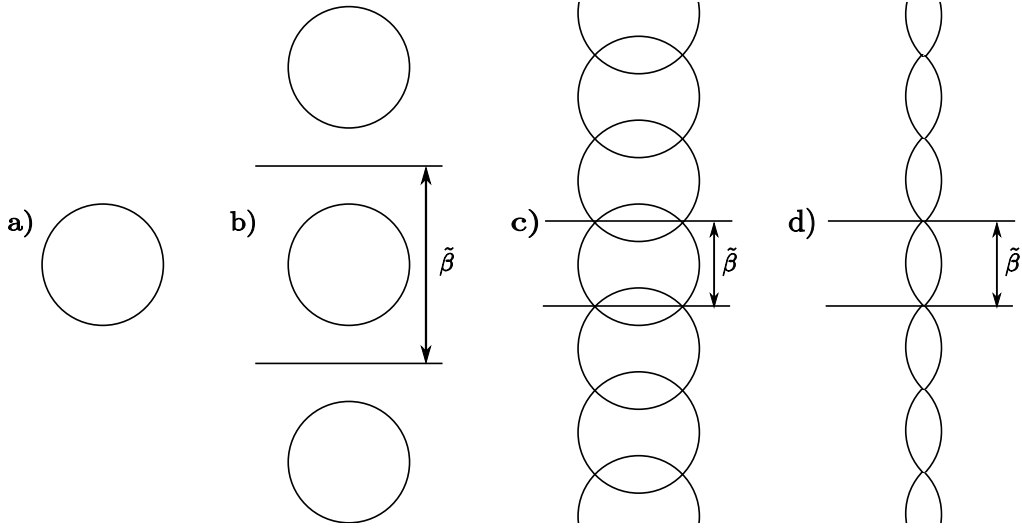


Figure 3.5: Instanton solutions at small  $\kappa$ : a) at zero temperature; b) at  $0 < \tilde{T} < 1/2$ ; c) at  $\tilde{T} > 1/2$ , the naive instanton of overlapping circles and d) at  $\tilde{T} > 1/2$ , the lemon instanton. Figure taken from Ref. [1].

“time” direction. Solutions to this nonrelativistic problem exist for  $d \gtrsim \kappa^{1/2}$ . This implies that the Legendre transform of Eq. (3.58) is only valid for  $\tilde{\mathcal{E}} \lesssim \kappa^{1/4}$ . For  $\tilde{\mathcal{E}} \lesssim \kappa$  taking the Legendre transform analytically is made difficult by the infinite sum. In the limited regime  $\kappa \ll \tilde{\mathcal{E}} \ll \kappa^{1/4}$  however I can fairly simply find the leading few terms.

$$\begin{aligned} \tilde{\Sigma}(\kappa, \tilde{\mathcal{E}}) &= \pi - 2\tilde{\mathcal{E}} - \frac{3}{4}\kappa^{2/3}\tilde{\mathcal{E}}^{1/3} + \frac{\kappa}{4} \left\{ 1 - \sum_{n=2}^{\infty} \left( \sqrt{1 - \frac{1}{n^2}} - 1 \right)^2 \left( 1 - \frac{1}{n^2} \right)^{-1/2} \right\} \\ &- \frac{11}{64}\kappa^{4/3}\tilde{\mathcal{E}}^{-1/3} + \sum_{n=2}^{\infty} \frac{\kappa^{5/3}\tilde{\mathcal{E}}^{-2/3}}{32n(n^2-1)^{3/2}} + \frac{35}{1536}\kappa^2\tilde{\mathcal{E}}^{-1} + O(\kappa^{7/3}\tilde{\mathcal{E}}^{-4/3}). \end{aligned} \quad (3.60)$$

The leading enhancement,  $-2\tilde{\mathcal{E}}$ , has been long known in the context of induced vacuum decay [277, 278].

For  $\tilde{T} \geq 1/2$  the circles intersect and the above calculation breaks down (see Fig. 3.5 c). The intersection must be resolved in a region of size  $\kappa$  as in Fig. 3.3. However, once I include intersections, a more general class of solutions to the full problem is possible: I can combine sections of circles with intersections. This is possible as solutions to Eq. (3.45) must only locally be arcs of a circle with curvature 1. Of all possible solutions describing pair production processes, that with minimum action will dominate the path integral and hence give the rate of pair production.

The minimum action solution of this kind has been found by several authors



[279, 247, 280, 281], though there is some dispute about this [282]. It is given by a lemon shape, Fig. 3.5 d), and not by the overlapping circles, 3.5 c). The angle of intersection (see Fig. 3.4) is given by

$$\gamma_{\tilde{T}} = 2 \arcsin \left( \frac{1}{2\tilde{T}} \right). \quad (3.61)$$

However, note that this worldline on IR scales is only a solution to the full problem if, for given  $\gamma_{\tilde{T}}$ , the corresponding UV solution exists. At small but finite  $\kappa$  my numerical calculations in Sec. 3.4 find instanton solutions which appear to approach the lemon instanton as  $\kappa \rightarrow 0$ .

The action of the thermal lemon-shaped instanton, to zeroth order in  $\kappa$ , is

$$\tilde{S}(0, \tilde{T}) = \gamma_{\tilde{T}} + \sin(\gamma_{\tilde{T}}) \quad (3.62)$$

where  $\tilde{T} > 1/2$ . Below  $\tilde{T} = 1/2$  the action is equal to  $\pi$ , at zeroth order in  $\kappa$ . The action and its first derivative are continuous at  $\tilde{T} = 1/2$ , though the second derivative diverges as  $-8/\sqrt{\tilde{T} - 1/2}$  as  $\tilde{T} \rightarrow 1/2$  from above. Hence I say that there is a second order phase transition at  $\tilde{T} = 1/2$ , for  $\kappa = 0$ . Below the phase transition the solution has circular symmetry. This is broken above it.

To get the leading order correction in  $\kappa$  it would seem I must solve the equation of motion derived from Eq. (3.46) in the region of the intersection (assuming such a solution exists). However, I can in fact bypass this hard problem using perturbative renormalisation. First, I evaluate the interaction term on the leading order IR instanton, the lemon. This gives an unphysical logarithmic UV divergence from the intersections

$$V_{\text{Lemon}} = \frac{\kappa}{\pi^2} \left\{ \left( \frac{\pi}{2} - \gamma_{\tilde{T}} \right) \cot(\gamma_{\tilde{T}}) + 1 \right\} \log(\lambda) + \text{finite terms}, \quad (3.63)$$

where I have used  $\lambda$  for the short distance regulator, rather than  $a$ , as this should be of the order of the matching scale, as in Sec. 3.3.4. Though I cannot solve the UV problem, I know that it must provide a compensating counterterm i.e.

$$\frac{\kappa}{\pi^2} \left\{ \left( \frac{\pi}{2} - \gamma_{\tilde{T}} \right) \cot(\gamma_{\tilde{T}}) + 1 \right\} \log \left( \frac{\kappa}{\lambda} \right). \quad (3.64)$$

From the perspective of the short distance physics this is an IR divergence, arising due to the matching scale  $\lambda$  being much larger than  $\kappa$ . The presence of  $\kappa$  in the logarithm is due to the scaling in the short distance problem. This meets my expectations, as explained at the end of Sec. 3.3.4, leading to a contribution of order

$\kappa \log(\kappa)$ ,

$$\begin{aligned} \tilde{S}(\kappa, \tilde{T}) &= \gamma_{\tilde{T}} + \sin(\gamma_{\tilde{T}}) \\ &+ \frac{1}{\pi^2} \left\{ \left( \frac{\pi}{2} - \gamma_{\tilde{T}} \right) \cot(\gamma_{\tilde{T}}) + 1 \right\} \kappa \log(\kappa) + O(\kappa). \end{aligned} \quad (3.65)$$

where  $\tilde{T} > 1/2$ . Note that the  $O(\kappa \log(\kappa))$  term starts to dominate over the leading term when  $\gamma_{\tilde{T}} = O(\kappa)$  and  $\pi - \gamma_{\tilde{T}} = O(\kappa)$ , or  $\tilde{T} = O(\kappa^{-1})$  and  $\tilde{T} - 1/2 = O(\kappa)$ . This signals a breakdown of the separation of scales assumed in deriving Eq. (3.65) and a breakdown of the approximate solution.

I have perturbatively renormalised the problem, in the sense of directly matching divergences with counterterms at a given order in the small parameter,  $\kappa$ . The subleading corrections at  $O(\kappa)$  depend on the solution to the short distance ( $\alpha = 1$ ) problem. My result could be nonperturbatively improved using the methods of the renormalisation group.

From Eq. (3.65) I can find the inclusive pair production rate at a fixed energy by Legendre transform,

$$\begin{aligned} \tilde{\Sigma}(\kappa, \tilde{\mathcal{E}}) &= \pi - \gamma_{\tilde{\mathcal{E}}} - \sin(\gamma_{\tilde{\mathcal{E}}}) \\ &+ \frac{1}{\pi^2} \left\{ \left( \frac{\pi}{2} - \gamma_{\tilde{\mathcal{E}}} \right) \cot(\gamma_{\tilde{\mathcal{E}}}) + 1 \right\} \kappa \log(\kappa) + O(\kappa), \end{aligned} \quad (3.66)$$

where I have defined  $\gamma_{\tilde{\mathcal{E}}} := 2 \arcsin(\tilde{\mathcal{E}}/2)$ . Note that the energy and temperature are monotonically increasing functions of each other in the allowed region of parameter space, the relationship is  $\tilde{\mathcal{E}} = \sqrt{4 - 1/\tilde{T}^2} + O(\kappa)$ .

The leading order result in Eq. (3.66) is the same as for pair production stimulated by the presence of a particle of mass  $\tilde{\mathcal{E}}$  [279] (or an off-shell photon [283]) or by a collision of particles with the same centre of mass energy [284, 285]. These calculations involve the same shaped instanton, though without the periodic copies. The (scaled) exponential suppression in that case, including the  $O(\kappa \log(\kappa))$  correction, is

$$\begin{aligned} &\pi - \gamma_{\tilde{\mathcal{E}}} - \sin(\gamma_{\tilde{\mathcal{E}}}) \\ &+ \frac{1}{2\pi^2} \left\{ -\gamma_{\tilde{\mathcal{E}}} \cot(\gamma_{\tilde{\mathcal{E}}}) + 1 \right\} \kappa \log(\kappa) + O(\kappa). \end{aligned} \quad (3.67)$$

Note that as  $0 < \kappa < 1$  and  $|\gamma_{\tilde{\mathcal{E}}}| < \pi$ , the corresponding rate is strictly lower than that given by the exponentiation of  $\tilde{\Sigma}(\kappa, \tilde{\mathcal{E}})$ . This is as expected: the inclusive rate at energy  $\tilde{\mathcal{E}}$  is greater than the rate of the specific process at the same energy.

### 3.3.5 Low temperature expansion

I now consider the case of low temperatures,  $\tilde{T} \ll 1$ , but arbitrary coupling,  $\kappa$ . The effect of nonzero temperature is felt through the interaction potential, coupling periodic copies of the circular worldline. Perturbation theory in  $\tilde{T}$  takes the form

$$\begin{aligned}\tilde{S}[x] &= \tilde{S}_0[x] + \tilde{T}^4 \tilde{S}_4[x] + \tilde{T}^6 \tilde{S}_6[x] + \tilde{T}^8 \tilde{S}_8[x] + \dots, \\ x^\mu(\tau) &= x_0^\mu(\tau) + \tilde{T}^4 x_4^\mu(\tau) + \tilde{T}^6 x_6^\mu(\tau) + \tilde{T}^8 x_8^\mu(\tau) + \dots\end{aligned}\quad (3.68)$$

The terms  $\tilde{S}_n[x]$  are simply defined to be the coefficients of  $\tilde{T}^n$  in the full action. Note that: (i) the coefficient of the quadratic term is zero due to the closure of the worldline loops and (ii) the coefficients of all odd powers of  $\tilde{T}$  in  $\tilde{S}[x]$  vanish due to cancellation between loops in the positive and negative Euclidean time directions. These properties of the  $\tilde{S}[x]$  expansion carry over to that of  $x^\mu(\tau)$  by standard perturbation theory.

First order perturbation theory gives

$$\tilde{S}(\kappa, \tilde{T}) = \pi - \frac{\kappa}{4} - \zeta(4)\kappa\tilde{T}^4 - 4\zeta(6)\kappa\tilde{T}^6 + O(\tilde{T}^8). \quad (3.69)$$

The higher order terms contain at least one power of kappa. These first two terms are the same as those coming from the expansion of Eq. (3.58). To calculate the coefficient of the  $O(\tilde{T}^8)$  term requires second order perturbation theory, which amounts to solving a somewhat complicated integrodifferential equation.

As pointed out in Refs. [222, 276], expanding the exponential of Eq. (3.69) captures the two-loop corrections for weak fields and low temperatures (Eq. (76) in Ref. [253] and Eq. (65) in Ref. [256]),

$$e^{-\frac{1}{\epsilon}(\pi - \frac{\kappa}{4} - \zeta(4)\kappa\tilde{T}^4)} \approx \left(1 + \pi\alpha + \frac{2\pi^5\alpha\tilde{T}^4}{45m^4\epsilon^4}\right) e^{-\pi/\epsilon}, \quad (3.70)$$

where  $\alpha = g^2/(4\pi)$ . At higher loop orders one would need to calculate also the semiclassical prefactor for comparison.

The Legendre transform of (3.69) gives the inclusive pair production rate at

fixed, perturbatively low energies. It is

$$\begin{aligned} \tilde{\Sigma}(\kappa, \tilde{\mathcal{E}}) = \pi - \frac{\kappa}{4} - \frac{5\zeta(4)^{1/5}\kappa}{2^{8/5}} \left(\frac{\tilde{\mathcal{E}}}{\kappa}\right)^{4/5} \\ - \frac{\zeta(6)\kappa}{2^{2/5}\zeta(4)^{6/5}} \left(\frac{\tilde{\mathcal{E}}}{\kappa}\right)^{6/5} + O\left(\frac{\tilde{\mathcal{E}}}{\kappa}\right)^{8/5} \end{aligned} \quad (3.71)$$

where the requirement of low temperatures translates into the requirement that  $(\tilde{\mathcal{E}}/\kappa) \ll 1$ .<sup>5</sup>

### 3.3.6 High temperature

At sufficiently high temperatures the process of pair production becomes classical. The instanton is then independent of the Euclidean time direction and is called a sphaleron [243, 244, 94, 95]. The problem reduces from four to three dimensions. Further, due to the irrelevance of the one and two directions ( $\mu = 1, 2$ ) the problem becomes one dimensional. The action gives the Boltzmann factor.

In my case the instanton consists of two worldlines: a stationary charged particle,  $x^\mu(\tau)$ , and its antiparticle,  $y^\mu(\tau')$ , at a fixed distance,  $|x^3(\tau) - y^3(\tau')| = r$ . On such a path the action reduces to

$$\tilde{S}_{\text{Straight}}[r; \kappa, \tilde{T}] = \left(2 - r - \frac{\kappa}{4\pi r}\right) \frac{1}{\tilde{T}}. \quad (3.72)$$

There is an unstable stationary point of the action at  $r_0 = \sqrt{\kappa/4\pi}$  which gives the thermal instanton. The action is then

$$\tilde{S}_{\text{Straight}}(\kappa, \tilde{T}) = 2\left(1 - \sqrt{\frac{\kappa}{4\pi}}\right) \frac{1}{\tilde{T}}, \quad (3.73)$$

which can also be written as  $\tilde{S} = \tilde{\mathcal{E}}/\tilde{T}$ , where  $\tilde{\mathcal{E}}$  is the energy of the solution. Note that as  $\tilde{T} = \epsilon T/m$ , the factors of  $\epsilon$  cancel in the exponent of the rate leaving just the usual Boltzmann suppression in physical units.

The instanton may give the rate of thermal pair production when it is the lowest action solution for given parameters  $(\kappa, \tilde{T})$ . In a broad class of theories, though not including SQED or QED, it has been shown that a solution must satisfy a further constraint for it to describe tunnelling: the spectrum of linear perturbations

---

<sup>5</sup>The structure of this expansion is reminiscent of diagrammatic low energy expansions about instantons, such as arose in the discussion of electroweak baryon number conservation (see for example [186, 278]).

about the solution must have one negative mode [192]. Loosely speaking, this is because only when there is a single negative mode does the solution correspond to the minimum barrier penetration path. Variation of  $r$  is one negative mode, present for all  $\kappa$  and  $\tilde{T}$ .

Due to the periodic boundary conditions, the components of both worldlines are each expressible as a Fourier series. I define  $\zeta^\mu(\tau) := x^\mu(\tau) - y^\mu(\tau)$  and  $\xi^\mu(\tau) := x^\mu(\tau) + y^\mu(\tau)$ . The linearised eigenvalue equations about the straight line solution inherit the nonlocality of the full action. They are thus linear integrodifferential equations, the expressions being very long, so I omit them here.

For  $\kappa \ll 1$ , the integrands of the nonlocal interactions become highly peaked, approaching delta functions which make the eigenvalue equations local. In this regime the dynamics is nonrelativistic and the eigenvalue equations can be straightforwardly solved. In the spectrum of eigenfunctions there are two sets of potentially unstable linear fluctuations, one given by  $\zeta^3(\tau) = r_0 + \delta \cos(2\pi n\tau)$  and the other by  $\xi^3(\tau) = \delta \sin(2\pi n\tau)$ , where  $\delta \ll 1$ ,  $n \in \mathbb{N}$ , and in each case all other components are zero. The eigenvalues are

$$\lambda_n(\kappa, \tilde{T}) \approx \frac{1}{2}(2\pi n)^2 \tilde{T} - \frac{4\pi}{\sqrt{\pi\kappa\tilde{T}}}. \quad (3.74)$$

The lowest frequency mode is thus least stable, and is unstable when  $\tilde{T} < \tilde{T}_{\lambda_1=0}(\kappa) \approx \sqrt{2}\pi^{-3/4}\kappa^{-1/4}$ . This signals the existence of another solution of lower action which is continuously connected to the straight line solution but which breaks time translation invariance. Hence there is a second order phase transition in the rate at this temperature. The instability is exactly analogous to the Plateau-Rayleigh instability in fluid dynamics [286, 287]; the Gregory-Laflamme instability in black strings [288]; nuclear scission [289] and an instability in vacuum bubbles at finite temperature [243, 244].

These linear fluctuations remain eigenvectors of the full integrodifferential equations at larger values of  $\kappa$ . The eigenvalue of the lowest frequency mode is then somewhat more complicated,

$$\begin{aligned} \lambda_1(\kappa, \tilde{T}) = & \frac{1}{2}(2\pi)^2 \tilde{T} - \frac{2}{3}\pi^2 \kappa \tilde{T}^2 - \frac{2\pi}{\sqrt{\pi\kappa\tilde{T}}} \\ & - 2\pi \left( 1 + \frac{1}{\sqrt{\pi\kappa\tilde{T}}} \right) e^{-\sqrt{\pi\kappa\tilde{T}}}. \end{aligned} \quad (3.75)$$

For the higher frequency modes, the eigenvalue is given by  $\lambda_n(\kappa, \tilde{T}) = n\lambda_1(\kappa, n\tilde{T})$ . The term,  $-\frac{2}{3}\pi^2 \kappa \tilde{T}^2$ , is due to the interactions of each worldline with itself. It is

the much-discussed, electromagnetic self-force [290, 291, 292] and its contribution destabilises the straight worldlines, increasingly so at higher temperatures. This issue has been discussed in a similar context in Ref. [123], where it was argued that the photon-charged particle interaction is modified on sufficiently short scales, so diminishing the self-force.

Setting Eq. (3.75) to zero defines the boundary between stability and instability to the lowest frequency perturbation. The boundary is described by a function,  $\tilde{T}_{\lambda_1=0}(\kappa)$ , consisting of two branches which meet at  $\kappa \approx 3.06534$ . This is shown in Fig. 3.6. For sufficiently small  $\kappa$ , the lower branch coincides with the long wavelength instability found in the nonrelativistic analysis and the upper branch is approximately given by  $\tilde{T}_{\lambda_1=0}(\kappa) \approx 3/\kappa$ . The instability above the upper branch is due to the self-force.

Higher frequency modes are more stable to the long wavelength instability but less stable to the self-force instability. As  $n$  increases the self-force term grows fastest so all sufficiently high harmonics are unstable. This instability is present for all  $\kappa$  and  $\tilde{T}$ . In fact, as this instability only depends on the shape of the worldlines at short distances,  $O(1/(n\tilde{T}))$ , it is present for all smooth worldlines (and likely for more general worldlines too). Due to the translational symmetry in the Euclidean time direction, the unstable harmonics of the sphaleron come in pairs, one a sine and the other a cosine.

The self-force instability may be a sign of the breaking down of the cluster expansion at larger values of  $\kappa$ . In support of this view, the self-force does not arise for  $\kappa \ll 1$  at leading order in  $\kappa$ . In the cluster expansion, only a small number of charged particle worldlines are included. Charged particle loops of size  $\kappa/(8\pi)$  have a small action, due to cancellation between the kinetic and interaction terms. These loops make up the bubbling sea of virtual charged particle pairs, part of the quantum vacuum. Their presence modifies the photon-charge interaction on scales of order  $\kappa/(8\pi)$ , an effect which is not included in the cluster expansion. A quantitative inclusion of these effects is beyond the scope of this chapter but, as argued in Ref. [123], photon-charge interactions should be weaker on scales of order  $\kappa/(4\pi)$  ( $g^2/(4\pi m)$  in dimensionful units) and below. This is interpreted as an effective spreading-out of the charge, which prevents the self-force instability.

For small deviations below the lower branch of  $\tilde{T}_{\lambda_1=0}(\kappa)$ , and for sufficiently small  $\kappa$ , the dynamics is nonrelativistic. In this case the equations of motion can be solved, even beyond the linearised approximation, by straightforward integration.

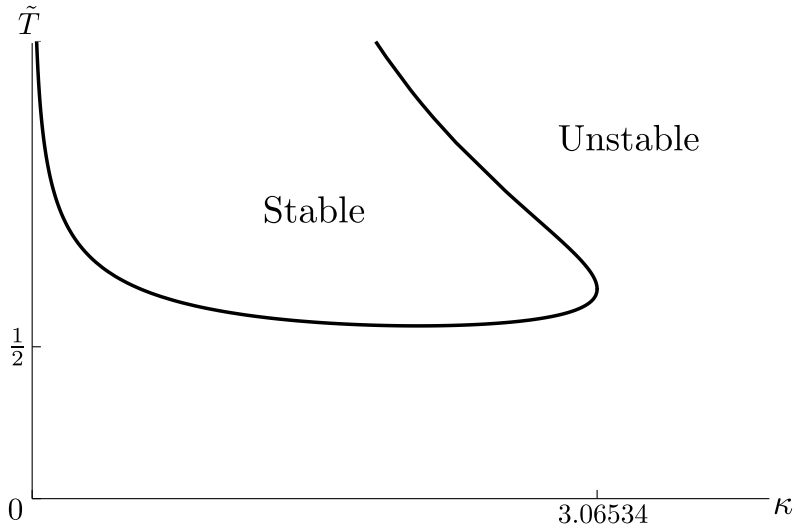


Figure 3.6: Regions within which the straight line instanton is stable and unstable to the lowest frequency perturbations. The boundary is defined by setting Eq. (3.75) to zero and defines a function,  $\tilde{T}_{\lambda_1=0}(\kappa)$ , with two branches. Figure taken from Ref. [1].

The first integral of the motion is the energy,  $\tilde{\mathcal{E}}$ ,

$$-\frac{1}{4}\dot{r}^2 + U(r) = \tilde{\mathcal{E}}, \quad (3.76)$$

where overdot signifies differentiation with respect to the Euclidean time coordinate,  $t$ , and  $U(r) = 2 - r - \kappa/(4\pi r)$ . Integrating this equation gives  $t(r)$ , which can be inverted to give  $r(t)$ . The solutions are periodic, with period  $\tilde{\beta}(\kappa, \tilde{\mathcal{E}})$ .

In the nonrelativistic regime the action is given by

$$\tilde{S}_{\text{Nonrel}}(\kappa, \tilde{T}) = \int_{r_L}^{r_R} \frac{2U(r) - \tilde{\mathcal{E}}}{\sqrt{U(r) - \tilde{\mathcal{E}}}} dr, \quad (3.77)$$

where  $\tilde{\mathcal{E}}$  is treated as a function of  $\tilde{\beta}$  and  $\kappa$  and where  $r_L$  and  $r_R$  are the classical turning points on the left and right. The nonrelativistic approximation is valid for  $\Delta\tilde{T} := \tilde{T}_{\lambda_1=0} - \tilde{T} \ll 1$ , hence I expand the integral thuswise

$$\begin{aligned} \tilde{S}_{\text{Nonrel}}(\kappa, \tilde{T}) &= \tilde{S}_{\text{Straight}}(\kappa, \tilde{T}) - \frac{1}{3}\sqrt{2}\pi^{7/4}\kappa^{5/4}\Delta\tilde{T}^2 \\ &\quad - \frac{41}{54}\pi^{5/2}\kappa^{3/2}\Delta\tilde{T}^3 + O(\Delta\tilde{T}^4), \end{aligned} \quad (3.78)$$

Note that the nonrelativistic solution has a lower action than the straight lines, so

it dominates the rate where it exists,

$$\tilde{S}(\kappa, \tilde{T}) = \begin{cases} \tilde{S}_{\text{Straight}}(\kappa, \tilde{T}) & , \Delta\tilde{T} \leq 0, \\ \tilde{S}_{\text{Nonrel}}(\kappa, \tilde{T}) & , 0 < \Delta\tilde{T} \ll 1. \end{cases}$$

Also note that the difference between the two rates arises at second order in  $\Delta\tilde{T}$ , showing that the transition between the two solutions is a second order phase transition.

The Legendre transform of these results gives

$$\tilde{\Sigma}(\kappa, \tilde{\mathcal{E}}) = \begin{cases} \tilde{\Sigma}_{\text{Straight}}(\kappa, \tilde{\mathcal{E}}) & , \Delta\tilde{\mathcal{E}} \leq 0, \\ \tilde{\Sigma}_{\text{Nonrel}}(\kappa, \tilde{\mathcal{E}}) & , 0 < \Delta\tilde{\mathcal{E}} \ll 1. \end{cases}$$

where  $\Delta\tilde{\mathcal{E}} := \tilde{\mathcal{E}}_c - \tilde{\mathcal{E}}$  and  $\tilde{\mathcal{E}}_c := 2(1 - \sqrt{\kappa/4\pi})$ , the threshold energy. The two functions are

$$\tilde{\Sigma}_{\text{Straight}}(\kappa, \tilde{\mathcal{E}}) = 0, \quad (3.79)$$

and

$$\begin{aligned} \tilde{\Sigma}_{\text{Nonrel}}(\kappa, \tilde{\mathcal{E}}) &= \frac{\pi^{3/4}\kappa^{1/4}}{\sqrt{2}}\Delta\tilde{\mathcal{E}} + \frac{3\pi^{5/4}}{16\sqrt{2}\kappa^{1/4}}\Delta\tilde{\mathcal{E}}^2 \\ &\quad - \frac{5\pi^{7/4}}{256\sqrt{2}\kappa^{3/4}}\Delta\tilde{\mathcal{E}}^3 + O(\Delta\tilde{\mathcal{E}}^4). \end{aligned} \quad (3.80)$$

The inclusive rate of pair production at a fixed energy is unsuppressed at the threshold energy. Just below the threshold,  $\Delta\tilde{\mathcal{E}} \ll 1$ , the suppression is given by the nonrelativistic result here. Note that the leading term in  $\Delta\tilde{\mathcal{E}}$  can be written as  $\Delta\tilde{\mathcal{E}}/\tilde{T}_{\lambda_1=0}$ .

### 3.4 Arbitrary temperature and $\kappa$

For arbitrary temperature and  $\kappa$  there is no symmetry and no small parameter which can help me proceed analytically<sup>6</sup>. As noted in Sec. 3.3.3, the cluster expansion we have made is expected to break down for  $\kappa/(8\pi) \geq O(1)$ . In this section I perform calculations in the range  $\kappa \in [0, 1]$ .

I adopt a numerical approach, in particular I discretise the loop, representing it

---

<sup>6</sup>Note that solutions of the equations of motion are only instantons if their actions are positive. At zero temperature this restricts me to  $\kappa < 4\pi$ . The same condition holds at high temperatures for the straight line instanton.



by a large number,  $N$ , of points,  $x_i$ ,  $i = 0, \dots, N - 1$ , and then write an approximation to the action where derivatives are replaced by finite differences (see Appendix A.5 for details). Note that though the worldline is replaced by a one dimensional lattice of points, there is no spacetime lattice regularisation as the points are not constrained to lie on a spacetime lattice but may lie anywhere in  $\mathbb{R}^4$ , up to numerical accuracy. However, the worldline is itself regularised by a lattice.

The number  $N$  must be chosen such that the distance between neighbouring points,  $|dx_i| := |x_{i+1} - x_i|$ , is much smaller than the smallest scale in the problem, the cutoff,  $a$ . Note that for a continuous worldline, the global reparameterisation symmetry  $\tau \rightarrow \tau + c$  means that  $\dot{x}^2$  is constant. Thus, to leading order in  $1/N$ ,  $|dx_i|$  is independent of  $i$  and hence equal to  $L[x]/N$ , where  $L[x]$  is the length of the loop. Further, the cutoff  $a$  must be chosen to be much smaller than any other scale in the problem. In summary I require

$$\frac{L[x]}{N} \ll a \ll \text{Min}(\kappa, A^{-1}[x; i]), \quad (3.81)$$

where  $A[x; i]$  is the proper acceleration of the worldline at the point  $i$ . Note that the interactions between two disconnected worldlines do not need regularisation, so I may treat them exactly (up to discretisation errors). Computational constraints impose a maximum possible  $N$  ( $\sim 2^{12} = 4096$  in my case). This in turn imposes a minimum  $a$  and hence a minimum  $\kappa$  and a maximum proper acceleration.

The equations of motion are then  $4N$  (ignoring for the moment the symmetries and the zero modes) coupled, nonlinear algebraic equations which I solve numerically. The discretisation is presented in detail in Appendix A.5. A relatively smooth, one dimensional object embedded in a higher dimensional space is aptly described by its Fourier decomposition. However, due to the difficulty of evaluating the non-local interaction term in Fourier space, I adopted a real-space discretisation of the worldline. Starting with an initial guess at the solution I iteratively solve the linearised equations until converging on a solution of the nonlinear equations, i.e. the Newton-Raphson method. The ratio of the norm of the equations of motion (a  $4N$  dimensional vector) to the norm of the solution was used as a measure of convergence. Using this measure, an accuracy of better than  $10^{-7}$  was usually reached in about three iterations. Simpler gradient methods cannot be used here as the solution is a saddle point, having one negative mode.

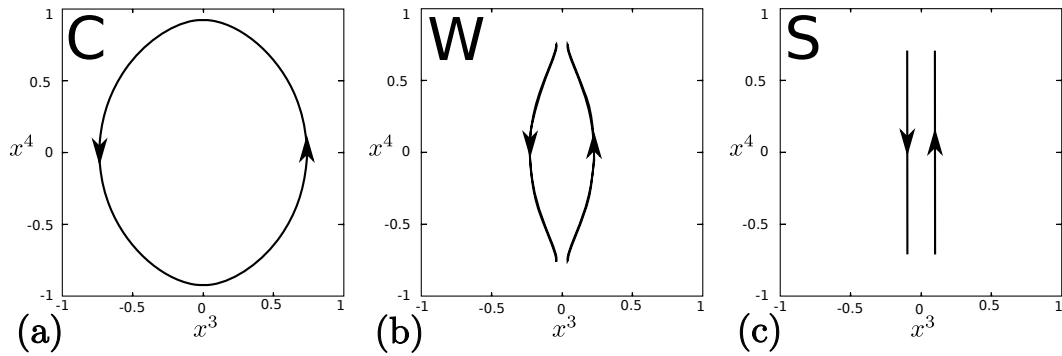


Figure 3.7: Examples of the three types of numerical solutions, all with  $\kappa = 0.5$  and  $a = 0.02$ . From left to right: (a) a C instanton with  $\tilde{T} = 0.5$ ; (b) a W instanton with  $\tilde{T} = 0.66$ ; and (c) an S instanton with  $\tilde{T} = 0.71 \approx \tilde{T}_{\lambda_1=0}$  (lower branch). Figure taken from Ref. [1].

### 3.4.1 Finite temperature results

At low temperatures I can use the zero temperature instanton as an initial guess. Once the iterations have converged, I can then increase the temperature slightly and repeat the procedure using the solution from the last run as the initial guess for the next. In this way I can find all solutions in the  $(\kappa, \tilde{T})$  plane which are continuously connected to the low temperature solutions. These all have the topology of a circle and I refer to them as C instantons.

There are also instantons with the topology of railway tracks: two infinitely long disconnected pieces. In this case, the charged particles do not tunnel from zero distance as the initial (thermal) state has nonzero energy. Over the whole  $(\kappa, \tilde{T})$  plane there exist such solutions consisting of two straight lines (see Sec. 3.3.6) which I refer to as S instantons. Below the lower branch of  $\tilde{T}_{\lambda_1=0}$  (see Fig. 3.6), there exists another class of solutions with this topology and with lower action. These consist of two wavy lines and I refer to them as W instantons. For small  $\kappa$  and for temperatures just below the lower branch of  $\tilde{T}_{\lambda_1=0}$ , I can use the nonrelativistic approximation of Sec. 3.3.6 as an initial guess. From there I can step in  $\kappa$  and  $\tilde{T}$  to find all the continuously connected solutions. As I approach the lower branch of  $\tilde{T}_{\lambda_1=0}$  from below, the W instantons become straighter and merge with the S instantons.

As discussed in Sec. 3.3.3, I must regularise the interaction potential. This introduces a third parameter,  $a$ , the short distance cut off. For each point in the  $(\kappa, \tilde{T})$  plane, I find the corresponding solution for a range of  $a$  and evaluate the action,  $\tilde{S}(\kappa, \tilde{T}; a)$ , and its Legendre transform,  $\tilde{\Sigma}(\kappa, \tilde{T}; a)$ . For small enough  $a$  I

should be able to fit these to a linear function

$$\tilde{S}(\kappa, \tilde{T}; a) \approx \tilde{S}(\kappa, \tilde{T}) + c(\kappa, \tilde{T})a, \quad (3.82)$$

for some  $c(\kappa, \tilde{T})$ . To find  $\tilde{S}(\kappa, \tilde{T})$  I then extrapolate to  $a \rightarrow 0$ , ensuring that the  $a$  dependence is linear (see Fig. 3.11).

The Newton-Raphson method does not converge in the presence of zero modes, essentially because the solution is not unique. As described in Sec. 3.3, I fix the translation zero modes by demanding that the centre of mass of the worldline be at the origin,  $\bar{x}^\mu = 0$ . There is also a fifth zero mode corresponding to the remaining global symmetry of reparameterisation invariance. For worldlines with circular topology I fix this by demanding that  $x_0^3 - x_{N/2-1}^3 = 0$ . Given a suitable initial guess this essentially fixes the point  $x_0$  to be at the bottom of the loop and  $x_{N/2-1}$  to be at the top. In the high temperature case, where the instanton splits up into two separate worldlines, the global part of the reparameterisation invariance must be fixed on each side separately. I do so by demanding that there be a turning point at  $x_0$  on the right hand side and at  $x_{N-1}$  on the left hand side; i.e. I fix the spatial derivative to be zero there. In all cases I use Lagrange multipliers to impose constraints.

In the high temperature case I found that there is also a quazero mode associated with translating one of the halves forward in Euclidean time and the other downwards. The presence of this quazero mode slows the convergence of the Newton-Raphson method. To prevent this slowing down I fixed  $\bar{x}_L^4 = 0$  and  $\bar{x}_R^4 = 0$ , rather than simply  $(\bar{x}_L^4 + \bar{x}_R^4) = 0$  (subscripts  $L$  and  $R$  refer to left and right hand sides). This overconstrains the problem but the solutions thereby found are also solutions of the original problem. Further, from the parity symmetry I expect solutions to satisfy this extra constraint.

In this way I can start to fill in the  $(\kappa, \tilde{T})$  plane with instanton solutions, building up a contour plot of the action and a phase diagram. Each of the three different classes of solutions (C, W and S instantons) has a region of existence and a region within which it has the lowest Euclidean action (the actions denoted respectively by  $\tilde{S}_C$ ,  $\tilde{S}_W$  and  $\tilde{S}_S$ ). If two solutions exist at a given point in the plane, that with lower Euclidean action determines the rate, and hence defines the phase. The semiclassical tunnelling approximation is only valid when the action is positive. Fig. 3.8 is a contour plot of the Euclidean action as calculated numerically.

The phase diagram that emerges is quite interesting. The S instantons exist over the whole  $(\kappa, \tilde{T})$  plane. The C and W instantons do not. Where I have found the W instantons to exist, they have lower action than the S instantons. It also

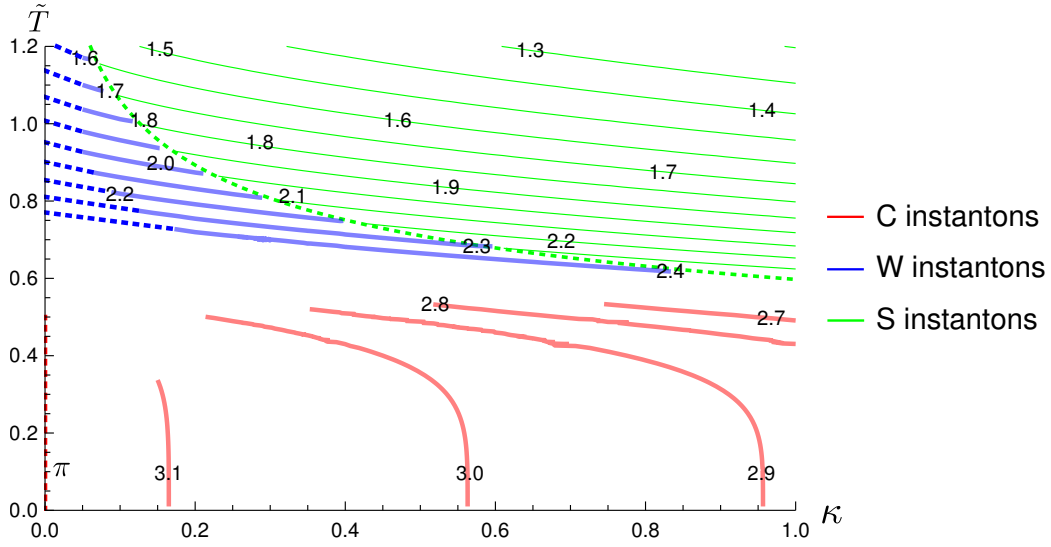


Figure 3.8: Contour plot of the action,  $\tilde{S}(\kappa, \tilde{T})$ , as calculated numerically. The solid red and blue lines are my numerical results and the solid green lines are given by Eq. (3.73). The region in the top right, bounded by the green dotted line, is the region within which the S instanton is the only known solution. The blank region between the solid red and blue lines and for small  $\kappa$  is where I could not maintain the hierarchies of Eq. (3.81) with  $N = 2^{12}$  points. The dashed blue lines are linear extrapolations from the contours found numerically to the same value of the action at  $\kappa = 0$  (Eq. (3.62)). Figure taken from Ref. [1].

seems to be the case for the C instantons. It is the case at  $\kappa = 0$  and I can give an argument for it at  $\kappa = 4\pi$ . The action of the C instantons goes to zero at  $(4\pi, 0)$  whereas that of the S instantons goes to zero at  $(4\pi, 1/\pi)$ . Further, if I can assume that  $\tilde{S}_C$  and  $\tilde{S}_S$  decrease with increasing temperature (i.e. the solutions have positive energy), then, where the C instantons exist for  $\kappa = 4\pi$  and  $\tilde{T} > 0$ , they must have lower action. I have not found numerically a region within which both the C and W instantons exist, though I do expect them to meet as they appear to abut each other on the phase diagram. It may be that they exist in disjoint regions, sharing a boundary of existence, or it may be that they coexist near their phase boundary where my numerical calculations fail.

From Fig. 3.8 I can see the existence of two lines of phase transitions:  $\tilde{T}_{CW}(\kappa)$  separating the C instantons from the W instantons and  $\tilde{T}_{WS}(\kappa)$  separating the W instantons from the S instantons. From my numerical results, within the range of parameters explored, the line defined by  $\tilde{T} = \tilde{T}_{WS}(\kappa)$  appears to coincide with the lower branch of  $\tilde{T}_{\lambda_1=0}(\kappa)$ . This line is a line of second order phase transitions, as discussed in Sec. 3.3.6. The order of the phase transitions at  $\tilde{T} = \tilde{T}_{CW}(\kappa)$  is not clear, except at  $\kappa = 0$ . From Fig. 3.8, and assuming that the W instantons change continuously as  $\kappa \rightarrow 0$ , it appears that the W instantons match up with

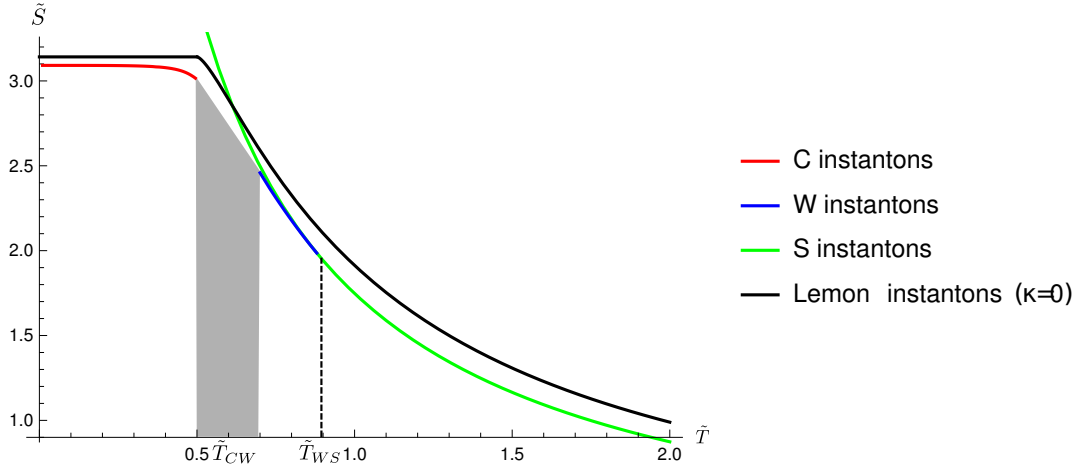


Figure 3.9: A slice through the  $(\kappa, \tilde{T})$  plane at fixed  $\kappa = 0.2$ . The action of the W instantons (blue) is lower than that of the S instantons (green) where they exist. The lemon-shaped instantons are only exact solutions for  $\kappa = 0$ . The expression for their action is  $\pi$  for  $\tilde{T} < 1/2$  and Eq. (3.62) for  $\tilde{T} > 1/2$ . The transition temperature,  $\tilde{T}_{CW}$ , lies somewhere in the grey shaded region. The difficulty in maintaining the hierarchies of Eq. (3.81) has prevented me from calculating it more accurately. Figure taken from Ref. [1].

the lemon instantons in this limit. Thus, at  $\kappa = 0$  the transition between  $C$  and  $W$  instantons is of second order, as discussed in Sec. 3.3.4. At  $\kappa = 0$ , I also have that  $\tilde{T}_{CW}(0) = 1/2$ . Above this I can say nothing precise as, in the region around  $\tilde{T} = \tilde{T}_{CW}$ , I have not been able to maintain the hierarchies of Eq. (3.81). However it appears that  $\tilde{T}_{CW}(\kappa) \approx 1/2$ , at least for  $\kappa \leq 1$ .

For  $(\kappa, \tilde{T})$  outside the region spanned by my numerical calculations (see Fig. 3.8), there is little I can say about the form of the phase diagram. The two lines of phase transitions may cross at some point  $\tilde{T}_{CW}(\kappa_*) = \tilde{T}_{WS}(\kappa_*)$ , which I denote by  $(\kappa_*, \tilde{T}_*)$ , or even at multiple points. Alternatively the line of phase transitions between  $C$  and  $W$  instantons may remain forever below that of  $W$  and  $S$  instantons, i.e.  $\tilde{T}_{CW}(\kappa) < \tilde{T}_{WS}(\kappa)$  for all  $\kappa$ . More work is needed to better understand the phase diagram for larger  $\kappa$  and  $\tilde{T}$ .

For comparison with the analytic results enumerated in Secs. 3.3.4, 3.3.5 and 3.3.6, in Fig. 3.9 I also give a plot comparing the action as a function of  $\tilde{T}$ , for fixed  $\kappa = 0.2$ .

### 3.4.2 Fixed energy results

I also calculate the Legendre transform of these results, which gives the inclusive rate of pair production at a given energy. To calculate the energy of a solution I

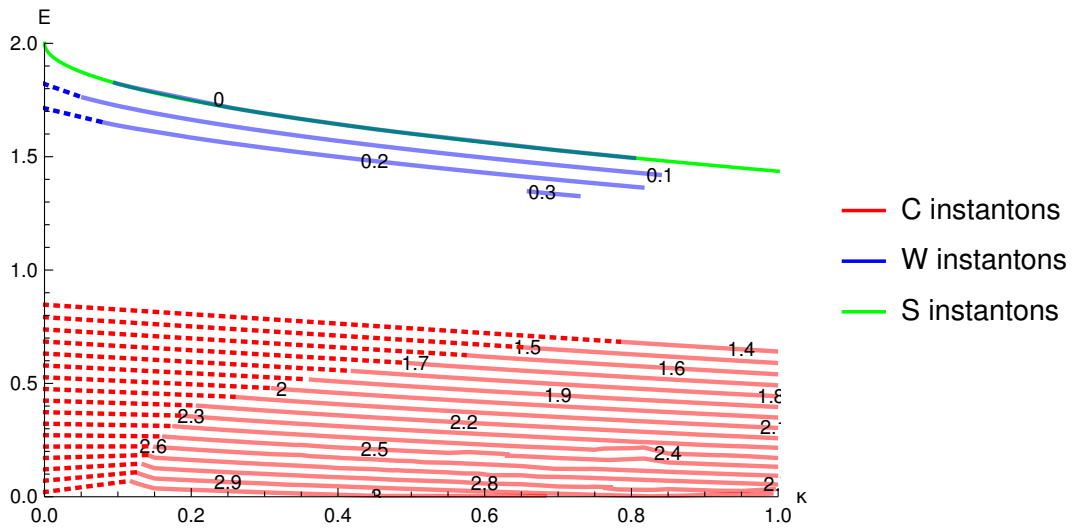


Figure 3.10: Contour plot of  $\tilde{\Sigma}(\kappa, \tilde{\mathcal{E}})$ , the exponential suppression of the inclusive rate of Schwinger pair production at fixed energy. The blank region in the top right, bounded by the green line, is the region within which the exponential suppression of the S instanton is negative. The blank region between the solid red and blue lines and for small  $\kappa$  is where I could not maintain the hierarchies of Eq. (3.81) with  $N = 2^{12}$  points. The dashed blue lines are linear extrapolations from the contours found numerically to the same value of  $\tilde{\Sigma}$  at  $\kappa = 0$  (Eq. (3.66)). Figure taken from Ref. [1].

use Eq. (3.38). Fig. 3.10 is a contour plot in the  $(\kappa, \tilde{\mathcal{E}})$  plane of the exponential suppression,  $\tilde{\Sigma}$ .

At  $\kappa = 0$  the relevant instanton is the lemon-shaped one discussed in Sec. 3.3.4. The corresponding suppression is given by Eq. (3.66) and there is no phase transition for any  $0 < \tilde{\mathcal{E}} < \tilde{\mathcal{E}}_c$ . On the other hand for  $\kappa > 0$  there is a phase transition between the C and W instantons.

In Fig. 3.10 I have also plotted extrapolations from my numerical results to the same value of  $\tilde{\Sigma}$  at  $\kappa = 0$  (Eq. (3.66)). The extrapolations for both C and W instantons look good. How these instantons match onto the lemon instantons at  $\kappa = 0$ , and where the phase transition between them lies, is not clear. Note that for small, nonzero  $\kappa$  and small  $\tilde{\mathcal{E}}$  the leading terms for both C and W instantons agree (Eqs. (3.60) and (3.66)).

### 3.4.3 Numerical errors

For a selection of my numerical solutions I performed various checks. For the C and W instantons I computed the lowest few eigenvalues of perturbations about the solutions and always found that there was one negative mode (in the

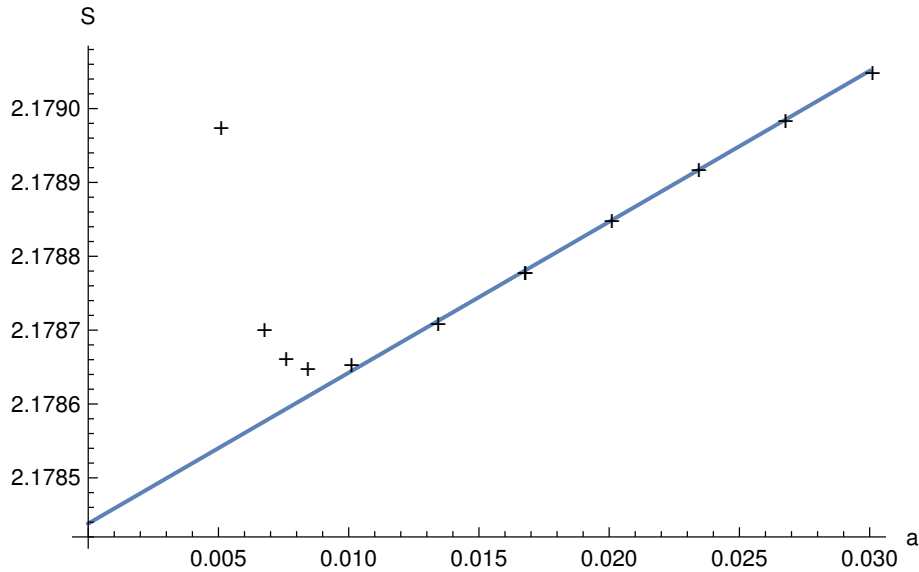


Figure 3.11: Plot of extrapolation of data to remove cutoff,  $a \rightarrow 0$ . Here are plotted data points for  $\tilde{S}(\kappa, \tilde{T}; a)$  for W instantons at  $(\kappa, \tilde{T}) = (0.2, 0.8)$ . The linear extrapolation is also plotted. The wild behaviour at very small  $a$  is expected to be due to the effect of the discreteness scale; here  $L[x]/N \approx 0.0006$ . Figure taken from Ref. [1].

plane), as required for the solution to be interpreted as a tunnelling solution. I also computed the spectrum of eigenvalues about some S instantons, finding one negative eigenvalue for temperatures above the lower branch of  $\tilde{T}_{\lambda_1=0}$  and more than one below this temperature. The apparent absence of the self-force instability due to higher harmonic fluctuations may be due to the cutoff,  $a$ , and due to the discretisation of the worldlines. The conservation of  $\dot{x}^2$  was accurate to about 1 part in  $10^4$  or better. The solutions were found to be symmetric under a rotation by  $\pi$  in the 3-4 plane, to numerical accuracy.

The dominant errors in my numerical calculation are due to the difficulty of maintaining the hierarchies of Eq. (3.81). I have rejected solutions for which  $L[x]/(Na) > 0.15$  or for which  $a/\text{Min}(\kappa, A^{-1}[x; i]) > 0.2$ . The errors due to the finiteness of these quantities manifest in the extrapolation  $a \rightarrow 0$  (see Eq. (3.82)).

See Fig. 3.11. For very small  $a$ , the dependence of the action on  $a$  is strongly nonlinear. This is due to  $a$  becoming comparable with the distance between points,  $L[x]/N$ , and hence the discreteness of the representation of the worldline becomes significant. I implemented an algorithm to fit to only the linear part of the plot. For each point in the  $(\kappa, \tilde{T})$  plane I assemble the data  $\{a, \tilde{S}(\kappa, \tilde{T}; a)\}$  in an array, ordered by the value of  $a$ . I then fit straight lines to all subsets of at least four consecutive data points, ensuring that this covers a range of  $a$  such that the maximum value is at least twice the minimum value. For each fit I calculate the standard error in

the result. For my final result,  $\tilde{S}(\kappa, \tilde{T})$ , I take that with least standard error. I also throw away results for which the standard error due to the fit is greater than 0.01, though in most cases it is much smaller.

For  $\tilde{T} = 0$ , I have both approximate, numerical results and an exact, analytic expression, Eq. (3.48). The difference between the two is found to increase with  $\kappa$  up to about 0.01 at  $\kappa = 1$ , using  $N = 2^{12}$  points. This error scales with the number of points as  $1/N^2$ . I also have an exact, analytic expression for large temperatures, Eq. (3.73). Unfortunately though, for the corresponding instanton, the S instanton, due to the enhanced symmetry the zero modes corresponding to time translation and to reparameterisation invariance cannot be fixed as for the other instantons, preventing convergence of the Newton-Raphson method.

As I approach the phase transition between C and W instantons,  $\tilde{T}_{CW}(\kappa)$ , it becomes more difficult to maintain the hierarchies of Eq. (3.81). Hence I expect errors there to be greater.

### 3.5 Summary

In this chapter, I have extended previous results on Schwinger pair production to arbitrary couplings and arbitrary temperatures. To achieve this I restricted myself to weak, constant external fields. This restriction was shown to result in a semiclassical approximation and within this approximation I have calculated the leading behaviour of the logarithm of the rate. As a by-product, I was also able to obtain inclusive pair production rates at fixed energy.

I adopted the worldline description. In this framework the problem reduced to one of solving the instanton equations of motion for a self-interacting worldline, an interesting geometric problem.

For weak couplings, like in QED, my results complement the extensive literature on the subject, providing an alternative approach which holds at all temperatures and in which some issues are clearer. In this case  $\kappa < \epsilon$  and my approach, which includes all orders in  $\kappa$  but just the leading order in  $\epsilon$ , does not seem necessary. However, as I have discussed, the singular nature of the small  $\kappa$  perturbation means that one ought not to simply set  $\kappa = 0$  from the outset. Doing this may lead to the incorrect instanton and hence to incorrect results at leading order in  $\epsilon$ .

In this weak coupling regime, and at temperatures  $\tilde{T} < 1/2$ , my results give small corrections to the leading order results. When expanded they capture the two-loop, thermal correction for weak fields. I also find no thermal correction at one-loop



in this temperature range. Though I have calculated analytically the correction to the exponent to leading and next to leading order in  $\kappa$ , a full calculation of higher order loop corrections would require also the thermal corrections to the prefactor.

At higher temperatures,  $\tilde{T} > 1/2$ , the singular nature of the weak coupling expansion gives nontrivial corrections to the naive  $\kappa \rightarrow 0$  limit. My numerical solutions at finite  $\kappa$  appear to approach the well-known lemon-shaped instanton as  $\kappa \rightarrow 0$ . At leading order, this solution gives a nonzero thermal enhancement to the rate. Note however that this enhancement is not present in the one-loop approximation, which breaks down due to the singular nature of the weak coupling expansion. The lemon-shaped instanton also shows an enhanced correction to the exponential suppression of order  $\kappa \log(\kappa)/\epsilon$ . This dominates over the order  $\epsilon^0$  correction for sufficiently small  $\epsilon$ .

At intermediate and strong couplings the results open new avenues. Using them one can make reliable estimates for the pair production rate of strongly charged particles via the thermal Schwinger process. In particular one could apply these results to the pair production of magnetic monopoles. Sufficiently light magnetic monopoles would be produced amply in the strong magnetic fields and high temperatures present in heavy ion collisions, in neutron stars and in the early Universe.

In this chapter I have only calculated the exponential suppression of the rate. For direct phenomenological application, one should also calculate the prefactor. Refs. [280, 293, 294] would be an apt place to start. They all find similar instantons to those in this chapter, though in theories without dynamical long-range forces. For the S instanton, I calculate the prefactor in the following chapter.

The appearance of the self-force instability in the semiclassical evaluation of the path integral raises some intriguing questions that require further work. This I pursue further in the following chapter.

The worldline description that I have developed here could be used to calculate pair production rates for other induced Schwinger processes at arbitrary coupling. For example one could consider a nonconstant external field. The numerical approach I have adopted would then directly apply.

# Chapter 4

## Magnetic monopole mass bounds

As discussed in Sec. 1.4 there have been many searches for magnetic monopoles [68, 69], but so far none have been found. Astrophysical [70, 71, 72] and cosmic ray [73, 74, 75, 76, 77] searches have provided constraints on the monopole flux in the Universe, and collider searches [78, 89, 81, 90, 295] have constrained the production cross section over a given mass range. However, in the absence of reliable theoretical predictions for the flux or the cross section, these cannot be converted into direct bounds on the monopole mass.

Further, as discussed in Chapter 2, it is expected that cross sections for production of composite magnetic monopoles from few particle collisions are strongly exponentially suppressed (see Eq. (2.1)). If this suppression is indeed present, it would effectively rule out the production of composite magnetic monopoles in, for example, proton-proton collisions at the Large Hadron Collider (LHC). For elementary (Dirac) monopoles the arguments of Refs. [104, 65] do not apply and cross sections for pair production are completely unknown.

The thermal Schwinger process, discussed in Chapter 3, provides an alternate mechanism to create magnetic monopoles. Although the rate is indeed exponentially suppressed for weak magnetic fields and low temperatures, the exponential suppression diminishes with increasing magnetic field strengths and temperatures. For sufficiently strong magnetic fields or sufficiently high temperatures, it is expected that magnetic monopoles will be produced amply. I suggest that this is because the energy is spread across many degrees of freedom in the initial state. This is what was found in the case of  $(B+L)$  violation [92, 93, 95, 106, 107, 296] (see Sec. 2.2.1), in the language of which the higher temperature process I consider is a sphaleron induced decay.

Strong magnetic fields and high temperatures arise, for example, in heavy ion collisions and around neutron stars. In this chapter I explore the consequences of

this. I construct the cross section for pair production of magnetic monopoles in heavy ion collisions. By comparison to an experimental upper bound on the cross section [91], I derive lower bounds on the mass of possible magnetic monopoles. Further, in the strong, long-lived magnetic fields present around neutron stars, sufficiently light magnetic monopoles would be produced and would dissipate the magnetic field. By comparison with the observed magnetic field strengths I derive another set of lower mass bounds. These bounds are model-independent in the sense that they apply to both elementary and composite (e.g. 't Hooft-Polyakov) monopoles and do not rely on (inapplicable) perturbation theory. However, as I will show in Chapter 5 an instability present in higher order corrections to the rate casts doubt on these conclusions. In this chapter though, I will take the rates as derived in Chapter 3 at face value, leaving discussion of the validity of this approach until Chapter 5.

For comparison to the bounds derived here, the current best, model-independent, lower bound on the mass of magnetic monopoles derives from thermal production of magnetic monopoles during reheating. As discussed in Sec. 1.4, due to the huge uncertainty in the reheating temperature, the bound is surprisingly weak,  $m \gtrsim 0.45\text{GeV}$ .

I briefly summarise the results of Chapter 3 for use in this chapter, referring explicitly to an external magnetic field. I show the dependence on: the magnetic coupling,  $g$ ; the external magnetic field,  $B$ ; the mass of the magnetic monopoles,  $m$ ; and the temperature,  $T$ . The results of Chapter 3 are valid for sufficiently heavy magnetic monopoles in slowly varying external magnetic fields, in which case the semiclassical approximation applies. The small semiclassical parameter in the calculation, akin to  $\hbar$ , is  $gB/m^2$ . In the leading semiclassical approximation, the rate of pair production per unit volume,  $\Gamma_T$ , is of the form

$$\log(\Gamma_T) = -\frac{m^2}{gB} \left\{ \tilde{S}(g, m, B, T) + O\left(\frac{gB}{m^2} \log\left(\frac{gB}{m^2}\right)\right) \right\}. \quad (4.1)$$

where  $m^2 \gg gB$  and the action,  $\tilde{S}$ , is a function only of the dimensionless ratios  $g^3B/m^2$  and  $mT/gB$ . It is not smooth, having discontinuities which can be described as phase transitions. In Chapter 3 it was calculated analytically in various limits as well as numerically.

Within these approximations, when  $m^2 \gg gB$  and the external field is slowly varying, any spin of the magnetic monopoles is invisible (see Appendix A.3). For composite monopoles I must also assume that the monopoles are small compared with other scales in the problem (see Appendix A.4). For the usual grand unified theory monopoles, this approximation fails when  $m^2 \lesssim g^3B/(4\pi)$ . For elementary

monopoles, virtual monopole pairs will modify the photon-monopole interaction on sufficiently short scales. One can make a simple estimate of the scales at which this effect becomes significant by setting the rest mass of a monopole pair equal to the Coulomb attraction. This defines the scale  $r \sim g^2/(8\pi m)$ . The semiclassical calculation of Chapter 3, which does not fully include this effect, thus breaks down when the scale of the instanton probes these short length scales, i.e. when  $m^2 \lesssim g^3 B/(8\pi)$ .

In this chapter, I will be interested in two particular cases. For heavy ion collisions, the relevant temperatures are high (see Sec. 3.3.6). When  $m^2 \gtrsim g^3 B$ , high temperatures are such that  $T \gtrsim \sqrt{2}\pi^{-3/4}(gB^3/m^2)^{1/4}$ . In this regime the action is given by Eq. (3.73), or expressed in terms of dimensionful parameters,

$$\tilde{S}(g, m, B, T) = 2 \left( 1 - \sqrt{\frac{g^3 B}{4\pi m^2}} \right) \frac{gB}{mT}. \quad (4.2)$$

When  $g^3 B/m^2$  is larger, it may be that the action is smaller than that given by Eq. (4.2). This depends on the nature of the phase diagram as discussed in Chapter 3. However, the action cannot be larger than that given by Eq. (4.2) and hence the rate of pair production cannot be lower, within the semiclassical approximation.

For neutron stars the relevant temperatures are low,  $T \ll gB/m$  (see Sec. 3.3.5). In this case the action is given by Eq. (3.69), or expressed in terms of dimensionful parameters,

$$\begin{aligned} \tilde{S}(g, m, B, T) = \pi - \frac{g^3 B}{4m^2} - \zeta(4) \frac{g^3 B}{m^2} \left( \frac{mT}{gB} \right)^4 \\ - 4\zeta(6) \frac{g^3 B}{m^2} \left( \frac{mT}{gB} \right)^6 + O \left( \frac{mT}{gB} \right)^8. \end{aligned} \quad (4.3)$$

At zero temperature, and at leading order in  $g^3 B/m^2$ , the leading and next to leading corrections to the logarithm of the rate have been calculated [25, 221]. Together they give the rate, Eq. (3.49), or expressed in terms of dimensionful parameters,

$$\Gamma_0 = (2s + 1) \frac{g^2 B^2}{8\pi^3} e^{-\frac{\pi m^2}{gB} + \frac{g^2}{4}} \left( 1 + O \left( \frac{g^3 B}{m^2} \right) \right), \quad (4.4)$$

where  $s$  is the spin of the charged particle.

## 4.1 Heavy ion collisions

In a high energy heavy ion collision a fireball is created which thermalises quickly and within which there are strong magnetic fields because of the fast-moving electrically charged nuclei [297, 298, 299, 300, 301, 302]. The presence of both the thermal bath and the magnetic fields means that thermal Schwinger pair production of magnetic monopoles is possible. However, only sufficiently light magnetic monopoles will be produced in measurable quantities.

For a given event, with impact parameter  $b$ , the fireball will be contained in some spacetime region,  $\mathcal{R}(b)$ . If the temperature,  $T(x; b)$ , and magnetic field,  $B(x; b)$  are sufficiently slowly varying, then to find the total probability,  $p(b)$ , that a pair of magnetic monopoles is produced in a given collision, I can simply integrate the rate over the spacetime volume of the fireball,

$$p(b) = \int_{\mathcal{R}(b)} d^4x \Gamma_T(m, g, B(x; b), T(x; b)). \quad (4.5)$$

From this I can write down the cross section for pair production,

$$\sigma_{M\bar{M}} = \int db \frac{d\sigma_{HI}^{\text{inel}}}{db} p(b), \quad (4.6)$$

where  $d\sigma_{HI}^{\text{inel}}/db$  is the total, differential, inelastic cross section for the relevant heavy ion collision. Due to the exponential dependence of  $\Gamma_T$  on the magnetic field and temperature, all of these integrals can be carried out in the stationary phase approximation. However, as I have thus far only calculated the logarithm of the rate to leading order in  $gB/m^2$ , I will instead make the following simple estimate

$$\sigma_{M\bar{M}} \approx \sigma_{HI}^{\text{inel}} \mathcal{V} \Gamma_T(m, g, B, T), \quad (4.7)$$

where  $\mathcal{V}$  is the spacetime volume of a typical collision and  $B$  and  $T$  are taken to be the maximum values of the functions  $B(x; b)$  and  $T(x; b)$  respectively. This expression should capture the approximate order of magnitude of the result.

In heavy ion collisions there have been both direct searches for magnetic monopoles [91] and (preliminary) searches for trapped monopoles in obsolete parts of the beam pipe [303, 304]. Ref. [91] reported the results of a search at the Super Proton Synchrotron (SPS) for magnetic monopoles in fixed-target lead ion collisions with beam energy 160A GeV. In this, they derived an upper bound on the magnetic monopole pair production cross section,  $\sigma_{M\bar{M}} < \sigma_{M\bar{M}}^{UB} = 1.9\text{nb}$ . By comparing this with Eq.

(4.7), I can derive a lower bound on the mass of any possible magnetic monopoles.

Assuming that the prefactor of  $\Gamma_T$  (as in  $A$  in Ref. [270]) multiplied by  $\mathcal{V}$  is not exponentially large in  $m^2/gB$ , I arrive at

$$\log \left( \frac{\sigma_{HI}^{\text{inel}}}{\sigma_{MM}^{UB}} \right) \lesssim \frac{m^2}{gB} \tilde{S}(g, m, B, T). \quad (4.8)$$

The magnetic field strength in lead ion collisions at these energies was estimated to be  $B_{160\text{GeV}} \approx 0.0097\text{GeV}^2$  [298]. From an analysis of the spectrum of neutral pions, the temperature was estimated to be  $T_{160\text{GeV}} \approx 0.185\text{GeV}$  [305]. I take  $\sigma_{HI}^{\text{inel}} \approx 6.3b$ , the minimum-bias cross section for the experiment [306].

Substituting Eq. (4.2) and the parameters into Eq. (4.8) leads to the following bound on the mass of any magnetic monopoles

$$m \gtrsim \left( 2.0 + 2.6 \left( \frac{g}{g_D} \right)^{3/2} \right) \text{GeV}. \quad (4.9)$$

Note that the experiment was only sensitive to magnetic charges  $g \geq 2g_D$ . For  $g = 2g_D$  the bound reads  $m \gtrsim 9.5\text{GeV}$ .

The semiclassical approximation, made in deriving Eq. (4.9), requires that the exponential suppression be large. At the lower bound this amounts to  $22 \gg 1$ . The approximation of constant magnetic field requires that the magnetic field varies significantly on time and length scales much larger than those of the instanton. The instanton has a spatial extent of  $\sqrt{g/4\pi B} \approx 18\text{GeV}^{-1}$  for  $g = 2g_D$  in the direction of the magnetic field (transverse to the beam) and a temporal extent of  $1/T \approx 5.4\text{GeV}^{-1}$ . At SPS energies the magnetic field varies significantly over the length and timescales of the fireball. The transverse size of the fireball is of the order of the size of a lead nucleus,  $2R_{Pb} \approx 100\text{GeV}^{-1}$ , which is somewhat larger than the spatial size of the instanton. The lifetime of the magnetic field,  $t_B \approx 2R_{Pb}/\gamma \approx 11\text{GeV}^{-1}$ , is reduced by,  $\gamma$ , the Lorentz factor in the centre of mass frame [299, 301, 302] (though it has been suggested that the lifetime may be longer [307, 308, 309]). This lifetime,  $t_B$ , is somewhat larger than the temporal extent of the instanton.

At higher energies one would expect to produce higher mass magnetic monopoles, if such particles exist. The magnetic field strength increases linearly with the centre of mass energy,  $\sqrt{s}$ , [300, 299, 301] and the temperature increases approximately as a small power [310] both effects increasing the range of accessible masses. However at higher energies the magnetic field becomes more transient, its lifetime being proportional to  $1/\sqrt{s}$ . This leads to a breakdown of the constant field approximation.

To account for this, the calculation of Chapter 3 would need to be modified. One would expect the temporal variation of the magnetic field to increase the rate of pair production, and spatial variation to decrease it [311, 312, 313, 314, 283].

There is promise for magnetic monopole searches in the next scheduled Pb-Pb collisions at the LHC in 2018, at which ALICE, ATLAS, CMS, LHCb and MoEDAL may be able to detect monopoles. The trapping detectors of MoEDAL are ideally suited for this because they have no background noise [90]. I make the simple, though perhaps naive, assumption that the rate derived for a constant magnetic field provides a lower bound on the true rate. Using the magnetic field,  $B \approx 1.1\text{GeV}^2$ , and integrated luminosity,  $L_{int} \approx 4\mu\text{b}^{-1}$ , from the 2015 lead ion collisions at  $\sqrt{s_{NN}} = 5.02\text{TeV}$  [315] and the temperature,  $T \approx 0.30\text{GeV}$ , and cross section,  $\sigma_{HI}^{inel} \approx 7.7\text{b}$ , from the lower energy collisions in 2010-2011 [316, 317], and assuming an acceptance better than or equal to  $O(10^{-4})$ , I would predict that magnetic monopoles with masses up to approximately  $(1+28(g/g_D)^{3/2})\text{GeV}$  could be experimentally observed.

Note that the rate of magnetic monopole pair production in heavy ion collisions has been discussed before in [318, 319]. They also consider thermal production, though they do not include the effect of the magnetic field.

## 4.2 Neutron stars

There are also strong magnetic fields and high temperatures in neutron stars. Magnetic fields have been estimated to be up to  $B_{\text{Magnetar}} \approx 10^{-4}\text{GeV}^2$  [320] for the so called magnetars. The temperatures of such neutron stars lie in the range  $10^{-8}\text{GeV}$  to  $10^{-6}\text{GeV}$  for most of the stars' lifetime, though in the early stages they can be as high as  $10^{-2}\text{GeV}$  [321, 322].

Magnetic monopoles present in such circumstances would be accelerated by the magnetic field thuswise dissipating its energy. A calculation of this effect can be used to put upper bounds on the number density of magnetic monopoles [70, 71, 72, 323]. I can go a step further and equate the number density to that produced by thermal Schwinger pair production, and thuswise bound the mass of any magnetic monopoles.

The magnetic field of a neutron star can be approximated as dipolar [324]. I focus on the magnetic fields above the surface of the star, which are fairly well established. I assume that on the microscopic scale  $m/gB$  the magnetic field can be treated as constant. Note that, due to the superconducting core, the internal magnetic fields would be contained into flux tubes increasing the field strength

locally and enhancing the production rate. Hence a consideration of the interior of the neutron star may lead to stronger bounds [323], though one would need to consider interactions between magnetic monopoles and matter particles [325, 326, 327, 328, 329].

I consider typical neutron star mass and radius parameters,  $M_{NS} = 1.4M_{\odot}$  and  $R \approx 1.0 \times 10^{20} \text{GeV}^{-1}$  respectively. At the surface of the star, where the gravitational field is strongest, the ratio of gravitational to magnetic forces on such a magnetic monopole is

$$\frac{F_G}{F_B} \approx \frac{G_N M_{NS} m}{g B R^2} \approx 7.14 \times 10^{-19} \left( \frac{g_D}{g} \right) \left( \frac{m}{\text{GeV}} \right), \quad (4.10)$$

where  $G_N$  is Newton's constant. So, for magnetic monopoles with masses much less than  $10^{19} \text{GeV}$ , the magnetic force dominates over the gravitational one. In this regime magnetic monopoles will be accelerated by the magnetic field over a timescale  $O(m/gB)$  to nearly the speed of light and will escape both the gravitational attraction of the star and the dipolar magnetic field, leaving with a kinetic energy  $O(gBR)$ . Due to their inertia, the magnetic monopoles do not follow the dipolar magnetic field lines back round into the neutron star but follow straighter, unbound trajectories, as can be checked by integrating the dual Lorentz force law with suitable parameters.

Locally the energy density of the magnetic field and thermal bath act as a source of magnetic monopoles. If the density of magnetic monopoles is low enough, which indeed it will turn out to be, I can ignore their annihilation and hence

$$\nabla_{\mu} n^{\mu} = \Gamma_T, \quad (4.11)$$

where  $n^{\mu} := n_c u^{\mu}$ ,  $n_c$  is the (comoving) number density of magnetic monopoles and  $u^{\mu}$  is their fluid velocity. Now consider a spatial region just above the surface of the neutron star, small enough so that across it the magnetic field and temperature can be treated as approximately constant but large enough so that its spatial dimensions are all large compared with the low temperature instanton size,  $m/gB$ . I denote the area of the surface by  $A$  and the volume by  $V$ . Integrating Eq. (4.11) over this spatial region gives

$$\frac{dN}{dt} \approx V \Gamma_T - \alpha A n u, \quad (4.12)$$

where  $N = nV$  is the number of magnetic monopoles in the spatial region,  $n := n^0$  is the number density measured in the frame of the neutron star,  $u$  is the spatial velocity in the same frame and  $\alpha$  is a numerical coefficient of order 1, the fraction



of the surface area through which magnetic monopoles may escape. The magnetic current will be aligned with the magnetic field and  $u \approx 1$ .

At equilibrium, the rate of change of  $N$  with time will be zero, hence the number density of magnetic monopoles is equal to

$$n \approx \frac{V\Gamma_T}{\alpha A}. \quad (4.13)$$

I define by  $r := V/\alpha A$ , the coefficient in front of  $\Gamma_T$ , which is of the order of the radius of the spatial region. The presence of the magnetic monopoles, being accelerated by the magnetic field, will dissipate the energy of the magnetic field at a rate

$$\frac{d}{dt} \left( \frac{1}{2} B^2 \right) = -\mathbf{J}_M \cdot \mathbf{B} \quad (4.14)$$

where  $\mathbf{J}_M = gn\mathbf{u}$ . Using that  $\mathbf{J}_M \cdot \mathbf{B} \approx gnB$  and Eq. (4.13) this simplifies to

$$\frac{dB}{dt} \approx -gr\Gamma_T. \quad (4.15)$$

This dissipation will provide a ceiling for the growth of the magnetic field. Consider a simplified model of the *fast dynamo process*, argued in [330] to be responsible for the strong magnetic fields in magnetars. In the presence of this process the rate of change of the magnetic field is modified to

$$\frac{dB}{dt} \approx -gr\Gamma_T + \frac{B}{2\tau_D}, \quad (4.16)$$

where  $\tau_D$  is the characteristic enhancement time of the dynamo. For sufficiently small magnetic fields the rate,  $\Gamma_T$ , is strongly exponentially suppressed and the dynamo action dominates. Conversely, the exponential dependence of  $\Gamma_T$  on  $B$  means that  $\Gamma_T$  will always dominate at sufficiently large values of  $B$ . In between is the point of maximum  $B$ , at which the two effects are equal and the right hand side of Eq. (4.16) is zero. This argument is sound if the semiclassical approximation still holds at this point.

The rate  $\Gamma_T$  is bounded below by the rate at zero temperature, Eq. (3.49). Thus I may use this to bound the effect of the dissipation of  $B$  due to the creation of magnetic monopoles. Equating the right hand side of (4.16) to zero, and using this zero temperature rate, I derive the following bound,

$$B \lesssim \frac{\pi m^2}{gW \left( \frac{e^{\frac{g^2}{4}} (2s+1) g^2 m^2 r \tau_D}{4\pi^2} \right)}, \quad (4.17)$$

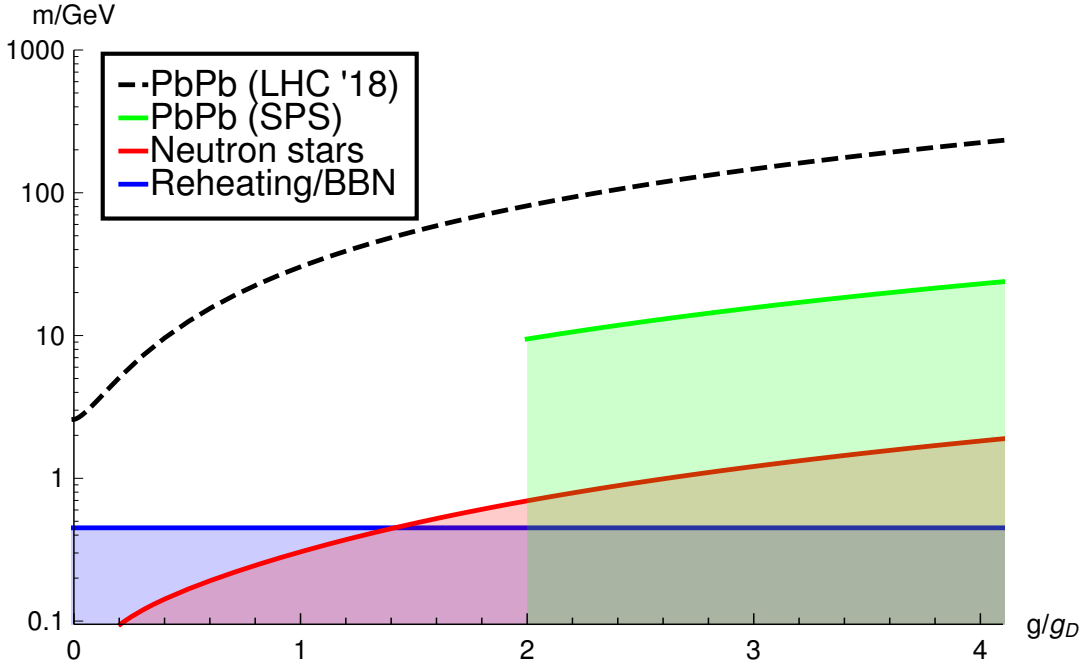


Figure 4.1: Summary of the lower bounds for the mass of magnetic monopoles. The dotted line is a projection.

where  $W$  is the principal part of the Lambert-W function. Inverting the argument which led to the maximum magnetic field, I may use the observation of a strong magnetic field to give a lower bound on the mass of possible magnetic monopoles,

$$m \gtrsim \sqrt{\frac{gB}{\pi} \left[ \frac{g^2}{4} + \log \left( \frac{(2s+1)g^3 Br \tau_D}{4\pi^3} \right) \right]}. \quad (4.18)$$

So, the largest bounds will be found from the observation of strong magnetic fields,  $B$ , existing over large spatial extents,  $r$ , and created by processes with long characteristic times,  $\tau_D$ . Note though that the dependence on  $s$ ,  $r$  and  $\tau_D$  is only logarithmic and hence the dependence on  $B$  dominates.

If I take  $r \approx R/10$ , a tenth the radius of the neutron star, and  $\tau_D \approx 1.5 \times 10^{21} \text{GeV}^{-1}$  (one millisecond, a short characteristic dynamo time) and  $B \approx B_{\text{Magnetar}}$ , I derive the following lower bounds:  $m \gtrsim 0.30 \text{GeV}$  for  $g = g_D$  and  $m \gtrsim 0.69 \text{GeV}$  for  $g = 2g_D$ . More generally we find that the following equation provides a good approximation:

$$m \gtrsim \left( 0.05 + 0.22 \left( \frac{g}{g_D} \right)^{3/2} \right) \text{GeV}. \quad (4.19)$$

If there were to exist magnetic monopoles lighter than these lower bounds, their production and acceleration would strongly dissipate the magnetic field before it could

ever reach  $B_{\text{Magnetar}}$ . Note that for the bounding values the exponential suppression is numerically about  $87 \gg 1$ , and hence the semiclassical approximation is valid.

A similar approach to that I have presented here was given recently in Ref. [331], though they considered somewhat different types of particles.

### 4.3 Summary

From the arguments of this chapter, magnetic monopoles with masses below those indicated in Fig. 4.1 cannot exist in nature. My key approximations, that the relevant magnetic fields are sufficiently weak and slowly varying, appear more or less justified. However, as mentioned in the introduction to this chapter, in calculating higher order corrections to the rate used here, one encounters an instability which casts doubt on the validity of the approximations. This will be discussed more fully in the following chapter.

Future higher energy heavy ion collisions can improve these bounds significantly though, at higher energies, accounting for the spacetime dependence of the magnetic field requires further theoretical work. Further, an understanding of the kinematic distribution of the created monopoles is important for comparison with experiments. In neutron stars, a consideration of the superconducting regions below the surface may lead to significant improvements in the lower mass bounds, though in this case monopole-matter interactions would have to be accounted for.

# Chapter 5

## Thermal Schwinger sphaleron

As discussed in Chapter 3, at zero temperature Schwinger pair production is determined by a circular worldline instanton. At nonzero temperatures the rate of this process is enhanced by the energy of the thermal bath, and the worldline instanton is deformed away from circular. At sufficiently high temperatures the process becomes essentially thermal and is determined by a worldline sphaleron<sup>1</sup> (which, in Chapter 3, I referred to as the S instanton). In this chapter I briefly review the derivation of the worldline sphaleron and then calculate the sphaleron rate, including the fluctuation prefactor.

Following the work in Chapter 3, my calculations will be carried out in both quantum electrodynamics (QED) and scalar quantum electrodynamics (SQED), for strong charge coupling,  $g^2 \gg 1$ . In SQED I will assume that the scalar self-coupling is weak,  $\lambda \ll 1$ . I consider circumstances when the calculation is semiclassical and hence the rate is slow. In this regime the results are independent of many properties of the charged particles. The results are applicable to the dual Schwinger process, the creation of magnetic monopoles in magnetic fields. The electric and magnetic production rates are related by simply swapping electric and magnetic quantities in the final result. The results are applicable to both elementary and composite monopoles (see Appendix A.4).

Unlike the zero temperature worldline instanton of the Schwinger process, the worldline sphaleron is not visible at any finite loop order. If I denote symbolically the interaction between the dynamical (as opposed to external) photon field and the charged particles as  $J \cdot A$ , then the loop expansion of the Schwinger rate,  $\Gamma$ , takes

---

<sup>1</sup>Note that the worldline sphaleron referred to in this chapter is not the original sphaleron of Refs. [94, 95], though it is closely analogous.

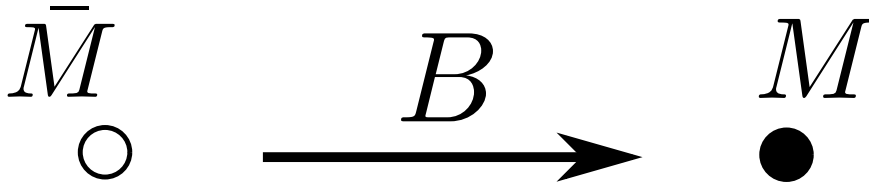


Figure 5.1: The simple worldline sphaleron, for the dual thermal Schwinger process. The attraction between monopole and antimonopole is balanced by the external magnetic field,  $B$ , which pushes them apart.

the form,

$$\Gamma \sim \sum_{n=0}^{\infty} \langle c_n (J \cdot A)^n \rangle. \quad (5.1)$$

The leading term,  $c_0$ , gives the one loop result, that of Schwinger [201] or, at finite temperature, Refs. [249, 247, 250, 251, 332, 242, 333, 334, 281, 282]. The next order term has also been calculated, both at zero [253, 254, 222, 255] and at finite but low temperature [256]. Now, the presence of the sphaleron requires the interaction  $J \cdot A$  in the exponent of the semiclassical expansion. Hence, it requires all orders in the loop expansion.

Despite this, the worldline sphaleron itself is rather simple. The electric version consists of an electron and a positron a finite distance apart, such that the force of interaction between them is balanced by the force of the external electric field pushing them apart. The magnetic version is the electromagnetic dual of this. It is shown in Fig. 5.1.

My interest in calculating the sphaleron rate of the thermal Schwinger process is for its relevance to the production of magnetic monopoles in heavy ion collisions, as discussed in Chapter 4. As such I will refer only to magnetic charges in the rest of this chapter, though the results are equally applicable to electric particles. The minimum magnetic charge squared is  $g_D^2 = (2\pi/e)^2 \approx 430$ , so  $g^2 \gg 1$  is well satisfied. In the fireball of a heavy ion collision there are strong magnetic fields and high temperatures. Hence, magnetic monopoles may be produced by the dual thermal Schwinger process. There is much promise for magnetic monopole searches in current and future heavy ion collisions, in particular the MoEDAL experiment [90] at the LHC, so spurring this work. Here I extend the results of Chapter 3 by calculating the prefactor of the rate, an important quantity for making comparison to experiment. In doing so, I encounter the well-know self-force instability which marks a breaking down of the approximations made, so calling into question the validity of the mass bounds of Chapter 4.

I should add a quick note on what I mean by my initial thermal state. I

consider temperatures,  $T$ , much less than the mass of any magnetic monopoles,  $m$  (or for the electric case, much less than the mass of the electron). In this case there are no magnetic monopoles in the initial state. Upon turning on the magnetic field, magnetic monopoles are produced by the thermal Schwinger process. The initial rate of production is what I calculate. This process is relevant only for the lightest magnetic monopole (or the lightest electrically charged particle), because the lightest particles will be produced exponentially more quickly than heavier particles and, once produced, their presence will cause Debye screening.

In Sec. 5.1 I define the sphaleron rate and set up the calculation of it. Following this, in Sec. 5.2 I calculate the sphaleron and the spectrum of fluctuations about it. In Sec. 5.3 I note that the spectrum of fluctuations manifests the well known self-force instability. In sec. 5.4 I specialise to a particular region of parameter space where the self-force instability does not rear its head. I then calculate the sphaleron rate, including the prefactor, the main result of this chapter. In Sec. 5.6, I summarise my results.

## 5.1 General approach

The thermal rate of decay of a metastable state has been studied by many authors [245, 246, 243, 244]. In regards to the thermal Schwinger process, in Chapter 3 I calculated the logarithm of the rate, the factor  $S$  in

$$\Gamma_T \sim e^{-S}. \quad (5.2)$$

To go beyond this, I need an explicit expression for the rate, including the prefactor. As argued for in Refs. [245, 246], for high temperatures, where the process is dominated by a static configuration, a sphaleron, the rate is given by <sup>2</sup>

$$\Gamma_T \approx \frac{-|\omega_-|}{\pi V} \text{Im} \log(Z_T), \quad (5.3)$$

where  $V$  is the spatial volume,  $Z_T$  is the canonical partition function excluding the states containing the decay products and  $|\omega_-|$  is the rate of growth with time of the unstable mode, responsible for the imaginary part of  $\log(Z_T)$ . It is assumed that the rate of decay is slow, so that the process is out of equilibrium.

I first consider the dual thermal Schwinger process in SQED, with the mag-

---

<sup>2</sup>At lower temperatures the rate is given instead by Eq. (3.12), related by replacing  $|\omega_-| \rightarrow 2\pi T$ .

netic field pointing along the  $x^3$  direction. In Chapter 3 I gave the following exact worldline path integral (Eq. 3.20),

$$\frac{1}{V} \text{Im} \log(Z_T) = \frac{1}{V} \text{Im} \log \left[ 1 + \sum_{n=1}^{\infty} \frac{1}{n!} \prod_{j=1}^n \left( \int_0^{\infty} \frac{ds_j}{s_j} \int \mathcal{D}x_j^\mu e^{-\frac{1}{\epsilon} \tilde{S}[x_j; s_j; \kappa; \tilde{T}]} e^{\frac{\kappa}{\epsilon} \sum_{k < j} \oint dx_j^\mu dx_k^\nu G_{\mu\nu}(x_j, x_k; \tilde{T})} \right) \right], \quad (5.4)$$

where  $\epsilon := gB/m^2$ ,  $\kappa := g^3 B/m^2$  and  $\tilde{T} := mT/gB$ . I will refer to  $s_j$  as Schwinger parameters. The problem is formulated in Euclidean space with periodic  $x^4$  direction, with period  $1/\tilde{T}$ . The free thermal photon propagator is  $G_{\mu\nu}$ , where  $\mu, \nu$  run over Euclidean indices 1, 2, 3, 4. The scaled action,  $\tilde{S}$ , for a single worldline, is (Eq. 3.21)

$$\begin{aligned} \tilde{S}[x; s; \kappa, \tilde{T}] &:= s + \frac{1}{4s} \int_0^1 d\tau \dot{x}^\mu \dot{x}_\mu - \int_0^1 d\tau x_3 \dot{x}^4 \\ &- \frac{\kappa}{2} \int_0^1 d\tau \int_0^1 d\tau' \dot{x}^\mu(\tau) \dot{x}^\nu(\tau') G_{\mu\nu}(x(\tau), x(\tau'); \tilde{T}). \end{aligned} \quad (5.5)$$

The worldlines are coupled by the terms involving the photon propagator. This interaction has a short distance divergence, corresponding to the electromagnetic contribution to the self-energy of the magnetic monopoles. In this chapter I regularise this divergence following Ref. [237] (using the length counterterm of Eq. (3.40)).

As in Chapter 3, I perform a cluster expansion of Eq. (5.4) (Eq. (3.24)),

$$\Gamma_T = \sum_{n=1}^{\infty} \Gamma_T^{(n)}, \quad (5.6)$$

where  $\Gamma_T^{(n)}$  is the contribution to  $\Gamma_T$  from clusters of  $n$  worldlines. For  $\epsilon \ll 1$ , the path integral of each cluster can be evaluated in the saddle point approximation. In this case the cluster expansion can be viewed as a dilute instanton expansion. The leading contribution to the thermal Schwinger rate is given by the instanton with smallest action. This leading order term is approximately equal to the density of these instantons, and is exponentially small. Higher order terms in the cluster expansion are expected to be suppressed by powers of this density, or by subleading instanton densities.

At low temperatures,  $\tilde{T} \ll 1$ , the dominant instanton is the circular worldline instanton [221, 25], a saddle point of  $\Gamma_T^{(1)}$ . At higher temperatures, thermal cor-

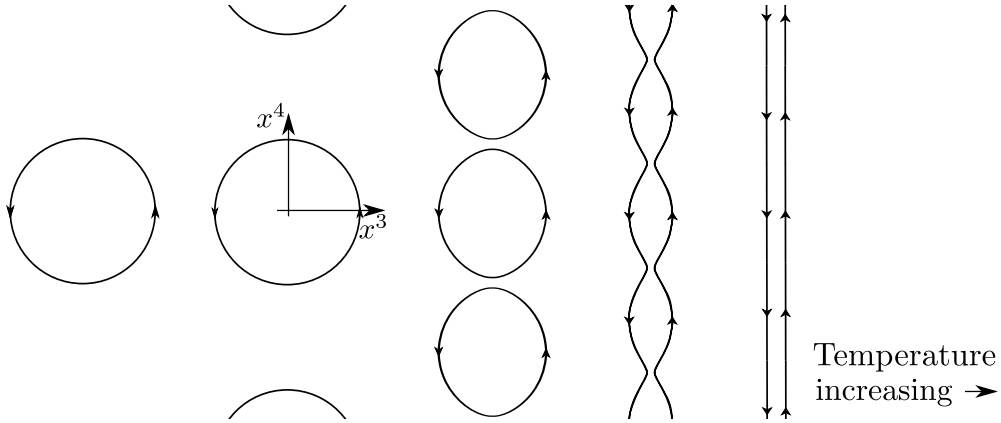


Figure 5.2: Worldline instantons relevant for the thermal Schwinger process. Each column represents a different instanton, each relevant for a given temperature. The rightmost instanton is the worldline sphaleron, which dominates the rate at the highest temperatures. The magnetic field points along the 3-direction and the 4-direction is the Euclidean time direction.

rections deform this instanton, so increasing the rate. Above some temperature,  $\tilde{T}_{CW}$ , a second instanton, with different topology, dominates, called a W instanton in Chapter 3. It consists of a monopole and antimonopole oscillating back and forth, parallel to the magnetic field, and is a saddle point of  $\Gamma_T^{(2)}$ . At higher temperatures still, above  $\tilde{T}_{WS}$ , this W instanton ceases to exist and the dominant instanton is the static worldline sphaleron solution, also a saddle point of  $\Gamma_T^{(2)}$ . The instanton phase diagram outlined here has been established for  $0 \leq \kappa \leq 1$  and may be subject to change at larger values of  $\kappa$ .

## 5.2 The sphaleron and fluctuations about it

Eq. (5.5) gives the action for one worldline,  $x^\mu(\tau)$ , with proper length  $s$ , and it gives the exponent of the integrand of  $\Gamma_T^{(1)}$ , when divided by  $\epsilon$ . In terms of the action for one worldline, the action for two worldlines, the scaled exponent of the integrand of  $\Gamma_T^{(2)}$ , is

$$\begin{aligned} \tilde{S}[x, y; s_x, s_y; \kappa, \tilde{T}] &:= \tilde{S}[x; s_x; \kappa, \tilde{T}] + \tilde{S}[y; s_y; \kappa, \tilde{T}] \\ &\quad - \kappa \int_0^1 d\tau \int_0^1 d\tau' \dot{x}^\mu(\tau) \dot{y}^\nu(\tau') G_{\mu\nu}(x(\tau), y(\tau'); \tilde{T}). \end{aligned} \quad (5.7)$$

Due to the double integral terms in the action, the corresponding equations of motion are integrodifferential equations.



The sphaleron is a static solution to these equations of motion. It consists of particle and antiparticle sitting a fixed distance apart along the  $x^3$  axis. It is given by

$$\begin{aligned} x(\tau) = x_0(\tau) &:= \left\{ 0, 0, \frac{1}{2} \sqrt{\frac{\kappa}{4\pi}}, \frac{1}{2\tilde{T}}(2\tau - 1) \right\}, \\ y(\tau) = y_0(\tau) &:= \left\{ 0, 0, -\frac{1}{2} \sqrt{\frac{\kappa}{4\pi}}, -\frac{1}{2\tilde{T}}(2\tau - 1) \right\}, \\ s_x = s_{x0} &:= \frac{1}{2\tilde{T}}, \\ s_y = s_{y0} &:= \frac{1}{2\tilde{T}}. \end{aligned} \quad (5.8)$$

The action of the sphaleron is

$$\tilde{S}(\kappa, \tilde{T}) = \frac{2}{\tilde{T}} \left( 1 - \sqrt{\frac{\kappa}{4\pi}} \right). \quad (5.9)$$

The saddle point approximation requires also the determinant of fluctuations about this solution. Expanding the action to second order about this solution gives a surprisingly large number of terms,  $O(100)$ , most of which are due to the nonlocal interactions. To proceed I define  $\zeta^\mu(\tau) := x^\mu(\tau) - y^\mu(\tau)$  and  $\xi^\mu(\tau) := x^\mu(\tau) + y^\mu(\tau)$ . The solution given in Eq. (5.8) can then be written as

$$\begin{aligned} \zeta(\tau) = \zeta_0(\tau) &:= \left\{ 0, 0, \sqrt{\frac{\kappa}{4\pi}}, \frac{1}{\tilde{T}}(2\tau - 1) \right\}, \\ \xi(\tau) = \xi_0(\tau) &:= \left\{ 0, 0, 0, 0 \right\}. \end{aligned} \quad (5.10)$$

Due to the periodicity, I may expand the fluctuations about the solution in a Fourier series,

$$\begin{aligned} \zeta^\mu(\tau) - \zeta_0^\mu(\tau) &= a_0^\mu + \sum_{n=1}^{\infty} \left( a_n^\mu \sqrt{2} \cos(2\pi n\tau) + b_n^\mu \sqrt{2} \sin(2\pi n\tau) \right), \\ \xi^\mu(\tau) - \xi_0^\mu(\tau) &= c_0^\mu + \sum_{n=1}^{\infty} \left( c_n^\mu \sqrt{2} \cos(2\pi n\tau) + d_n^\mu \sqrt{2} \sin(2\pi n\tau) \right). \end{aligned} \quad (5.11)$$

The second order action is diagonal in these Fourier coefficients. It can thus be

expressed as

$$\begin{aligned} \tilde{S}^{(2)} = & \frac{1}{2}4\tilde{T}(s_x - s_{x0})^2 + \frac{1}{2}4\tilde{T}(s_y - s_{y0})^2 + \frac{1}{2}\sum_{n=0}^{\infty}\sum_{\mu=1}^4(\alpha_n^\mu a_n^\mu a_n^\mu + \gamma_n^\mu c_n^\mu c_n^\mu) \\ & + \frac{1}{2}\sum_{n=1}^{\infty}\sum_{\mu=1}^4(\beta_n^\mu b_n^\mu b_n^\mu + \delta_n^\mu d_n^\mu d_n^\mu). \end{aligned} \quad (5.12)$$

The eigenvalues for  $n = 0$  are

$$\begin{aligned} \alpha_0 = & \left\{ \frac{2\pi}{\sqrt{\pi\kappa\tilde{T}}}, \frac{2\pi}{\sqrt{\pi\kappa\tilde{T}}}, -\frac{4\pi}{\sqrt{\pi\kappa\tilde{T}}}, 0 \right\}, \\ \gamma_0 = & \{0, 0, 0, 0\}. \end{aligned} \quad (5.13)$$

The four zero modes of  $\gamma_0$  correspond to translations of the instanton. The fifth,  $\alpha_0^4$ , corresponds to translation in the parameter  $\tau$ . The negative eigenvalue corresponds to increasing, or decreasing, the separation between the particles. It is negative for all  $\kappa$  and  $\tilde{T}$ . The eigenvalues for  $n = 1$  are

$$\begin{aligned} \alpha_1 = & \left\{ \frac{1}{2}(2\pi)^2\tilde{T} - \frac{2}{3}\pi^2\kappa\tilde{T}^2 + \pi \left( \sqrt{\pi\kappa\tilde{T}} + 1 + \frac{1}{\sqrt{\pi\kappa\tilde{T}}} \right) e^{-\sqrt{\pi\kappa\tilde{T}}} + \frac{\sqrt{\pi}}{\sqrt{\kappa\tilde{T}}}, \right. \\ & \frac{1}{2}(2\pi)^2\tilde{T} - \frac{2}{3}\pi^2\kappa\tilde{T}^2 + \pi \left( \sqrt{\pi\kappa\tilde{T}} + 1 + \frac{1}{\sqrt{\pi\kappa\tilde{T}}} \right) e^{-\sqrt{\pi\kappa\tilde{T}}} + \frac{\sqrt{\pi}}{\sqrt{\kappa\tilde{T}}}, \\ & \frac{1}{2}(2\pi)^2\tilde{T} - \frac{2}{3}\pi^2\kappa\tilde{T}^2 - 2\pi \left( 1 + \frac{1}{\sqrt{\pi\kappa\tilde{T}}} \right) e^{-\sqrt{\pi\kappa\tilde{T}}} - \frac{2\sqrt{\pi}}{\sqrt{\kappa\tilde{T}}}, \\ & \left. \frac{1}{2}(2\pi)^2\tilde{T} \right\}, \end{aligned} \quad (5.14)$$

$$\begin{aligned} \beta_1 = & \left\{ \frac{1}{2}(2\pi)^2\tilde{T} - \frac{2}{3}\pi^2\kappa\tilde{T}^2 - \pi \left( \sqrt{\pi\kappa\tilde{T}} + 1 + \frac{1}{\sqrt{\pi\kappa\tilde{T}}} \right) e^{-\sqrt{\pi\kappa\tilde{T}}} + \frac{\sqrt{\pi}}{\sqrt{\kappa\tilde{T}}}, \right. \\ & \frac{1}{2}(2\pi)^2\tilde{T} - \frac{2}{3}\pi^2\kappa\tilde{T}^2 - \pi \left( \sqrt{\pi\kappa\tilde{T}} + 1 + \frac{1}{\sqrt{\pi\kappa\tilde{T}}} \right) e^{-\sqrt{\pi\kappa\tilde{T}}} + \frac{\sqrt{\pi}}{\sqrt{\kappa\tilde{T}}}, \\ & \frac{1}{2}(2\pi)^2\tilde{T} - \frac{2}{3}\pi^2\kappa\tilde{T}^2 + 2\pi \left( 1 + \frac{1}{\sqrt{\pi\kappa\tilde{T}}} \right) e^{-\sqrt{\pi\kappa\tilde{T}}} - \frac{2\sqrt{\pi}}{\sqrt{\kappa\tilde{T}}}, \\ & \left. \frac{1}{2}(2\pi)^2\tilde{T} \right\}, \end{aligned} \quad (5.15)$$

and  $\gamma_1 = \beta_1$ , and  $\delta_1 = \alpha_1$ . The eigenvalues for  $n > 1$  are given in terms of the  $n = 1$

eigenvalues by

$$\alpha_n(\kappa, \tilde{T}) = n\alpha_1(\kappa, n\tilde{T}), \quad (5.16)$$

and likewise for the others. This can be seen by noting that an  $n$ th harmonic at a given temperature,  $\tilde{T}$ , can be seen as an  $n = 1$  harmonic at the higher temperature  $n\tilde{T}$ .

### 5.3 Self-force instability

These higher harmonics lead to a problem. For sufficiently large  $n$ , the self-force term,  $-\frac{2}{3}\pi^2\kappa\tilde{T}^2n^3$ , dominates. Hence, there are an infinite number of negative eigenvalues (see Fig. 5.3). This is a serious problem. It puts into doubt the relevance of this solution as an instanton (or sphaleron), which would be expected on general grounds to only have a single negative eigenvalue [192].

The self-force instability is well known in both classical [290, 291, 292] and quantum [335, 123, 336, 337, 338, 339, 340] electrodynamics. Its existence in quantum mechanical systems has been linked to the unboundedness of the spectrum of the Hamiltonian [341, 342, 343].

In Refs. [336, 337] it was found that a nonrelativistic electron interacting with a quantised photon field does not show the self-force instability, at least for  $\alpha \lesssim 1$ . Starting from an extended charge distribution, with finite mass, they found that one could take the size of the charge distribution to zero and the result was free of the self-force instability. However, if they first took the Compton wavelength to zero (or the mass to infinity), the self-force instability reared its ugly head. Taking the mass to infinity amounts to dropping charged particle loop corrections.

In the dilute instanton gas approximation, extra monopole loops with  $\tilde{S} \geq O(1)$  are suppressed by the instanton density, as argued in Sec. 5.1, and Chapter 3, and hence can justifiably be dropped. On the other hand, extra monopole loops with  $\tilde{S} = o(1)$ , as  $\epsilon \rightarrow 0$ , are not present in the semiclassical approximation and are not necessarily suppressed. As  $\epsilon \rightarrow 0$  there are nontrivial such loops when there is a cancellation between the rest mass and Coulomb interaction terms. These are virtual particles, and they have a size  $\sim \kappa/(8\pi)$ , or  $g^2/(8\pi m)$  in physical units. When there is a separation of scales between the virtual particle loop size,  $O(\kappa)$ , and the instanton size,  $O(1/\tilde{T})$ , i.e. when  $\kappa\tilde{T} = g^2T/m \ll 1$ , the virtual particle loops should simply renormalise the parameters of the theory [221], in particular the charge. This is assumed in my analysis. However, when  $\kappa\tilde{T} = O(1)$ , the saddle-point approximation plus renormalisation is not expected to adequately take virtual

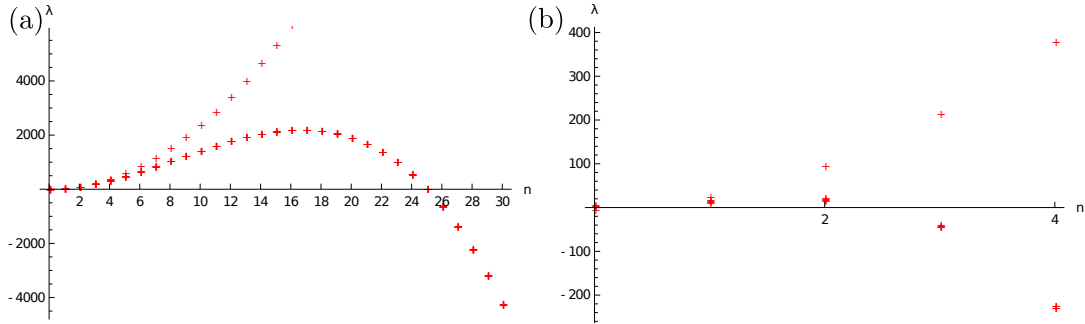


Figure 5.3: The first few eigenvalues, ordered by  $n$ , showing the self-force instability: (a) at  $(\kappa, \tilde{T}) = (0.1, 1.2)$ , the first 490 eigenvalues, showing the instability at  $n = 30$ ; (b) at  $(\kappa, \tilde{T}) = (1, 1.2)$ , the first 74 eigenvalues showing the instability at  $n = 3$ .

monopole loops into account. The self-force instability, which arises at  $O(\kappa\tilde{T})$ , may be symptomatic of this.

I define  $n_{SF}$  such that the self-force turns those harmonics negative with  $n \geq n_{SF}$ . For  $\tilde{T} = O(1)$  and  $\kappa = O(1)$ , I find that  $n_{SF} = O(1)$  as can be seen in Fig. 5.3 (b), where for  $(\kappa, \tilde{T}) = (1, 1.2)$  I can see that  $n_{SF} = 3$ . Above  $\kappa \approx 3.0653$  and for all  $\tilde{T}$ , the instability is at  $n_{SF} = 1$ . For  $\kappa\tilde{T} \ll 1$ , instead I find that

$$n_{SF} \approx \frac{3}{\kappa\tilde{T}} \left( 1 - \frac{\kappa^{3/2}}{9\pi^{3/2}} + O(\kappa^3) \right), \quad (5.17)$$

as can be seen in Fig. 5.3 (a), where for  $(\kappa, \tilde{T}) = (0.1, 1.2)$  I can see that  $n_{SF} = 31$ . For  $\kappa\tilde{T} \ll 1$  the self-force problem is moved to parametrically high harmonics, or short distances, where the effects of virtual monopole pairs are significant and hence the naive semiclassical approximation is expected to break down. One should therefore cut off the higher harmonics below  $O(1/(\kappa\tilde{T}))$  and apply standard renormalisation theory to the result. The self-force instability is thereby avoided within the semiclassical approximation, and the issue moved into the ultraviolet, where it can be considered separately.

Magnetic and electric charges are related inversely, via the Dirac quantisation condition,  $ge = 2\pi j$ , where  $j \in \mathbb{Z}$ . This relationship is expected to hold for the running couplings [344, 38, 345]. Hence, as one probes shorter distances the effective magnetic charge decreases; magnetic charge is anti-shielded. This has been argued to be an effective spreading-out of magnetic charge over scales  $O(\kappa)$  [123]. Classically, a charge distribution spread out on these scales is stable [336, 337], hence, for magnetic monopoles, one might expect that the ultraviolet physics does not suffer from the self-force instability.

For physical electric charges, on the other hand, the coupling is weak,  $g^2 \ll 1$ .

In this case  $\kappa \ll \epsilon \ll 1$ , and, given  $\tilde{T} = o(1/\epsilon)$ , the self-force problem is not present at leading order in  $\epsilon$ , which is the approximation I make.

## 5.4 The scalar prefactor for small $\kappa\tilde{T}$

In this section I consider the regime  $\kappa\tilde{T} \ll 1$ , for which, as I have argued in the previous section, the self-force instability is not present. I adopt zeta function regularisation for the high harmonics and assume the running coupling is known at the relevant energy scale.

The temperature,  $\tilde{T}_{WS}$ , above which the worldline sphaleron dominates the thermal Schwinger process satisfies  $\tilde{T}_{WS} \gtrsim 0.5$ , at least for  $\kappa \leq 1$ . For small  $\kappa$ , it grows and is given approximately by

$$\tilde{T}_{WS} \approx \frac{\sqrt{2}}{\pi^{3/4}\kappa^{1/4}}. \quad (5.18)$$

Given that  $\tilde{T} > \tilde{T}_{WS}$ , we must have that  $\kappa \ll 1$  and  $\tilde{T}$  must lie in the window

$$\frac{\sqrt{2}}{\pi^{3/4}\kappa^{1/4}} < \tilde{T} \ll \frac{1}{\kappa}. \quad (5.19)$$

Note too that, due to the strong coupling,  $\kappa$  must lie in the window

$$\epsilon \ll \kappa \ll 1. \quad (5.20)$$

Above  $\tilde{T}_{WS}$ , the rate is dominated by the sphaleron and hence by the second term in the cluster expansion,

$$\frac{1}{V} \text{Im} \log(Z_T) \approx \frac{1}{V} \text{Im} \frac{1}{2!} \prod_{j=1}^2 \left( \int_0^\infty \frac{ds_j}{s_j} \int \mathcal{D}x_j^\mu e^{-\frac{1}{\epsilon} \tilde{S}[x_j; s_j; \kappa, \tilde{T}]} e^{\frac{\kappa}{\epsilon} \sum_{k < j} \oint dx_j^\mu dx_k^\nu G_{\mu\nu}(x_j, x_k; \tilde{T})} \right). \quad (5.21)$$

I wish to evaluate this in the saddle point approximation about the sphaleron.

The action of the sphaleron is

$$\tilde{S}(\kappa, \tilde{T}) = \frac{2}{\tilde{T}} \left( 1 - \sqrt{\frac{\kappa}{4\pi}} \right) \approx \frac{2}{\tilde{T}}, \quad (5.22)$$

and the Schwinger parameters at the saddle point are

$$\frac{1}{s_1} \frac{1}{s_2} = (2\tilde{T})^2. \quad (5.23)$$

Using the results of Sec. 5.2 I can perform the Gaussian integrations over the fluctuations about the saddle point, dropping all terms  $o(1)$  as  $\kappa \rightarrow 0$ . The integrations over the fluctuations in the Schwinger parameters give

$$(2\pi) \left( \frac{4\tilde{T}}{\epsilon} \right)^{-1} = \frac{\pi\epsilon}{2\tilde{T}}. \quad (5.24)$$

In the integrations over all the other parameters I must keep in mind that the change of variables,  $(x^\mu(\tau), y^\mu(\tau)) \rightarrow (\zeta^\mu(\tau) = x^\mu(\tau) - y^\mu(\tau), \xi^\mu(\tau) = x^\mu(\tau) + y^\mu(\tau))$ , was carried out. The Jacobian of the transformation is  $1/2$  for each pair of degrees of freedom or  $1/\sqrt{2}$  for each degree of freedom. This can be seen easily in the two dimensional transformation  $(x, y) \rightarrow (u = x - y, v = x + y)$ ,

$$|J| = \begin{vmatrix} \frac{\partial x}{\partial u} & \frac{\partial x}{\partial v} \\ \frac{\partial y}{\partial u} & \frac{\partial y}{\partial v} \end{vmatrix} = \begin{vmatrix} \frac{1}{2} & \frac{1}{2} \\ -\frac{1}{2} & \frac{1}{2} \end{vmatrix} = \frac{1}{2}. \quad (5.25)$$

For the nonzero modes, multiplication by this Jacobian factor is equivalent to multiplying the eigenvalues by 2.

Integration over the four zero modes associated with spacetime translation gives the spacetime volume (in units of  $1/(m\epsilon)^4$  due to the scaling of  $x$  and  $y$ ) multiplied by the Jacobian factor,  $1/\sqrt{2}$ , for each of the four degrees of freedom,

$$\frac{1}{4} m^4 \epsilon^4 \mathcal{V}, \quad (5.26)$$

where  $\mathcal{V}$  is the (dimensionful) Euclidean spacetime volume, i.e.  $V/T$  where  $V$  is the spatial volume and  $T$  is the temperature.

The integration over the zero mode associated with proper time translation becomes, after using the Faddeev-Popov method [346, 347],

$$\frac{1}{\sqrt{2}} \sqrt{\frac{\int_0^1 d\tau \left( \dot{\zeta}_0^4 \right)^2}{2\pi}} = \frac{1}{\sqrt{\pi\tilde{T}}}. \quad (5.27)$$

Integration over the single negative mode gives

$$\frac{1}{2}(2\pi)^{1/2} \left( -\frac{8\sqrt{\pi}}{\epsilon\sqrt{\kappa\tilde{T}}} \right)^{-1/2} = \pm i \frac{1}{4} (\pi\kappa)^{1/4} \sqrt{\tilde{T}\epsilon} \quad (5.28)$$

where the  $\pm i$  comes from taking the square root of the negative eigenvalue. For the decay rate I must choose the negative sign. The explicit factor of 1/2 is due to the requirement to integrate only over half the real line for the negative mode, as famously pointed out in Ref. [268]. Gaussian integration over the other two constant fluctuations gives

$$(2\pi)^{2/2} \left( \frac{4\sqrt{\pi}}{\epsilon\sqrt{\kappa\tilde{T}}} \right)^{-2/2} = \frac{1}{2} \sqrt{\pi} \sqrt{\kappa\tilde{T}\epsilon}. \quad (5.29)$$

Formally carrying out the Gaussian integrals (to leading order in  $\kappa$  and  $\kappa\tilde{T}$ ) over the infinite number of harmonic fluctuations gives

$$\begin{aligned} & \prod_{n=1}^{\infty} (2\pi)^{16/2} \left( \frac{(2\pi n)^2 \tilde{T}}{\epsilon} \right)^{-10/2} \left( \frac{(2\pi n)^2 \tilde{T}}{\epsilon} + \frac{4\sqrt{\pi}}{\sqrt{\kappa\tilde{T}\epsilon}} \right)^{-4/2} \left( \frac{(2\pi n)^2 \tilde{T}}{\epsilon} - \frac{8\sqrt{\pi}}{\sqrt{\kappa\tilde{T}\epsilon}} \right)^{-2/2} = \\ & \prod_{n=1}^{\infty} \left( \frac{\epsilon}{2\pi\tilde{T}} \right)^8 \left( 1 + \frac{1}{\pi^{3/2} \sqrt{\kappa\tilde{T}^2 n^2}} \right)^{-2} \left( 1 - \frac{2}{\pi^{3/2} \sqrt{\kappa\tilde{T}^2 n^2}} \right)^{-1} n^{-16}. \end{aligned} \quad (5.30)$$

To define the (regularised) infinite products I use zeta function regularisation following Ref. [294]. The key (formal) equations for the zeta function regularisation I use are

$$\begin{aligned} \prod_{n=1}^{\infty} a &= a^{\sum_{n=1}^{\infty} 1} = a^{\zeta(0)} = a^{-1/2}, \\ \prod_{n=1}^{\infty} n &= \lim_{s \rightarrow 0} e^{\sum_{n=1}^{\infty} \log(n)/n^s} = e^{-\zeta'(0)} = (2\pi)^{1/2}. \end{aligned} \quad (5.31)$$

I also use the following identity

$$\prod_{n=1}^{\infty} \left( 1 - \frac{c^2}{n^2} \right)^{-1} = \frac{\pi c}{\sin(\pi c)}. \quad (5.32)$$

Applying Eqs. (5.31) and (5.32) to Eq. (5.30) gives

$$\left( \frac{2\pi\tilde{T}}{\epsilon} \right)^4 \left( \frac{\pi}{\sqrt{\pi^{3/2} \sqrt{\kappa\tilde{T}^2} \sinh\left(\frac{\pi}{\sqrt{\pi^{3/2} \sqrt{\kappa\tilde{T}^2}}}\right)}} \right)^2 \left( \frac{\pi}{\sqrt{\pi^{3/2} \sqrt{\kappa\tilde{T}^2} \sin\left(\frac{\pi\sqrt{2}}{\sqrt{\pi^{3/2} \sqrt{\kappa\tilde{T}^2}}}\right)}} \right)^2 (2\pi)^{-8} \quad (5.33)$$

Putting it all together, and noting that I get an overall factor of  $2!$  from interchanging the particles, cancelling the  $1/2!$ , I find

$$\frac{1}{V} \text{Im} \log(Z_T) \approx - \frac{m^4 (\tilde{T}\epsilon)^{3/2}}{128\sqrt{2}\pi^2 \sin\left(\frac{\pi\tilde{T}_{WS}}{\tilde{T}}\right) \sinh^2\left(\frac{\pi\tilde{T}_{WS}}{\sqrt{2}\tilde{T}}\right)} \exp\left\{-\frac{2}{\tilde{T}\epsilon}\right\}, \quad (5.34)$$

where we have reintroduced  $\tilde{T}_{WS} = \sqrt{2}/(\pi^{3/4}\kappa^{1/4})$  to simplify the expression. Note that this expression is divergent at  $\tilde{T} = \tilde{T}_{WS}$ , where the sphaleron develops another zero mode. Below this temperature the sphaleron is unstable due to the existence of another saddle point with lower action, the W instanton of Chapter 3. This may signal a parametric enhancement of the dependence on the semiclassical parameter,  $\epsilon$  [122]. Whether or not there are phenomenological consequences of this enhancement depend on precise values in a given situation, though the exponential dependence may well dominate over such power law enhancements in the prefactor. The higher harmonic divergences, at  $\tilde{T} = \tilde{T}_{WS}/n$ , are at lower temperatures where the sphaleron (or S instanton) does not dominate the rate.

The last ingredient required to construct the sphaleron rate is  $|\omega_-|$ , the rate of growth with time of the unstable mode. This is

$$|\omega_-| = 2\pi T_{WS} \approx 2\pi \left(\frac{4gB^3}{\pi^3 m^2}\right)^{1/4}. \quad (5.35)$$

The rate of pair production is thus given by

$$\Gamma_{T,s=0} \approx 2\pi T_{WS} \left(\frac{mT_{WS}}{2\pi}\right)^{3/2} F\left(\frac{T}{T_{WS}}\right) e^{-\frac{2m}{T}} \left[1 + O\left(\frac{g^3 B}{m^2}, \frac{g^2 T}{m}\right)\right], \quad (5.36)$$

where I have restored the dimensionful variables,  $s$  refers to the spin of the charged particles and the function  $F$  is given by

$$F(\tau) := \frac{\left(\frac{\tau}{\pi}\right)^{3/2}}{64 \sin\left(\frac{\pi}{\tau}\right) \sinh^2\left(\frac{\pi}{\sqrt{2}\tau}\right)}. \quad (5.37)$$

The logarithm of the function is plotted in Fig. 5.4. Note that the result is valid for  $g^2 \gg 1$  and hence only for very low temperatures and very weak magnetic fields. Unfortunately, in this regime any enhancement of the rate due to the magnetic field is only in the prefactor<sup>3</sup>. For the dual electric result simply make the exchange:

<sup>3</sup>Assuming there exists some other background rate of production, proportional to  $\exp(-2m/T)$ .



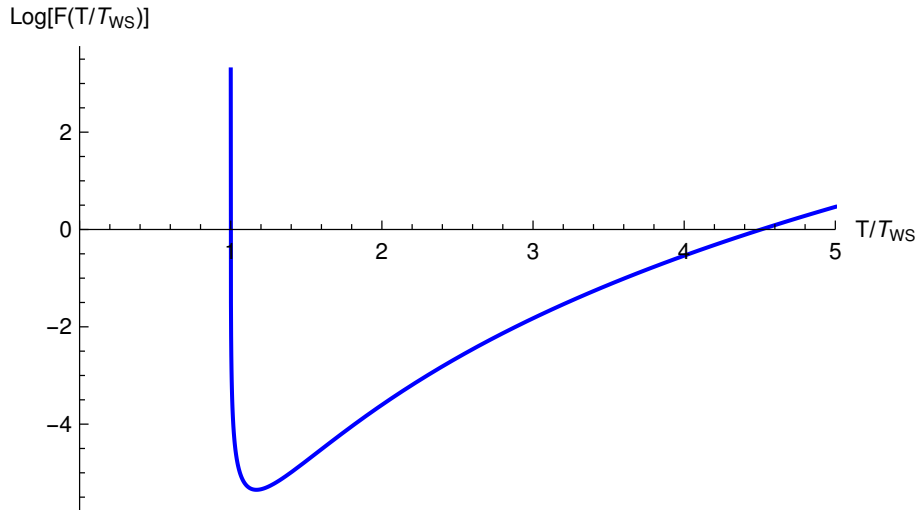


Figure 5.4: The logarithm of the function  $F$ , Eq. (5.37). The sharp rise at  $T = T_{WS}$  is a divergence of the form  $F \sim c/(T - T_{WS})$ , where  $c$  is a constant. It is due to the presence of an extra zero mode.

$g \rightarrow e$  and  $B \rightarrow E$ , in Eqs. (5.36) and (5.37)<sup>4</sup>.

This result can be compared with the rate of pair production of weakly coupled electron-positron pairs from a thermal bath of photons [348, 334],

$$\Gamma_{2\gamma \rightarrow e^- e^+} \approx 2m^4 \left( \frac{e^2}{8\pi^2} \right)^2 \left( \frac{T}{m} \right)^3 e^{-\frac{2m}{T}} \left[ 1 + O\left( e^2, \frac{T}{m} \right) \right]. \quad (5.38)$$

This process is due to the collision of pairs of photons in the thermal bath.

## 5.5 The spinor prefactor for small $\kappa\tilde{T}$

For (Dirac) spinor charged particles, the worldline path integral contains an additional spin-dependent factor. As shown in Appendix A.3, for  $\epsilon \ll 1$  this factor is subdominant and does not affect the sphaleron action. It does however modify the prefactor which, for each worldline,  $x$ , is multiplied by

$$\begin{aligned} & -\frac{1}{2} \text{Tr}_{\gamma_x} \mathcal{P}_x \exp \left\{ s_x \Sigma_x^{34} + \kappa s_x \int_0^1 d\tau \int_0^1 d\tau' \Sigma_x^{\mu\rho} \left( \partial_\rho^x G_{\mu\nu}(x, y') \dot{y}'^\nu + \partial_\rho^x G_{\mu\nu}(x, x') \dot{x}'^\nu \right) \right\} \\ & = -\frac{1}{2} \text{Tr}_{\gamma_x} \mathcal{P}_x \exp \left\{ \Sigma_x^{34} \left( \frac{1}{2\tilde{T}} - \frac{1}{2\tilde{T}} \right) \right\}, \\ & = -2, \end{aligned} \quad (5.39)$$

<sup>4</sup>Note that this result is only valid for  $e^2 \gg 1$ .

where  $\text{Tr}_{\gamma_x}$  denotes a trace over spinor indices of the  $x$  worldline,  $\mathcal{P}_x$  is the path ordering operator along the  $x$  worldline,  $\Sigma^{\mu\nu} := [\gamma^\mu, \gamma^\nu]/2$ , where  $\gamma^\mu$  are the Euclidean Dirac (gamma) matrices satisfying  $\{\gamma^\mu, \gamma^\nu\} = 2\delta^{\mu\nu}$  and  $'$  denotes dependence on  $\tau'$  as opposed to  $\tau$ . There is second factor, for the other worldline,  $y$ , which differs by interchange of  $x$  and  $y$ . The two factors are equal to each other. Hence the rate of pair production of spinor charged particles is

$$\Gamma_{T,s=1/2} \approx 4\Gamma_{T,s=0}. \quad (5.40)$$

The 4 comes from a product of traces over gamma matrices and hence can be seen as a factor of  $(2s+1)^2$ , to be compared with the single power of  $(2s+1)$  which arises in Schwinger pair production at zero temperature. This is due to the sphaleron consisting of two worldlines, whereas the zero temperature instanton consists of only one.

## 5.6 Summary

Eqs. (5.36), (5.37) and (5.40) are the chief results of this chapter. They give the sphaleron rate for the thermal Schwinger process at strong coupling, including the prefactor. The result is valid for sufficiently weak fields, such that

$$B \ll \frac{m^2}{g^3}, \quad (5.41)$$

and for temperatures such that

$$\left(\frac{4gB^3}{\pi^3 m^2}\right)^{1/4} < T \ll \frac{m}{g^2}. \quad (5.42)$$

In this regime the rate is strongly exponentially suppressed, by the Boltzmann factor,  $2m/T \gg g^2$ . For magnetic monopoles,  $g^2 \geq g_D^2 \approx 430$ , and hence the results derived here are unfortunately too suppressed to be of relevance to monopole searches in heavy ion collisions.

For larger,  $O(1)$ , values of  $g^3 B/m^2$  and  $g^2 T/m$ , the exponential suppression of the rate is greatly reduced, leading to predictions of a measurable rate of pair production. It was such a regime that led to the mass bounds in Chapter 4. However, the validity of the dilute instanton approximation is suspect in this case, due to the presence of the self-force instability. This casts doubt on the mass bounds I derived.

One hope might be that the calculated exponential suppression may still give a good approximation to the rate at  $O(1)$  values of  $g^3 B/m^2$  and  $g^2 T/m$ , though the corrections to this cannot be calculated systematically.

Regardless, the self-force instability is merely a pathology of the approximation scheme and may be overcome. For both elementary and 't Hooft-Polyakov magnetic monopoles, the anti-screening of magnetic charge, or the effective size of magnetic monopoles, is expected to ameliorate the problem. For 't Hooft-Polyakov monopoles an explicit classical field theory calculation is possible, within which there is no self-force instability. This may allow one to extend the calculation of the thermal Schwinger rate to a parameter regime where it is large enough to be measurable.

Alternatively, within the worldline approach, the W instantons of Chapter 3 offer some promise. These instantons have a well defined  $\kappa \rightarrow 0$  limit, the lemon instanton, for which one may consistently calculate the rate, including the prefactor, at higher temperatures [279, 247, 280, 281, 282] (though for even weaker magnetic fields). Whether or not this will lead to a measurable production rate in, for example, heavy ion collisions remains to be seen.

# Chapter 6

## Conclusion

So, where do we stand on my central question: assuming that magnetic monopoles exist, can we create them, and if so, how? The tentative answer of this thesis is: yes, if they are sufficiently light, we may be able to create magnetic monopoles in strong magnetic fields and high temperatures by colliding heavy ions at high speeds.

In Chapter 2, I reviewed the arguments suggesting that the cross section for pair production of composite magnetic monopoles in few particle collisions is exponentially suppressed at all energies. There is even a suggestion that the same suppression may be present for elementary magnetic monopoles, due to their large effective size. These arguments cannot be taken as conclusive and I outlined several possible approaches to rigorously establish or refute them. Perhaps the most promising method I discussed is the RST method, which I investigated in the context of kink pair production.

The results of the calculation of Chapter 3 suggest that, in strong magnetic fields and high temperatures, any sufficiently light magnetic monopoles may be produced amply. The zero temperature [25] and zero magnetic field [83] limits of my calculation were previously known, and hence the main qualitative features of my generalisation were intuitively clear. Mine was nevertheless an important step, both because it expanded the range of relevant physical situations and because the approach lends itself to further extensions. The result is also of interest as an example of an all orders calculation in QED, of which very few are known.

The work of Chapter 4 gave new model-independent lower bounds on the mass of any possible magnetic monopoles. Despite being only  $O(\text{GeV})$ , they are the strongest such bounds known in the literature. The bounds from heavy ion collisions derive from the fairly low energy collisions at the SPS. Current and future heavy ion collisions at the LHC have centre-of-mass energies almost three orders of magnitude higher [90]. As such, it is expected that much higher energy magnetic monopoles

---

could be produced. However, at higher energies the magnetic field has a shorter lifetime and is more inhomogeneous, the effects of which need to be understood. For direct experimental comparison, it is also important to understand the kinematic distribution of magnetic monopoles produced.

Chapter 5 developed the work of Chapter 3. In Chapter 5 I derived the rate (rather than just the logarithm of the rate) to leading order in  $\epsilon$ . In the calculation, the well known self-force instability of electrodynamics arose at  $\kappa = O(1)$ . This led to the suggestion that the saddle-point approximation breaks down at this point, throwing some doubt on my conclusions in Chapter 4. This may be remedied by an explicit calculation of the Schwinger sphaleron rate for 't Hooft-Polyakov monopoles, where the  $\kappa = O(1)$  behaviour is modified classically by the composite structure. In this case a saddle-point approximation should still be valid.

It is 86 years since Dirac's groundbreaking paper introduced the modern study of magnetic monopoles [6]. In this thesis, I have proposed a new approach to directly constrain the masses of any possible magnetic monopoles, an approach which may finally allow us to unambiguously test Dirac's guess that magnetic monopoles may have a mass of about 0.5GeV [11] (see Fig. 4.1). Unfortunately the very heavy monopoles predicted by Grand Unified Theories, as well as the even heavier Kaluza-Klein magnetic monopoles predicted by Planck scale compactifications in String Theory, are far beyond the reach of terrestrial collider experiments for the foreseeable future. However my work suggests that intermediate mass monopoles, with masses perhaps up to  $O(\text{TeV})$ , could be produced in LHC heavy ion collisions. More theoretical work still needs to be done, but, as Pierre Curie suggested, it is not absurd to think we might find one.

# Appendix A

## A.1 Induced Schwinger pair production at weak coupling

There does not exist a local relativistic Hamiltonian for a charged relativistic particle, whether electric or magnetic (once the photon has been integrated out). However, one can write down various approximate Hamiltonians, each valid in a certain regime. One such approximation, the *test particle* approximation, applies when the field due to the charged particles can be ignored. As such it is a weak coupling approximation. In this case, the forces on the charged particles are due solely to a fixed external field, described by a gauge potential  $A^\mu = (\phi, \mathbf{A})$ . The Hamiltonian,  $\mathcal{H}$ , for the motion of a charged particle with mass  $m$  is then given by

$$(\mathcal{H} - g\phi(t, \mathbf{x}))^2 - (\mathbf{p} - g\mathbf{A}(t, \mathbf{x}))^2 = m^2, \quad (\text{A.1})$$

where  $t$  is the time coordinate,  $\mathbf{x}$  is the spatial position of the charged particle with charge  $g$  and  $\mathbf{p}$  is the conjugate momentum.

I consider the production of pairs of charged particles by a constant external field,  $E$ , and from an initial state with energy  $\mathcal{H}$ . In the test particle approximation the particles do not interact so they can be treated separately, each starting from a state with energy  $\mathcal{H}/2$ . The problem is then effectively one-dimensional and I denote the position and momentum by  $x$  and  $p$  respectively. I choose the gauge potential to be  $A^\mu = (Ex, 0)$ . The tunnelling begins from a state with no charged particles (or where the charged particle and its anti-particle are at the same location,  $x = 0$ ). The positively charged particle tunnels to the classically allowed position,  $x = (m - \mathcal{H}/2)/(gE)$ , and the negatively charged particle to  $x = -(m - \mathcal{H}/2)/(gE)$ . The positive and negative particles give equal tunnelling rates. The semiclassical

expression for the exponential suppression of the combined tunnelling rate is [172]

$$\begin{aligned}
4 \int_0^{(m+\mathcal{H}/2)/(gE)} p(x) dx &= 4 \int_0^{(m+\mathcal{H}/2)/(gE)} \sqrt{m^2 - \left(\frac{\mathcal{H}}{2} - gEx\right)^2} dx, \\
&= 4 \frac{m^2}{gE} \int_0^{1-\omega/2} \sqrt{1 - \left(\frac{\omega}{2} - y\right)^2} dy, \\
&= \frac{m^2}{gE} \left[ \pi - \omega \sqrt{1 - \left(\frac{\omega}{2}\right)^2} - 2 \arcsin\left(\frac{\omega}{2}\right) \right] \quad (\text{A.2})
\end{aligned}$$

where  $\omega = \mathcal{H}/m$ . At  $\omega = 0$  this reproduces the usual suppression of Schwinger's result [201]. For  $\omega > 0$  the suppression is reduced, giving the known rate of pair production from an off-shell photon [283]. At the pair production threshold,  $\omega = 2$ , the exponential suppression is zero. Note that nature of the energy of the initial state nowhere entered the calculation. Neither did any particular characteristics of electrodynamics, hence the same result holds for the vacuum decay rate in other theories [279, 284, 285].

## A.2 Coherent states

I briefly review the elements of the coherent state representation required for Sec. 2.5, following Refs. [349, 187]. Consider a one dimensional harmonic oscillator,

$$\begin{aligned}
\hat{H} &= \frac{1}{2} \hat{p}^2 + \frac{\omega^2}{2} \hat{x}^2, \\
&= \omega \left( \hat{a}^\dagger \hat{a} + \frac{1}{2} \right), \quad (\text{A.3})
\end{aligned}$$

where I have introduced the usual ladder operators, related to  $x$  and  $p$  by

$$\hat{x} = \frac{1}{\sqrt{2\omega}} (\hat{a} + \hat{a}^\dagger), \quad \hat{p} = -i\sqrt{\frac{\omega}{2}} (\hat{a} - \hat{a}^\dagger). \quad (\text{A.4})$$

The coherent states for this system,  $|a\rangle$ , are defined as the eigenstates of the lowering (or annihilation) operator  $\hat{a}$

$$\hat{a}|a\rangle = a|a\rangle, \quad (\text{A.5})$$

where  $a$  is the eigenvalue. In the coherent state basis,  $|a\rangle$ , any state of the system can be written as a holomorphic function of the complex variable  $a^*$ . For example

the normalised  $n$ th excited state has the form

$$\Psi_n(a^*) \equiv \langle a|n\rangle = \frac{(a^*)^n}{\sqrt{n!}}. \quad (\text{A.6})$$

The scalar product between two states is defined with respect to a complex Gaussian weight

$$\langle \Psi|\Phi\rangle = \int \frac{da^* da}{2\pi i} e^{-a^* a} \Psi[a^*]^* \Phi[a^*]. \quad (\text{A.7})$$

As is the action of an operator  $\hat{A}$  on the state  $\Psi$

$$(\hat{A}\Psi)(a^*) = \int \frac{db^* db}{2\pi i} e^{-b^* b} A(a^*, b) \Psi(b^*), \quad (\text{A.8})$$

where  $A(a^*, b) = \langle a|\hat{A}|b\rangle$  is the kernel of the operator. Any operator is completely determined by its kernel. The generalisation of this formalism to the case of a real scalar field theory is straightforward. The creation and annihilation operators are related to the field operator by

$$\hat{\phi}(x) = \int \frac{d\mathbf{p}}{\sqrt{2\omega_{\mathbf{p}}}} (\hat{a}_{\mathbf{p}} e^{-ip \cdot x} + \hat{a}_{\mathbf{p}}^\dagger e^{ip \cdot x}), \quad (\text{A.9})$$

where  $\omega_{\mathbf{p}} := \sqrt{m^2 + \mathbf{p}^2}$  and I have used the shorthand,

$$\int d\mathbf{p} := \int \frac{d^{D-1}\mathbf{p}}{(2\pi)^{D-1}}, \quad (\text{A.10})$$

and  $D$  is the dimension of spacetime. Then the coherent states will be defined as the common eigenstates of the annihilation operators  $\hat{a}_{\mathbf{p}}$  for all spatial momenta  $\mathbf{p}$ , and the complex Gaussian weight will be

$$\exp\left(-\int d\mathbf{p} a_{\mathbf{p}}^* a_{\mathbf{p}}\right). \quad (\text{A.11})$$

To calculate the inclusive cross section of the RST method, Eq. (2.27) in Sec. 2.5, I will need the kernel of the S-matrix,  $S(b^*, a)$ . This has a path integral representation

$$S(b^*, a) = \int d\phi_f d\phi_i e^{B_i(\phi_i, a) + B_f(\phi_f, b^*)} \int \mathcal{D}\phi e^{iS[\phi]}, \quad (\text{A.12})$$

where  $B_i(\phi_i, a)$  and  $B_f(\phi_f, b^*)$  are boundary terms. The integration  $\mathcal{D}\phi$  is over field configurations such that as  $t \rightarrow \pm\infty$ ,  $\phi \rightarrow \phi_{i/f}$  and  $S[\phi]$  is the action of the  $\phi$  fields.



The boundary terms are given by

$$\begin{aligned}
B_i(\phi_i, a) &= \frac{1}{2} \int \mathrm{d}\mathbf{p} \left[ -\omega_{\mathbf{p}} \tilde{\phi}_i(\mathbf{p}) \tilde{\phi}_i(-\mathbf{p}) - a_{\mathbf{p}} a_{-\mathbf{p}} e^{-2i\omega_{\mathbf{p}} T_i} \right. \\
&\quad \left. + 2\sqrt{2\omega_{\mathbf{p}}} e^{-i\omega_{\mathbf{p}} T_i} a_{\mathbf{p}} \tilde{\phi}_i(\mathbf{p}) \right], \\
B_f(\tilde{\phi}_f, b^*) &= \frac{1}{2} \int \mathrm{d}\mathbf{p} \left[ -\omega_{\mathbf{p}} \tilde{\phi}_f(\mathbf{p}) \tilde{\phi}_f(-\mathbf{p}) - b_{\mathbf{p}}^* b_{-\mathbf{p}}^* e^{2i\omega_{\mathbf{p}} T_f} \right. \\
&\quad \left. + 2\sqrt{2\omega_{\mathbf{p}}} e^{i\omega_{\mathbf{p}} T_f} b_{\mathbf{p}}^* \tilde{\phi}_f(\mathbf{p}) \right],
\end{aligned} \tag{A.13}$$

where  $\tilde{\phi}$  refers to the spatial Fourier transform of  $\phi$ .

As mentioned in Sec. 2.5, the projection operators in equation (2.27) take a particularly simple form in the coherent state representation. For any operator  $\hat{\mathcal{O}}$  of the form

$$\hat{\mathcal{O}} = \int \mathrm{d}\mathbf{p} f(p) \hat{a}_{\mathbf{p}}^\dagger \hat{a}_{\mathbf{p}}, \tag{A.14}$$

which has eigenvalues  $\{\mathcal{O}\}$ , the kernel of the projection operator which projects onto the subspace of states with given eigenvalue  $\mathcal{O}$  is

$$P_{\mathcal{O}}(b^*, a) = \int \frac{\mathrm{d}\theta}{2\pi} e^{-i\theta\mathcal{O} + \int \mathrm{d}\mathbf{p} e^{if(p)\theta} b_{\mathbf{p}}^* a_{\mathbf{p}}}. \tag{A.15}$$

### A.3 QED and SQED in weak external fields

For sufficiently small, scalar self-coupling,  $\lambda$ , the only difference between QED and SQED is the spin of the charged particles. Following the manipulations of SQED in Eq. (3.5) I see that the difference for a spin 1/2 charged particle manifests simply in replacing the determinant over the Klein-Gordon operator with a determinant over the Dirac operator, to the power of  $-1$ . Using the following identities

$$\begin{aligned}
\det(\not{D} + m) &= \det(-\not{D} + m), \\
&= \det((-\not{D}^2 + m^2))^{1/2}, \\
&= \det((-D^2 + m^2 - \frac{i}{2} g \Sigma^{\mu\nu} (F_{\mu\nu}^{ext}(x) + F_{\mu\nu}(x)))^{1/2}),
\end{aligned} \tag{A.16}$$

where the  $\Sigma^{\mu\nu}$  are proportional to the generators of Lorentz transformations in the spin 1/2 representation, i.e.  $\Sigma^{\mu\nu} = [\gamma^\mu, \gamma^\nu]/2$ , where  $\gamma^\mu$  are the Euclidean gamma matrices (see Ref. [350] for a definition). Using the final line of Eq. (A.16), one can see that the spin-1/2 functional trace can be written in terms of the spin-0 trace

and an additional spin factor [235, 238, 351]

$$\begin{aligned} \text{Tr}(e^{-(\mathcal{D}+m)s}) &= \text{Tr}(e^{-(-\mathcal{D}^2+m^2)s}) \\ &= \int \mathcal{D}x^\mu e^{-S_0[x^\mu, A_\mu^{ext} + A_\mu; s]} \text{Spin}[x^\mu, A_\mu^{ext} + A_\mu; s], \end{aligned} \quad (\text{A.17})$$

where  $S_0[x^\mu, A_\mu^{ext} + A_\mu; s]$  is given in Eq. (3.8) and the spin factor is given by

$$\text{Spin}[x^\mu, A_\mu^{ext} + A_\mu; s] := \text{Tr}_\gamma \mathcal{P} e^{i\frac{g}{2} \int_0^s d\tau \Sigma^{\mu\nu} (F_{\mu\nu}^{ext}(x) + F_{\mu\nu}(x))} \quad (\text{A.18})$$

where  $\text{Tr}_\gamma$  signifies the trace over spinorial indices and  $\mathcal{P}$  is the path ordering operator. The next step is to integrate over the gauge field  $A_\mu$ . Note that even with the inclusion of the spin factor the integration over  $A_\mu$  is Gaussian and hence can be done exactly. In the spin 0 case, the integration takes the following form

$$\int \mathcal{D}A_\mu e^{\frac{1}{2} \int_x \int_y A^\mu(x) G_{\mu\nu}^{-1}(x, y) A^\nu(y) + i \int_x A_\mu(x) j_0^\mu(x)}, \quad (\text{A.19})$$

where  $\int_x := \int d^4x$ , and  $j_0^\mu(x)$  is given by

$$j_0^\mu(x) = g \int_0^s d\tau \dot{x}^\mu(\tau) \delta^{(4)}(x - x(\tau)). \quad (\text{A.20})$$

Performing the integration leads to the following exponential,

$$\exp \left\{ \frac{1}{2} \int_x \int_y j_0^\mu(x) G_{\mu\nu}(x, y) j_0^\nu(y) \right\}. \quad (\text{A.21})$$

The difference in the spin 1/2 case amounts to the replacement

$$\begin{aligned} j_0^\mu(x) &\rightarrow j_0^\mu(x) - g \int_0^s d\tau \Sigma^{\mu\nu} \partial_\nu \delta^{(4)}(x - x(\tau)), \\ &:= j_0^\mu(x) + \xi^\mu(x). \end{aligned} \quad (\text{A.22})$$

Now, I scale all the dimensionful quantities as in Sec. 3.1, i.e.  $\tau \rightarrow \tau/s$ ,  $s \rightarrow s/gE$  and  $x^\mu \rightarrow x^\mu m/gE$ . This reduces all dependence on the parameters to dependence on  $\epsilon := gE/m^2 \ll 1$  and  $\kappa := g^3 E/m^2$ . I can now write the interaction terms in the

spin 1/2 case as

$$\begin{aligned} \exp \left\{ \frac{\kappa}{2\epsilon} \int_x \int_y j_0^\mu(x) G_{\mu\nu}(x, y) j_0^\nu(y) \right. \\ \left. + \kappa \int_x \int_y \xi^\mu(x) G_{\mu\nu}(x, y) j_0^\nu(y) \right. \\ \left. + \frac{\kappa\epsilon}{2} \int_x \int_y \xi^\mu(x) G_{\mu\nu}(x, y) \xi^\nu(y) \right\}, \end{aligned} \quad (\text{A.23})$$

where  $j^\mu$ ,  $\xi^\mu$  and  $G_{\mu\nu}$  are now independent of  $g$ ,  $E$  and  $m$ . In this paper, I have allowed  $\kappa$  to freely vary up to  $O(1)$  (that is because I only require  $\kappa \ll g^2$  and I consider strong coupling); however for the semiclassical approximation to be valid I require  $\epsilon \ll 1$ . Hence the spin dependent factors are subleading (as long as the dimensionless parts are at most  $O(1)$ ) and I can drop all  $\xi^\mu$  dependence.

The net result of all this is that, to leading order in  $\epsilon$ , the instanton describing pair production is the same for both theories, and hence so is the exponential suppression. However, the term proportional to  $\epsilon^0$  in the exponent of Eq. (A.23) and the external field contribution in (A.18) will contribute to the fluctuation prefactor about the instanton. Charge renormalisation, which is not included to leading order in  $\epsilon$ , is different in QED and SQED. In both cases I expect the final results to depend on the renormalised charge, as discussed in Sec. 3.3.3.

## A.4 Worldline description of extended particles

For elementary particles the geometric worldline description arises naturally and can be derived by standard methods from the field theoretic description, as shown in Sec. 3.1. For extended field configurations, such as solitons, no exact worldline description can exist. However, for circumstances where the extended field configuration is much smaller than all other scales, an effective worldline description can suffice [24, 227, 25, 279, 278]. This is analogous to the description of the motion of planets in the solar system in terms of the motion of points.

In Ref. [25] just such an effective description was explicitly derived for the 't Hooft-Polyakov monopole [23, 22]. The worldline instanton that they found was a circle and the effective worldline description was found to be valid when the radius of the circle was much larger than the size of the 't Hooft-Polyakov monopole. I wish to generalise this result for more general worldline curves.

The 't Hooft-Polyakov monopole is a static solution to the field equations for

the Georgi-Glashow model, and other similar theories. It is an extended solution and hence it cannot be said to be *at* a position, however it does have a well-defined centre and core region, beyond which all but the Abelian gauge field is exponentially damped. I can thus assign to the centre of the monopole solution a worldline, i.e. a map from the real line to the path in Minkowski space traced out by the centre of the monopole solution. The static solution and Lorentz transformations of it (which are also solutions) have straight, timelike worldlines. Static solutions of the Euclidean (Wick rotated) theory need not be timelike.

Combinations of straight worldlines are no longer exact solutions due to the interactions between them. However, in the limit that the monopoles are infinitely separated these should become exact solutions [266]<sup>1</sup>. At finite separation, due to the long-ranged interaction between monopoles, the solution is no longer exact. However, I can find an approximate solution following Ref. [25].

I consider for example the Georgi-Glashow theory. To find an approximate solution to the full (Euclidean) field equations I first solve the equations of motion for a pointlike monopole in a given external magnetic field, at a certain temperature, including the self-interaction. These are the classical worldline calculations I have carried out in this paper. For simplicity, I restrict the worldline to the 3–4 plane. I construct coordinates centred on the worldline and Fermi-Walker transported along it (see for example Ref. [353]). I denote the coordinate along the worldline as  $u$  and the normal coordinate in the plane as  $v$ , with  $(x_1, x_2, v) = (0, 0, 0)$  on the worldline. Other than photon excitations, which are taken into account, internal excitations of the 't Hooft-Polyakov monopole are assumed to be gapped and hence, for sufficiently low energies, these are not excited. That is, I can assume translation invariance along the monopole worldline. In this case, the field equations near the monopole worldline read

$$\begin{aligned} D_i F^{ij} + a(u) F^{vj} + O(a(u)^2 v^2) &= [D_i \phi, \phi], \\ D_i D^i \phi + a(u) D_v \phi + O(a(u)^2 v^2) &= \frac{\lambda}{g^2} (|\phi|^2 - M_W^2) \phi, \end{aligned} \quad (\text{A.24})$$

where  $D_a = \partial_a + igA_a$ ;  $i, j$  run over  $(x_1, x_2, v)$ ;  $\lambda$  is the four point self-coupling of the Higgs particle;  $M_W$  is the mass of a W boson and  $a(u)$  is the magnitude of the acceleration of the worldline. At zeroth order in the acceleration these equations

---

<sup>1</sup>In the Bogomolny-Prasad-Sommerfeld limit [64], i.e. when the scalar self-coupling is infinitesimally small and positive, such superpositions of static, like-charged monopoles are in fact exact solutions. That is because in this limit the attraction due to the Higgs field is exactly cancelled by the repulsion due to the gauge field [352]. At low energies the dynamics of such multimonomole solutions is given by geodesic motion of the collective coordinates on the configuration space of solutions [33, 34, 35].

are solved by the 't Hooft-Polyakov magnetic monopole, static along the worldline. Hence, at lowest order in the acceleration the full field theoretic calculation reduces to the geometric, worldline one which I have pursued in this paper. This also requires the radius of curvature of the worldline to be large compared with the classical radius of the monopole solution. In my dimensionless units the radius is  $O(\kappa)$  (for the Georgi-Glashow theory) and hence I get the constraint  $\kappa \ll a(u)^{-1}$ .

## A.5 Worldline finite difference formulation

In this appendix I give my discrete approximation to the action in Eq. (3.32) and the corresponding equations of motion. I use a simple finite difference approximation

$$\begin{aligned} \tilde{S}[x] = & \sqrt{N \sum_i (x_{i+1}^\mu - x_i^\mu)^2 - \sum_i x_i^3 (x_{i+1}^4 - x_i^4)} \\ & - \frac{\kappa}{2} \sum_{i,j} (x_{i+1}^\mu - x_i^\mu)(x_{j+1}^\mu - x_j^\mu) G_R(x_i, x_j; \tilde{T}, a) \end{aligned} \quad (\text{A.25})$$

where  $i$  and  $j$  run over  $0, 1, \dots, N-1$  and contractions of Lorentz indices are implied. As discussed in Sec. 3.3.3 I choose an exponential counterterm, rather than the simpler length counterterm of Polyakov, so that the bare mass is positive. Summing the infinite periodic copies of the regularised propagator gives

$$\begin{aligned} \sum_{n=-\infty}^{\infty} \frac{-1}{4\pi^2((t+n/\tilde{T})^2 + r^2 + a^2)} = \\ \frac{\tilde{T} \sinh\left(2\pi\tilde{T}\sqrt{a^2 + r^2}\right)}{4\pi\sqrt{a^2 + r^2} \left(\cos\left(2\pi\tilde{T}t\right) - \cosh\left(2\pi\tilde{T}\sqrt{a^2 + r^2}\right)\right)}, \end{aligned} \quad (\text{A.26})$$

and likewise for the exponential counterterm

$$\begin{aligned} \sum_{n=-\infty}^{\infty} \frac{\sqrt{\pi}}{4\pi^2 a^2} e^{-(r^2 + (t+n/\tilde{T})^2)/a^2} = \\ \frac{\tilde{T} e^{-r^2/a^2} \vartheta_3\left(\pi\tilde{T}t, e^{-\pi^2 a^2 \tilde{T}^2}\right)}{4\pi a} \end{aligned} \quad (\text{A.27})$$

where  $t$  and  $r$  are the temporal and spatial differences as in Sec. 3.1.2 and  $\vartheta_3$  is the Jacobi theta function of the third kind. Due to the lack of well optimised

numerical libraries for the Jacobi theta function, I in fact make a different choice of counterterm, which also reduces to the exponential regularisation for small  $\tilde{T}$ ,

$$G_R(x_i, x_j; \tilde{T}, a) = \frac{\tilde{T} \sinh\left(2\pi\tilde{T}\sqrt{a^2 + r^2}\right)}{4\pi\sqrt{a^2 + r^2} \left(\cos\left(2\pi\tilde{T}t\right) - \cosh\left(2\pi\tilde{T}\sqrt{a^2 + r^2}\right)\right)} + \frac{\sqrt{\pi}e^{-r^2/a^2} e^{(\cos(2\pi\tilde{T}t)-1)/(2\pi^2 a^2 \tilde{T}^2)}}{4\pi^2 a^2} \quad (\text{A.28})$$

This regularisation is smooth and periodic in  $1/\tilde{T}$ , as well as being relatively fast to numerically evaluate.

One further point, also mentioned in Sec. 3.3.3, is that there is no need to regularise the interactions between disconnected parts of worldlines, so one may use the unregularised propagator. This is useful as it removes some sources of error due to the finite cutoff,  $a$ . In my calculations, I have used the unregularised propagator for the interaction between the left and right hand sides of the W instantons. It could also be used, though I did not, for the interaction between thermal copies for the C instantons.

As discussed in Sec. 3.4, I fix the  $N_0$  zero and quasizero modes using Lagrange multipliers. Writing the constraint equations as  $C_a[x] = 0$ , where  $a$  runs over  $1, \dots, N_0$ , I define a new action including the Lagrange multiplier terms

$$\tilde{S}[x, \lambda] := \tilde{S}[x] + \sum_{a=1}^{N_0} \lambda_a C_a[x]. \quad (\text{A.29})$$

The  $\lambda_a$  are the Lagrange multipliers.

The equations of motion, which are simply  $4N + N_0$  coupled, nonlinear, algebraic equations are found by taking partial derivatives of (A.29), with respect to  $x_k^p$  and  $\lambda_b$ ,

$$\begin{aligned} \frac{\partial \tilde{S}[x]}{\partial x_k^p} &= 0, \\ C_b[x] &= 0. \end{aligned} \quad (\text{A.30})$$

The Newton-Raphson equations derived from these, and an initial guess, are a system of linear equations, which I solve by LU decomposition, using the numerical library Eigen 3 [195]. The 1 and 2 directions are trivial and decouple, leaving  $2N + \tilde{N}_0$  equations, where  $\tilde{N}_0 (< N_0)$  is the number of zero modes in the reduced

space.

## A.6 Thermal Schwinger rate numerical data

Along with this thesis, I have made available the numerical results presented in summary form in Sec. 3.4. They are in the file *gould2017thermal\_results.csv*. The first line gives the column headings and all following lines give the corresponding numerical data as comma-separated values. The meanings of the headings are as follows.

pot: The nature of the interaction potential, see below.

log2N:  $\log_2(N)$ , where  $N$  is the number of points in the worldline.

kappa: The coupling,  $\kappa := g^3 E/m^2$ .

T: The temperature,  $\tilde{T} := mT/gE$ .

a: The cutoff,  $a$ .

S: The action,  $\tilde{S} := S/\epsilon$ .

E: The energy,  $\tilde{\mathcal{E}} := \mathcal{E}/m$ .

len: The length of the worldline.

kinetic: The gauge-fixed length of the worldline,  $\tilde{L}$ , Eq. (3.33).

i0: Minus the area of the worldline,  $-\tilde{A}$ , Eq. (3.34).

vr: The interaction,  $\tilde{V}_R$ , Eq. (3.41) and the finite temperature generalisations.

zmax: The maximum distance between points in the  $x^3$  direction.

zmin: The minimum distance between points in the  $x^3$  direction.

tmax: The maximum distance between points in the  $x^4$  direction.

sol: The ratio of the norms of  $\partial\tilde{S}[x]/\partial x_k^\rho$  and  $x_k^\rho$ .

acc\_max: The maximum acceleration along the worldline, see below.

The first column, pot, takes three different values depending on the nature of the interaction potential. It takes the value 1 for zero temperature; 13 for the low temperature, C instanton topology; and 15 for the high temperature, W instanton topology.

The acceleration referred to in the last column is a finite difference approximation to  $|\ddot{x}|$ , defined by

$$N^2|2x_k - x_{k+1} - x_{k-1}|, \quad (\text{A.31})$$

where  $N$  is the number of points in the worldline.

# Bibliography

- [1] O. Gould and A. Rajantie, “Thermal Schwinger pair production at arbitrary coupling,” *Phys. Rev.* **D96** (2017) 076002, [arXiv:1704.04801 \[hep-th\]](#).
- [2] O. Gould and A. Rajantie, “Magnetic Monopole Mass Bounds from Heavy-Ion Collisions and Neutron Stars,” *Phys. Rev. Lett.* **119** (2017) 241601, [arXiv:1705.07052 \[hep-ph\]](#).
- [3] O. Gould and A. Rajantie, “Worldline sphaleron for Schwinger pair production,”. (Forthcoming).
- [4] P. Peregrinus, *The Letter of Petrus Peregrinus on the Magnet, AD 1269*, vol. 1. Library of Alexandria, 2015.
- [5] P. Curie, “Sur la possibilité d’existence de la conductibilité magnétique et du magnétisme libre,” in *Annales de la Fondation Louis de Broglie*, vol. 19, pp. 159–160, Fondation Louis de Broglie. 1994.
- [6] P. A. M. Dirac, “Quantized Singularities in the Electromagnetic Field,” *Proc. Roy. Soc. Lond.* **A133** (1931) 60–72.
- [7] M. Marinelli and G. Morpurgo, “The Electric Neutrality of Matter: A Summary,” *Phys. Lett.* **B137** (1984) 439–442.
- [8] J. Polchinski, “Monopoles, duality, and string theory,” *Int. J. Mod. Phys.* **A19S1** (2004) 145–156, [arXiv:hep-th/0304042 \[hep-th\]](#). [,145(2003)].
- [9] R. Foot, G. C. Joshi, H. Lew, and R. R. Volkas, “Charge quantization in the standard model and some of its extensions,” *Mod. Phys. Lett.* **A5** (1990) 2721–2732.
- [10] R. Foot, H. Lew, and R. R. Volkas, “Electric charge quantization,” *J. Phys.* **G19** (1993) 361–372, [arXiv:hep-ph/9209259 \[hep-ph\]](#). [Erratum: *J. Phys.* **G19**,1067(1993)].



- [11] P. A. M. Dirac, "The Theory of magnetic poles," *Phys. Rev.* **74** (1948) 817–830.
- [12] N. Cabibbo and E. Ferrari, "Quantum electrodynamics with Dirac monopoles," *Nuovo Cim.* **23** (1962) 1147–1154.
- [13] J. S. Schwinger, "Magnetic charge and quantum field theory," *Phys. Rev.* **144** (1966) 1087–1093.
- [14] J. S. Schwinger, "Sources and magnetic charge," *Phys. Rev.* **173** (1968) 1536–1544.
- [15] D. Zwanziger, "Local Lagrangian quantum field theory of electric and magnetic charges," *Phys. Rev.* **D3** (1971) 880.
- [16] M. Blagojevic and P. Senjanovic, "The Quantum Field Theory of Electric and Magnetic Charge," *Phys. Rept.* **157** (1988) 233.
- [17] R. A. Brandt, F. Neri, and D. Zwanziger, "Lorentz Invariance of the Quantum Field Theory of Electric and Magnetic Charge," *Phys. Rev. Lett.* **40** (1978) 147–150.
- [18] R. A. Brandt, F. Neri, and D. Zwanziger, "Lorentz Invariance From Classical Particle Paths in Quantum Field Theory of Electric and Magnetic Charge," *Phys. Rev.* **D19** (1979) 1153.
- [19] K. G. Wilson, "Confinement of Quarks," *Phys. Rev.* **D10** (1974) 2445–2459. [45(1974)].
- [20] A. M. Polyakov, "Compact Gauge Fields and the Infrared Catastrophe," *Phys. Lett.* **B59** (1975) 82–84.
- [21] A. M. Polyakov, "Quark Confinement and Topology of Gauge Groups," *Nucl. Phys.* **B120** (1977) 429–458.
- [22] G. t. Hooft, "Magnetic monopoles in unified gauge theories," *Nucl. Phys. B* **79** no. 2, (1974) 276–284.
- [23] A. M. Polyakov, "Particle Spectrum in Quantum Field Theory," *JETP Lett.* **20** (1974) 194–195.
- [24] K. Bardakci and S. Samuel, "Local Field Theory for Solitons," *Phys. Rev.* **D18** (1978) 2849.

- [25] I. K. Affleck and N. S. Manton, “Monopole pair production in a magnetic field,” *Nuclear Physics B* **194** no. 1, (1982) 38–64.
- [26] H. Georgi and S. L. Glashow, “Unity of All Elementary Particle Forces,” *Phys. Rev. Lett.* **32** (1974) 438–441.
- [27] G. 't Hooft, “Topology of the Gauge Condition and New Confinement Phases in Nonabelian Gauge Theories,” *Nucl. Phys.* **B190** (1981) 455–478.
- [28] N. Seiberg and E. Witten, “Electric - magnetic duality, monopole condensation, and confinement in  $N=2$  supersymmetric Yang-Mills theory,” *Nucl. Phys.* **B426** (1994) 19–52, [arXiv:hep-th/9407087 \[hep-th\]](#). [Erratum: *Nucl. Phys.*B430,485(1994)].
- [29] V. A. Rubakov, “Adler-Bell-Jackiw Anomaly and Fermion Number Breaking in the Presence of a Magnetic Monopole,” *Nucl. Phys.* **B203** (1982) 311–348.
- [30] J. C. G. Callan, “Dyon-Fermion Dynamics,” *Phys. Rev.* **D26** (1982) 2058–2068.
- [31] B. Julia and A. Zee, “Poles with Both Magnetic and Electric Charges in Nonabelian Gauge Theory,” *Phys. Rev.* **D11** (1975) 2227–2232.
- [32] E. Witten, “Dyons of Charge  $e\theta/2\pi$ ,” *Phys. Lett.* **86B** (1979) 283–287.
- [33] N. S. Manton, “A Remark on the Scattering of BPS Monopoles,” *Phys. Lett.* **B110** (1982) 54–56.
- [34] M. F. Atiyah and N. J. Hitchin, “Low-Energy Scattering of Nonabelian Monopoles,” *Phys. Lett.* **A107** (1985) 21–25.
- [35] G. W. Gibbons and N. S. Manton, “Classical and Quantum Dynamics of BPS Monopoles,” *Nucl. Phys.* **B274** (1986) 183–224.
- [36] J. L. Cardy, “Duality and the Theta Parameter in Abelian Lattice Models,” *Nucl. Phys.* **B205** (1982) 17–26.
- [37] E. Witten, “On S duality in Abelian gauge theory,” *Selecta Math.* **1** (1995) 383, [arXiv:hep-th/9505186 \[hep-th\]](#).
- [38] S. R. Coleman, “The Magnetic Monopole Fifty Years Later,” in *Particles and Fields 2. Proceedings, Summer Institute, Banff, Canada, August 16-27, 1981*, pp. 461–552. 1982. [[461\(1982\)](#)].

- [39] J. Preskill, “Magnetic Monopoles,” *Ann. Rev. Nucl. Part. Sci.* **34** (1984) 461–530.
- [40] V. A. Rubakov, “Monopole Catalysis of Proton Decay,” *Rept. Prog. Phys.* **51** (1988) 189–241.
- [41] G. ’t Hooft, “Monopoles, instantons and confinement,” in *National Summer School for Graduate Students: We-Heraeus Doktorandenschule Saalburg: Grundlagen und Neue Methoden der Theoretischen Physik Saalburg, Germany, September 4-15, 2000*. 1999. [arXiv:hep-th/0010225](#) [hep-th].
- [42] K. A. Intriligator and N. Seiberg, “Lectures on supersymmetric gauge theories and electric-magnetic duality,” *Nucl. Phys. Proc. Suppl.* **45BC** (1996) 1–28, [arXiv:hep-th/9509066](#) [hep-th]. [,157(1995)].
- [43] F. J. Ernst, “Removal of the nodal singularity of the C-metric,” *Journal of Mathematical Physics* **17** no. 4, (1976) 515–516.
- [44] D. Garfinkle and A. Strominger, “Semiclassical Wheeler wormhole production,” *Phys. Lett.* **B256** (1991) 146–149.
- [45] F. Dowker, J. P. Gauntlett, D. A. Kastor, and J. Traschen, “Pair creation of dilaton black holes,” *Physical Review D* **49** no. 6, (1994) 2909.
- [46] G. W. Gibbons, “Selfgravitating magnetic monopoles, global monopoles and black holes,” *Lect. Notes Phys.* **383** (1991) 110–138, [arXiv:1109.3538](#) [gr-qc].
- [47] D. J. Gross and M. J. Perry, “Magnetic Monopoles in Kaluza-Klein Theories,” *Nucl. Phys.* **B226** (1983) 29–48.
- [48] M. J. Perry, “Non-Abelian Kaluza-Klein Monopoles,” *Phys. Lett.* **B137** (1984) 171–174.
- [49] J. Figueroa and O. Farrill, “Electromagnetic duality for children,” 1998.
- [50] W. Greub and H.-R. Petry, “Minimal coupling and complex line bundles,” *Journal of Mathematical Physics* **16** no. 6, (1975) 1347–1351.
- [51] T. T. Wu and C. N. Yang, “Concept of Nonintegrable Phase Factors and Global Formulation of Gauge Fields,” *Phys. Rev.* **D12** (1975) 3845–3857.
- [52] E. Lubkin, “Geometric definition of gauge invariance,” *Annals Phys.* **23** (1963) 233.

- [53] K. A. Milton, “Theoretical and experimental status of magnetic monopoles,” *Rept. Prog. Phys.* **69** (2006) 1637–1712, arXiv:hep-ex/0602040 [hep-ex].
- [54] R. F. Dashen, B. Hasslacher, and A. Neveu, “Nonperturbative Methods and Extended Hadron Models in Field Theory. 1. Semiclassical Functional Methods,” *Phys. Rev.* **D10** (1974) 4114.
- [55] R. F. Dashen, B. Hasslacher, and A. Neveu, “Nonperturbative Methods and Extended Hadron Models in Field Theory. 2. Two-Dimensional Models and Extended Hadrons,” *Phys. Rev.* **D10** (1974) 4130–4138.
- [56] R. F. Dashen, B. Hasslacher, and A. Neveu, “Nonperturbative Methods and Extended Hadron Models in Field Theory. 3. Four-Dimensional Nonabelian Models,” *Phys. Rev.* **D10** (1974) 4138.
- [57] F. Englert and R. Brout, “Broken Symmetry and the Mass of Gauge Vector Mesons,” *Phys. Rev. Lett.* **13** (1964) 321–323.
- [58] P. W. Higgs, “Broken Symmetries and the Masses of Gauge Bosons,” *Phys. Rev. Lett.* **13** (1964) 508–509.
- [59] G. S. Guralnik, C. R. Hagen, and T. W. B. Kibble, “Global Conservation Laws and Massless Particles,” *Phys. Rev. Lett.* **13** (1964) 585–587.
- [60] J. Frohlich, G. Morchio, and F. Strocchi, “Higgs Phenomenon Without Symmetry Breaking Order Parameter,” *Nucl. Phys.* **B190** (1981) 553–582.
- [61] P. Goddard, “Magnetic Monopoles in Grand Unified Theories,” *Philosophical Transactions of the Royal Society of London. Series A, Mathematical and Physical Sciences* **304** no. 1482, (1982) 87–95.
- [62] A. M. Jaffe and C. H. Taubes, *Vortices and Monopoles. Structure of Static Gauge Theories*. 1980.
- [63] E. B. Bogomolny, “Stability of Classical Solutions,” *Sov. J. Nucl. Phys.* **24** (1976) 449. [Yad. Fiz.24,861(1976)].
- [64] M. K. Prasad and C. M. Sommerfield, “An Exact Classical Solution for the ’t Hooft Monopole and the Julia-Zee Dyon,” *Phys. Rev. Lett.* **35** (1975) 760–762.
- [65] A. K. Drukier and S. Nussinov, “Monopole Pair Creation in Energetic Collisions: Is It Possible?,” *Phys. Rev. Lett.* **49** (1982) 102.

- [66] A. Rajantie, “Introduction to Magnetic Monopoles,” *Contemp. Phys.* **53** (2012) 195–211, [arXiv:1204.3077 \[hep-th\]](#).
- [67] G. Giacomelli, “Magnetic Monopoles,” *Riv. Nuovo Cim.* **7N12** (1984) 1–111.
- [68] L. Patrizii and M. Spurio, “Status of Searches for Magnetic Monopoles,” *Ann. Rev. Nucl. Part. Sci.* **65** (2015) 279–302, [arXiv:1510.07125 \[hep-ex\]](#).
- [69] A. Rajantie, “The search for magnetic monopoles,” *Phys. Today* **69** no. 10, (2016) 40–46.
- [70] E. N. Parker, “The Origin of Magnetic Fields,” *Astrophys. J.* **160** (1970) 383.
- [71] M. S. Turner, E. N. Parker, and T. J. Bogdan, “Magnetic Monopoles and the Survival of Galactic Magnetic Fields,” *Phys. Rev.* **D26** (1982) 1296.
- [72] F. C. Adams, M. Fatuzzo, K. Freese, G. Tarle, R. Watkins, and M. S. Turner, “Extension of the Parker bound on the flux of magnetic monopoles,” *Phys. Rev. Lett.* **70** (1993) 2511–2514.
- [73] **MACRO** Collaboration, M. Ambrosio *et al.*, “Final results of magnetic monopole searches with the MACRO experiment,” *Eur. Phys. J.* **C25** (2002) 511–522, [arXiv:hep-ex/0207020 \[hep-ex\]](#).
- [74] **ANITA-II** Collaboration, M. Detrixhe *et al.*, “Ultra-Relativistic Magnetic Monopole Search with the ANITA-II Balloon-borne Radio Interferometer,” *Phys. Rev.* **D83** (2011) 023513, [arXiv:1008.1282 \[astro-ph.HE\]](#).
- [75] **ANTARES** Collaboration, S. Adrian-Martinez *et al.*, “Search for Relativistic Magnetic Monopoles with the ANTARES Neutrino Telescope,” *Astropart. Phys.* **35** (2012) 634–640, [arXiv:1110.2656 \[astro-ph.HE\]](#).
- [76] **IceCube** Collaboration, M. G. Aartsen *et al.*, “Searches for Relativistic Magnetic Monopoles in IceCube,” *Eur. Phys. J.* **C76** no. 3, (2016) 133, [arXiv:1511.01350 \[astro-ph.HE\]](#).
- [77] S. Burdin, M. Fairbairn, P. Mermoud, D. Milstead, J. Pinfold, T. Sloan, and W. Taylor, “Non-collider searches for stable massive particles,” *Phys. Rept.* **582** (2015) 1–52, [arXiv:1410.1374 \[hep-ph\]](#).
- [78] M. Fairbairn, A. C. Kraan, D. A. Milstead, T. Sjostrand, P. Z. Skands, and T. Sloan, “Stable massive particles at colliders,” *Phys. Rept.* **438** (2007) 1–63, [arXiv:hep-ph/0611040 \[hep-ph\]](#).

- [79] P. B. Price, E. K. Shirk, W. Z. Osborne, and L. S. Pinsky, “Evidence for Detection of a Moving Magnetic Monopole,” *Phys. Rev. Lett.* **35** (1975) 487–490.
- [80] B. Cabrera, “First Results from a Superconductive Detector for Moving Magnetic Monopoles,” *Phys. Rev. Lett.* **48** (1982) 1378–1380.
- [81] **Particle Data Group** Collaboration, C. Patrignani *et al.*, “Review of Particle Physics,” *Chin. Phys.* **C40** no. 10, (2016) 100001.
- [82] M. J. Lewis, K. Freese, and G. Tarle, “Protogalactic extension of the Parker bound,” *Phys. Rev.* **D62** (2000) 025002, [arXiv:astro-ph/9911095](#) [[astro-ph](#)].
- [83] Ya. B. Zeldovich and M. Yu. Khlopov, “On the Concentration of Relic Magnetic Monopoles in the Universe,” *Phys. Lett.* **B79** (1978) 239–241.
- [84] A. H. Guth and S. H. H. Tye, “Phase Transitions and Magnetic Monopole Production in the Very Early Universe,” *Phys. Rev. Lett.* **44** (1980) 631. [Erratum: *Phys. Rev. Lett.* 44,963(1980)].
- [85] J. Preskill, “Cosmological Production of Superheavy Magnetic Monopoles,” *Phys. Rev. Lett.* **43** (1979) 1365.
- [86] M. S. Turner, “Thermal Production of Superheavy Magnetic Monopoles in the Early Universe,” *Phys. Lett.* **B115** (1982) 95–98.
- [87] W. Collins and M. S. Turner, “Thermal Production of Superheavy Magnetic Monopoles in the New Inflationary Universe Scenario,” *Phys. Rev.* **D29** (1984) 2158–2161.
- [88] P. R. Lindblom and P. J. Steinhardt, “Thermal Production of Superheavy Magnetic Monopoles in the New Inflationary Universe Scenario,” *Phys. Rev.* **D31** (1985) 2151.
- [89] **ATLAS** Collaboration, G. Aad *et al.*, “Search for magnetic monopoles and stable particles with high electric charges in 8 TeV *pp* collisions with the ATLAS detector,” *Phys. Rev.* **D93** no. 5, (2016) 052009, [arXiv:1509.08059](#) [[hep-ex](#)].
- [90] **MoEDAL** Collaboration, B. Acharya *et al.*, “Search for Magnetic Monopoles with the MoEDAL Forward Trapping Detector in 13 TeV

- Proton-Proton Collisions at the LHC,” *Phys. Rev. Lett.* **118** no. 6, (2017) 061801, [arXiv:1611.06817 \[hep-ex\]](#).
- [91] Y. D. He, “Search for a Dirac magnetic monopole in high-energy nucleus-nucleus collisions,” *Phys. Rev. Lett.* **79** (1997) 3134–3137.
- [92] G. ’t Hooft, “Symmetry Breaking Through Bell-Jackiw Anomalies,” *Phys. Rev. Lett.* **37** (1976) 8–11.
- [93] G. ’t Hooft, “Computation of the Quantum Effects Due to a Four-Dimensional Pseudoparticle,” *Phys. Rev.* **D14** (1976) 3432–3450. [Erratum: *Phys. Rev.* **D18**, 2199(1978)].
- [94] N. S. Manton, “Topology in the Weinberg-Salam Theory,” *Phys. Rev.* **D28** (1983) 2019.
- [95] F. R. Klinkhamer and N. S. Manton, “A Saddle Point Solution in the Weinberg-Salam Theory,” *Phys. Rev.* **D30** (1984) 2212.
- [96] V. A. Rubakov and M. E. Shaposhnikov, “Electroweak baryon number nonconservation in the early universe and in high-energy collisions,” *Usp. Fiz. Nauk* **166** (1996) 493–537, [arXiv:hep-ph/9603208 \[hep-ph\]](#). [*Phys. Usp.* **39**, 461(1996)].
- [97] F. Bezrukov, D. Levkov, C. Rebbi, V. Rubakov, and P. Tinyakov, “Semiclassical study of baryon and lepton number violation in high-energy electroweak collisions,” *Physical Review D* **68** no. 3, (2003) 036005.
- [98] D. G. Levkov and S. M. Sibiryakov, “Induced tunneling in QFT: Soliton creation in collisions of highly energetic particles,” *Phys. Rev.* **D71** (2005) 025001, [arXiv:hep-th/0410198 \[hep-th\]](#).
- [99] D. Levkov and S. Sibiryakov, “Real-time instantons and suppression of collision-induced tunneling,” *JETP Lett.* **81** (2005) 53–57, [arXiv:hep-th/0412253 \[hep-th\]](#). [*Pisma Zh. Eksp. Teor. Fiz.* **81**, 60(2005)].
- [100] S. Demidov and D. Levkov, “Soliton-antisoliton pair production in particle collisions,” *Physical review letters* **107** no. 7, (2011) 071601.
- [101] S. Demidov and D. Levkov, “High-energy limit of collision-induced false vacuum decay,” *JHEP* **06** (2015) 123, [arXiv:1503.06339 \[hep-ph\]](#).

- [102] S. V. Demidov and D. G. Levkov, “Semiclassical description of soliton-antisoliton pair production in particle collisions,” *JHEP* **11** (2015) 066, [arXiv:1509.07125 \[hep-th\]](#).
- [103] A. Kuznetsov and P. G. Tinyakov, “False vacuum decay induced by particle collisions,” *Physical Review D* **56** no. 2, (1997) 1156.
- [104] E. Witten, “Baryons in the  $1/n$  Expansion,” *Nucl. Phys.* **B160** (1979) 57–115.
- [105] A. A. Belavin, A. M. Polyakov, A. S. Schwartz, and Yu. S. Tyupkin, “Pseudoparticle Solutions of the Yang-Mills Equations,” *Phys. Lett.* **B59** (1975) 85–87.
- [106] V. A. Kuzmin, V. A. Rubakov, and M. E. Shaposhnikov, “On the Anomalous Electroweak Baryon Number Nonconservation in the Early Universe,” *Phys. Lett.* **155B** (1985) 36.
- [107] P. B. Arnold and L. D. McLerran, “Sphalerons, Small Fluctuations and Baryon Number Violation in Electroweak Theory,” *Phys. Rev.* **D36** (1987) 581.
- [108] V. A. Matveev, V. A. Rubakov, A. N. Tavkhelidze, and V. F. Tokarev, “Nonconservation of the Fermion Number in a Cold Dense Fermion Medium in  $V^-$ -a Gauge Theories,” *Theor. Math. Phys.* **69** (1986) 961–976. [Teor. Mat. Fiz.69,3(1986)].
- [109] V. A. Matveev, V. A. Rubakov, A. N. Tavkhelidze, and V. F. Tokarev, “Fermion Number Nonconservation and Cold Neutral Fermionic Matter in  $(V - A)$  Gauge Theories,” *Nucl. Phys.* **B282** (1987) 700–726.
- [110] V. A. Rubakov, “Unsuppressed Electroweak Fermion Number Nonconservation in Decays of Heavy Particles,” *Nucl. Phys.* **B256** (1985) 509–524.
- [111] V. A. Rubakov, “Electroweak Nonconservation of the Baryon Number in the Decay of Heavy Particles,” *JETP Lett.* **41** (1985) 266–268. [Pisma Zh. Eksp. Teor. Fiz.41,218(1985)].
- [112] A. Ringwald, “High-Energy Breakdown of Perturbation Theory in the Electroweak Instanton Sector,” *Nucl. Phys.* **B330** (1990) 1–18.



- [113] O. Espinosa, “High-Energy Behavior of Baryon and Lepton Number Violating Scattering Amplitudes and Breakdown of Unitarity in the Standard Model,” *Nucl. Phys.* **B343** (1990) 310–340.
- [114] A. H. Mueller, “Comparing two particle and multiparticle initiated processes in the one instanton sector,” *Nucl. Phys.* **B401** (1993) 93–115.
- [115] P. G. Tinyakov, “Multiparticle instanton-induced processes. Application to B violation in high energy collisions,” *Physics Letters B* **284** no. 3, (1992) 410–416.
- [116] P. G. Tinyakov, “Instanton like transitions in high-energy collisions,” *Int. J. Mod. Phys.* **A8** (1993) 1823–1886.
- [117] G. F. Bonini, A. G. Cohen, C. Rebbi, and V. A. Rubakov, “The Semiclassical description of tunneling in scattering with multiple degrees of freedom,” *Phys. Rev.* **D60** (1999) 076004, [arXiv:hep-ph/9901226](#) [hep-ph].
- [118] D. G. Levkov, A. G. Panin, and S. M. Sibiryakov, “Signatures of unstable semiclassical trajectories in tunneling,” *J. Phys.* **A42** (2009) 205102, [arXiv:0811.3391](#) [quant-ph].
- [119] V. Rubakov and P. G. Tinyakov, “Towards the semiclassical calculability of high energy instanton cross sections,” *Physics Letters B* **279** no. 1, (1992) 165–168.
- [120] V. A. Rubakov, D. T. Son, and P. G. Tinyakov, “Classical boundary value problem for instanton transitions at high-energies,” *Phys. Lett.* **B287** (1992) 342–348.
- [121] F. L. Bezrukov and D. Levkov, “Dynamical tunneling of bound systems through a potential barrier: complex way to the top,” *J. Exp. Theor. Phys.* **98** (2004) 820–836, [arXiv:quant-ph/0312144](#) [quant-ph]. [*Zh. Eksp. Teor. Fiz.*125,938(2004)].
- [122] D. G. Levkov, A. G. Panin, and S. M. Sibiryakov, “Unstable Semiclassical Trajectories in Tunneling,” *Phys. Rev. Lett.* **99** (2007) 170407, [arXiv:0707.0433](#) [quant-ph].
- [123] C. J. Goebel, “The Spatial Extent of Magnetic Monopoles,” in *Quanta: Essays in Theoretical Physics Dedicated to Gregor Wentzel*, P. G. O. Freund, C. J. Goebel, and Y. Nambu, eds., pp. 338–344. University of Chicago Press, 1970.

- [124] F. J. Dyson, “Divergence of perturbation theory in quantum electrodynamics,” *Phys. Rev.* **85** (1952) 631–632.
- [125] C. A. Hurst, “An example of a divergent perturbation expansion in field theory,” *Proc. Cambridge Phil. Soc.* **48** (1952) 625.
- [126] C. M. Bender and T. T. WU, “Large order behavior of Perturbation theory,” *Phys. Rev. Lett.* **27** (1971) 461.
- [127] L. N. Lipatov, “Divergence of the Perturbation Theory Series and the Quasiclassical Theory,” *Sov. Phys. JETP* **45** (1977) 216–223. [Zh. Eksp. Teor. Fiz.72,411(1977)].
- [128] E. Brezin, J. C. Le Guillou, and J. Zinn-Justin, “Perturbation Theory at Large Order. 1. The  $\phi^4$  Interaction,” *Phys. Rev.* **D15** (1977) 1544–1557.
- [129] G. 't Hooft, “Can We Make Sense Out of Quantum Chromodynamics?,” *Subnucl. Ser.* **15** (1979) 943.
- [130] B. E. Lautrup, “On High Order Estimates in QED,” *Phys. Lett.* **69B** (1977) 109–111.
- [131] C. Bachas, “On the breakdown of perturbation theory,” *Theor. Math. Phys.* **95** (1993) 491–498, [arXiv:hep-th/9212033](#) [hep-th]. [Teor. Mat. Fiz.95,187(1993)].
- [132] J. G. Russo, “A Note on perturbation series in supersymmetric gauge theories,” *JHEP* **06** (2012) 038, [arXiv:1203.5061](#) [hep-th].
- [133] H. Goldberg, “Sphaleron production in high-energy two particle collisions,” *Phys. Lett.* **B257** (1991) 346–350.
- [134] V. E. Korepin, P. P. Kulish, and L. D. Faddeev, “Soliton Quantization,” *JETP Lett.* **21** (1975) 138–139. [Pisma Zh. Eksp. Teor. Fiz.21,302(1975)].
- [135] S. R. Coleman, “Semiclassical Crossing Symmetry for Semiclassical Soliton Scattering,” *Phys. Rev.* **D12** (1975) 1650.
- [136] A. S. Goldhaber, “Role of Spin in the Monopole Problem,” *Phys. Rev.* **140** (1965) B1407–B1414.
- [137] D. Zwanziger, “Angular distributions and a selection rule in charge-pole reactions,” *Phys. Rev.* **D6** (1972) 458–470.

- [138] S. Mandelstam, “Determination of the pion - nucleon scattering amplitude from dispersion relations and unitarity. General theory,” *Phys. Rev.* **112** (1958) 1344–1360.
- [139] V. N. Gribov, *Strong interactions of hadrons at high energies: Gribov lectures on*. Cambridge University Press, 2012.  
<http://cambridge.org/catalogue/catalogue.asp?isbn=9780521856096>.
- [140] T. W. B. Kibble, “Kinematics of General Scattering Processes and the Mandelstam Representation,” *Phys. Rev.* **117** (1960) 1159–1162.
- [141] K. W. Ford and J. A. Wheeler, “Application of semiclassical scattering analysis,” *Annals of Physics* **7** no. 3, (1959) 287–322.
- [142] Y. Kazama, C. N. Yang, and A. S. Goldhaber, “Scattering of a Dirac Particle with Charge  $Ze$  by a Fixed Magnetic Monopole,” *Phys. Rev.* **D15** (1977) 2287–2299.
- [143] L. F. Urrutia, “Zeroth Order Eikonal Approximation in Relativistic Charged Particle Monopole Scattering,” *Phys. Rev.* **D18** (1978) 3031.
- [144] L. P. Gamberg and K. A. Milton, “Dual quantum electrodynamics: Dyon-dyon and charge monopole scattering in a high-energy approximation,” *Phys. Rev.* **D61** (2000) 075013, [arXiv:hep-ph/9910526](https://arxiv.org/abs/hep-ph/9910526) [hep-ph].
- [145] J.-L. Gervais and B. Sakita, “Extended Particles in Quantum Field Theories,” *Phys. Rev.* **D11** (1975) 2943.
- [146] K. E. Cahill, “Extended Particles and Solitons,” *Phys. Lett.* **53B** (1974) 174–176.
- [147] J. Goldstone and R. Jackiw, “Quantization of Nonlinear Waves,” *Phys. Rev.* **D11** (1975) 1486–1498.
- [148] J.-L. Gervais, A. Jevicki, and B. Sakita, “Perturbation Expansion Around Extended Particle States in Quantum Field Theory. 1.,” *Phys. Rev.* **D12** (1975) 1038.
- [149] R. F. Dashen, B. Hasslacher, and A. Neveu, “The Particle Spectrum in Model Field Theories from Semiclassical Functional Integral Techniques,” *Phys. Rev.* **D11** (1975) 3424.

- [150] E. Tomboulis, “Canonical Quantization of Nonlinear Waves,” *Phys. Rev.* **D12** (1975) 1678.
- [151] N. H. Christ and T. D. Lee, “Quantum Expansion of Soliton Solutions,” *Phys. Rev.* **D12** (1975) 1606.
- [152] V. G. Kiselev and K. G. Selivanov, “Quantum Corrections to Monopole Mass,” *Phys. Lett.* **B213** (1988) 165–167.
- [153] V. G. Kiselev, “A monopole in the Coleman-Weinberg model,” *Phys. Lett.* **B249** (1990) 269–272.
- [154] M. E. Peskin and D. V. Schroeder, *An Introduction to quantum field theory*. Addison-Wesley, Reading, USA, 1995.  
<http://www.slac.stanford.edu/~mpeskin/QFT.html>.
- [155] T. Banks, “Arguments Against a Finite N=8 Supergravity,”  
[arXiv:1205.5768](https://arxiv.org/abs/1205.5768) [hep-th].
- [156] C. Papageorgakis and A. B. Royston, “Revisiting Soliton Contributions to Perturbative Amplitudes,” *JHEP* **09** (2014) 128, [arXiv:1404.0016](https://arxiv.org/abs/1404.0016) [hep-th].
- [157] V. G. Kiselev and Ya. M. Shnir, “Forced topological nontrivial field configurations,” *Phys. Rev.* **D57** (1998) 5174–5183, [arXiv:hep-th/9801001](https://arxiv.org/abs/hep-th/9801001) [hep-th].
- [158] A. C. Davis, T. W. B. Kibble, A. Rajantie, and H. Shanahan, “Topological defects in lattice gauge theories,” *JHEP* **11** (2000) 010, [arXiv:hep-lat/0009037](https://arxiv.org/abs/hep-lat/0009037) [hep-lat].
- [159] A. Rajantie and D. J. Weir, “Nonperturbative study of the ’t Hooft-Polyakov monopole form factors,” *Phys. Rev.* **D85** (2012) 025003, [arXiv:1109.0299](https://arxiv.org/abs/1109.0299) [hep-lat].
- [160] H. Vidberg and J. Serene, “Solving the Eliashberg equations by means of N-point Padé approximants,” *Journal of Low Temperature Physics* **29** no. 3-4, (1977) 179–192.
- [161] M. Luscher and U. Wolff, “How to Calculate the Elastic Scattering Matrix in Two-dimensional Quantum Field Theories by Numerical Simulation,” *Nucl. Phys.* **B339** (1990) 222–252.

- [162] M. Asakawa, T. Hatsuda, and Y. Nakahara, “Maximum entropy analysis of the spectral functions in lattice QCD,” *Prog. Part. Nucl. Phys.* **46** (2001) 459–508, [arXiv:hep-lat/0011040 \[hep-lat\]](#).
- [163] F. E. Low, “Scattering of light of very low frequency by systems of spin 1/2,” *Phys. Rev.* **96** (1954) 1428–1432.
- [164] M. Gell-Mann and M. L. Goldberger, “Scattering of low-energy photons by particles of spin 1/2,” *Phys. Rev.* **96** (1954) 1433–1438.
- [165] R. d. L. Kronig, “On the theory of dispersion of x-rays,” *JOSA* **12** no. 6, (1926) 547–557.
- [166] H. A. Kramers, *La diffusion de la lumiere par les atomes*. 1927.
- [167] M. L. Goldberger, “Use of causality conditions in quantum theory,” *Physical Review* **97** no. 2, (1955) 508.
- [168] M. Gell-Mann, M. L. Goldberger, and W. E. Thirring, “Use of causality conditions in quantum theory,” *Phys. Rev.* **95** (1954) 1612–1627.
- [169] L. Landau, “On the theory of transfer of energy at collisions,” *Phys. Z. Sowjetunion* **1** no. 88, (1932) .
- [170] L. Landau, “On the theory of transfer of energy at collisions II,” *Phys. Z. Sowjetunion* **2** no. 46, (1932) 7.
- [171] L. Landau and E. Lifschitz, “On the theory of energy transfer during collisions III,” *JETP* **18** (1948) 750.
- [172] L. D. Landau and E. M. Lifshits, *Quantum Mechanics*, vol. v.3 of *Course of Theoretical Physics*. Butterworth-Heinemann, Oxford, 1991.
- [173] S. Iordanskii and L. Pitaevskii, “Multiphoton boundary of the excitation spectrum in He II,” *Soviet Journal of Experimental and Theoretical Physics* **49** (1979) 386.
- [174] A. S. Gorsky and M. B. Voloshin, “Nonperturbative production of multiboson states and quantum bubbles,” *Phys. Rev.* **D48** (1993) 3843–3851, [arXiv:hep-ph/9305219 \[hep-ph\]](#).
- [175] M. B. Voloshin, “On strong high-energy scattering in theories with weak coupling,” *Phys. Rev.* **D43** (1991) 1726–1734.

- [176] J. M. Cornwall and G. Tiktopoulos, “Functional Schrodinger equation approach to high-energy multiparticle scattering,” *Phys. Lett.* **B282** (1992) 195–200.
- [177] M. B. Voloshin, “Catalyzed decay of false vacuum in four-dimensions,” *Phys. Rev.* **D49** (1994) 2014–2018, [arXiv:hep-ph/9309237](#) [hep-ph].
- [178] D. Diakonov and V. Petrov, “Nonperturbative isotropic multiparticle production in Yang-Mills theory,” *Phys. Rev.* **D50** (1994) 266–282, [arXiv:hep-ph/9307356](#) [hep-ph].
- [179] D. T. Son, “Semiclassical approach for multiparticle production in scalar theories,” *Nucl. Phys.* **B477** (1996) 378–406, [arXiv:hep-ph/9505338](#) [hep-ph].
- [180] F. L. Bezrukov, M. V. Libanov, and S. V. Troitsky, “O(4) symmetric singular solutions and multiparticle cross-sections in  $\phi^4$  theory at tree level,” *Mod. Phys. Lett.* **A10** (1995) 2135–2141, [arXiv:hep-ph/9508220](#) [hep-ph].
- [181] F. L. Bezrukov, M. V. Libanov, D. T. Son, and S. V. Troitsky, “Singular classical solutions and tree multiparticle cross-sections in scalar theories,” in *High-energy physics and quantum field theory. Proceedings, 10th International Workshop, Zvenigorod, Russia, September 20-26, 1995*, pp. 228–238. 1995. [arXiv:hep-ph/9512342](#) [hep-ph].
- [182] F. L. Bezrukov, “Use of singular classical solutions for calculation of multiparticle cross-sections in field theory,” *Theor. Math. Phys.* **115** (1998) 647–657, [arXiv:hep-ph/9901270](#) [hep-ph]. [Teor. Mat. Fiz.115,358(1998)].
- [183] J. M. Cornwall and G. Tiktopoulos, “Semiclassical matrix elements for the quartic oscillator,” *Annals Phys.* **228** (1993) 365–410.
- [184] C. G. Darwin, “The dynamical motions of charged particles,” *The London, Edinburgh, and Dublin Philosophical Magazine and Journal of Science* **39** no. 233, (1920) 537–551.
- [185] L. D. Landau and E. M. Lifshitz, “The classical theory of fields,”.
- [186] P. B. Arnold and M. P. Mattis, “Baryon Violation at the SSC? Recent Claims Reexamined,” *Phys. Rev.* **D42** (1990) 1738–1743.
- [187] S. Yu. Khlebnikov, V. A. Rubakov, and P. G. Tinyakov, “Instanton induced cross-sections below the sphaleron,” *Nucl. Phys.* **B350** (1991) 441–473.

- [188] A. H. Mueller, “Leading power corrections to the semiclassical approximation for gauge meson collisions in the one instanton sector,” *Nucl. Phys.* **B353** (1991) 44–58.
- [189] A. H. Mueller, “First Quantum Corrections to Gluon-gluon Collisions in the One Instanton Sector,” *Nucl. Phys.* **B348** (1991) 310–326.
- [190] S. Yu. Khlebnikov and P. G. Tinyakov, “Constraint dependence of the instanton calculations and exponentiation of hard - soft corrections at high-energies,” *Phys. Lett.* **B269** (1991) 149–154.
- [191] M. B. Voloshin, “Quantum corrections on high-energy lines to amplitudes induced by Euclidean field solutions,” *Nucl. Phys.* **B359** (1991) 301–321.
- [192] S. R. Coleman, “Quantum Tunneling and Negative Eigenvalues,” *Nucl. Phys.* **B298** (1988) 178–186.
- [193] F. L. Bezrukov and D. Levkov, “Theta instantons in SU(2) Higgs theory,” *Theor. Math. Phys.* **138** (2004) 397–406, [arXiv:hep-th/0303136](https://arxiv.org/abs/hep-th/0303136) [hep-th]. [Teor. Mat. Fiz.138,422(2004)].
- [194] C. Rebbi and J. R. L. Singleton, “Computational study of baryon number violation in high-energy electroweak collisions,” *Phys. Rev.* **D54** (1996) 1020–1043, [arXiv:hep-ph/9601260](https://arxiv.org/abs/hep-ph/9601260) [hep-ph].
- [195] G. Guennebaud, B. Jacob, *et al.*, “Eigen v3.” [Http://eigen.tuxfamily.org](http://eigen.tuxfamily.org), 2010.
- [196] S. Balay, S. Abhyankar, M. F. Adams, J. Brown, P. Brune, K. Buschelman, L. Dalcin, V. Eijkhout, W. D. Gropp, D. Kaushik, M. G. Knepley, L. C. McInnes, K. Rupp, B. F. Smith, S. Zampini, H. Zhang, and H. Zhang, “PETSc Web page.” [Http://www.mcs.anl.gov/petsc](http://www.mcs.anl.gov/petsc), 2016.
- [197] T. Vachaspati, “Monopole-Antimonopole Scattering,” *Phys. Rev.* **D93** no. 4, (2016) 045008, [arXiv:1511.05095](https://arxiv.org/abs/1511.05095) [hep-th].
- [198] F. Sauter, “Uber das Verhalten eines Elektrons im homogenen elektrischen Feld nach der relativistischen Theorie Diracs,” *Z. Phys.* **69** (1931) 742–764.
- [199] W. Heisenberg and H. Euler, “Consequences of Dirac’s theory of positrons,” *Z. Phys.* **98** (1936) 714–732, [arXiv:physics/0605038](https://arxiv.org/abs/physics/0605038) [physics].

- [200] V. Weisskopf, “The electrodynamics of the vacuum based on the quantum theory of the electron,” *Kong. Dan. Vid. Sel. Mat. Fys. Med.* **14N6** (1936) 1–39.
- [201] J. S. Schwinger, “On gauge invariance and vacuum polarization,” *Phys. Rev.* **82** (1951) 664–679.
- [202] M. Stone, “The Lifetime and Decay of Excited Vacuum States of a Field Theory Associated with Nonabsolute Minima of Its Effective Potential,” *Phys. Rev.* **D14** (1976) 3568.
- [203] I. L. Bogolyubsky and V. G. Makhankov, “Dynamics of Heavy Spherically-Symmetric Pulsons,” *Pisma Zh. Eksp. Teor. Fiz.* **25** (1977) 120–123.
- [204] S. Kasuya, M. Kawasaki, and F. Takahashi, “I-balls,” *Phys. Lett.* **B559** (2003) 99–106, [arXiv:hep-ph/0209358](#) [hep-ph].
- [205] K. Mukaida, M. Takimoto, and M. Yamada, “On Longevity of I-ball/Oscillon,” *JHEP* **03** (2017) 122, [arXiv:1612.07750](#) [hep-ph].
- [206] C. M. Bender and S. A. Orszag, *Advanced mathematical methods for scientists and engineers I*. Springer Science & Business Media, 1999.
- [207] M. Hindmarsh and P. Salmi, “Numerical investigations of oscillons in 2 dimensions,” *Phys. Rev.* **D74** (2006) 105005, [arXiv:hep-th/0606016](#) [hep-th].
- [208] P. Salmi and M. Hindmarsh, “Radiation and Relaxation of Oscillons,” *Phys. Rev.* **D85** (2012) 085033, [arXiv:1201.1934](#) [hep-th].
- [209] E. J. Copeland, M. Gleiser, and H. R. Muller, “Oscillons: Resonant configurations during bubble collapse,” *Phys. Rev.* **D52** (1995) 1920–1933, [arXiv:hep-ph/9503217](#) [hep-ph].
- [210] P. M. Saffin and A. Tranberg, “Oscillons and quasi-breathers in D+1 dimensions,” *JHEP* **01** (2007) 030, [arXiv:hep-th/0610191](#) [hep-th].
- [211] E. A. Andersen and A. Tranberg, “Four results on  $\phi^4$  oscillons in D+1 dimensions,” *JHEP* **12** (2012) 016, [arXiv:1210.2227](#) [hep-ph].
- [212] M. Gleiser and J. Thorarinson, “A Phase transition in U(1) configuration space: Oscillons as remnants of vortex-antivortex annihilation,” *Phys. Rev.* **D76** (2007) 041701, [arXiv:hep-th/0701294](#) [HEP-TH].



- [213] V. Achilleos, F. K. Diakonou, D. J. Frantzeskakis, G. C. Katsimiga, X. N. Maintas, E. Manousakis, C. E. Tsagkarakis, and A. Tsapalis, “Oscillons and oscillating kinks in the Abelian-Higgs model,” *Phys. Rev.* **D88** (2013) 045015, [arXiv:1306.3868 \[hep-th\]](#).
- [214] C. E. Tsagkarakis, V. Achilleos, F. K. Diakonou, D. J. Frantzeskakis, G. C. Katsimiga, X. N. Maintas, E. Manousakis, and A. Tsapalis, “Oscillons and oscillating kinks in the Abelian-Higgs model,” *PoS CORFU2014* (2014) 122, [arXiv:1508.06209 \[hep-th\]](#).
- [215] E. Farhi, N. Graham, V. Khemani, R. Markov, and R. Rosales, “An Oscillon in the SU(2) gauged Higgs model,” *Phys. Rev.* **D72** (2005) 101701, [arXiv:hep-th/0505273 \[hep-th\]](#).
- [216] N. Graham, “An Electroweak oscillon,” *Phys. Rev. Lett.* **98** (2007) 101801, [arXiv:hep-th/0610267 \[hep-th\]](#). [Erratum: *Phys. Rev. Lett.* **98**, 189904(2007)].
- [217] G. Fodor and I. Racz, “What does a strongly excited ’t Hooft-Polyakov magnetic monopole do?,” *Phys. Rev. Lett.* **92** (2004) 151801, [arXiv:hep-th/0311061 \[hep-th\]](#).
- [218] P. Forgacs and M. S. Volkov, “Resonant excitations of the ’t Hooft-Polyakov monopole,” *Phys. Rev. Lett.* **92** (2004) 151802, [arXiv:hep-th/0311062 \[hep-th\]](#).
- [219] G. Fodor and I. Racz, “Numerical investigation of highly excited magnetic monopoles in SU(2) Yang-Mills-Higgs theory,” *Phys. Rev.* **D77** (2008) 025019, [arXiv:hep-th/0609110 \[hep-th\]](#).
- [220] T. Vachaspati, “Creation of Magnetic Monopoles in Classical Scattering,” *Phys. Rev. Lett.* **117** no. 18, (2016) 181601, [arXiv:1607.07460 \[hep-th\]](#).
- [221] I. K. Affleck, O. Alvarez, and N. S. Manton, “Pair Production at Strong Coupling in Weak External Fields,” *Nucl. Phys.* **B197** (1982) 509–519.
- [222] S. Lebedev and V. Ritus, “Virial representation of the imaginary part of the Lagrangian of an electromagnetic field,” *Zhurnal Eksperimental’noj i Teoreticheskoy Fiziki* **86** no. 2, (1984) 408–422.
- [223] G. V. Dunne and C. Schubert, “Multiloop information from the QED effective Lagrangian,” *J. Phys. Conf. Ser.* **37** (2006) 59–72, [arXiv:hep-th/0409021 \[hep-th\]](#).

- [224] I. Huet, D. G. C. McKeon, and C. Schubert, “Euler-Heisenberg lagrangians and asymptotic analysis in 1+1 QED, part 1: Two-loop,” *JHEP* **12** (2010) 036, [arXiv:1010.5315 \[hep-th\]](#).
- [225] I. Huet, M. Rausch de Traubenberg, and C. Schubert, “Asymptotic behavior of the QED perturbation series,” in *5th Winter Workshop on Non-Perturbative Quantum Field Theory (WWNPQFT) Sophia-Antipolis, France, March 22-24, 2017*. 2017. [arXiv:1707.07655 \[hep-th\]](#).  
<http://inspirehep.net/record/1611342/files/arXiv:1707.07655.pdf>.
- [226] D. G. Boulware, L. S. Brown, R. N. Cahn, S. D. Ellis, and C.-k. Lee, “Scattering on Magnetic Charge,” *Phys. Rev.* **D14** (1976) 2708.
- [227] N. S. Manton, “An Effective Lagrangian for Solitons,” *Nucl. Phys.* **B150** (1979) 397–412.
- [228] A. Casher, H. Neuberger, and S. Nussinov, “Chromoelectric Flux Tube Model of Particle Production,” *Phys. Rev.* **D20** (1979) 179–188.
- [229] A. Casher, H. Neuberger, and S. Nussinov, “Multiparticle production by bubbling flux tubes,” *Phys. Rev.* **D21** (1980) 1966.
- [230] A. Bialas, W. Czyz, A. Dyrek, and W. Florkowski, “Oscillations of Quark - Gluon Plasma Generated in Strong Color Fields,” *Nucl. Phys.* **B296** (1988) 611–624.
- [231] A. K. Ganguly, P. K. Kaw, and J. C. Parikh, “Thermal tunneling of  $q\bar{q}$  pairs in A-A collisions,” *Physical Review C* **51** no. 4, (1995) 2091.
- [232] W. Florkowski, “Schwinger tunneling and thermal character of hadron spectra,” *Acta Phys. Polon.* **B35** (2004) 799–808, [arXiv:nucl-th/0309049 \[nucl-th\]](#).
- [233] A. Ringwald, “Boiling the vacuum with an x-ray free electron laser,” in *Quantum aspects of beam physics. Proceedings, Joint 28th Advanced Beam Dynamics and Advanced and Novel Accelerator Workshop, QABP’03, Hiroshima, Japan, January 7-11, 2003*, pp. 149–163. 2003.  
[arXiv:hep-ph/0304139 \[hep-ph\]](#).  
<http://alice.cern.ch/format/showfull?sysnb=2372572>.
- [234] F. Bloch, “Zur Theorie des Austauschproblems und der Remanenzerscheinung der Ferromagnetika,” *Zeitschrift für Physik* **74** no. 5, (1932) 295–335.

- [235] R. P. Feynman, “An Operator calculus having applications in quantum electrodynamics,” *Phys. Rev.* **84** (1951) 108–128.
- [236] I. M. Gelfand and A. M. Yaglom, “Integration in functional spaces and its applications in quantum physics,” *J. Math. Phys.* **1** (1960) 48.
- [237] A. M. Polyakov, “Gauge Fields as Rings of Glue,” *Nucl. Phys.* **B164** (1980) 171–188.
- [238] A. Polyakov, “Two-dimensional quantum gravity. Superconductivity at high  $T_c$ ,” *Les Houches* (1988) 305–368.
- [239] E. S. Fradkin and D. M. Gitman, “Path integral representation for the relativistic particle propagators and BFV quantization,” *Phys. Rev.* **D44** (1991) 3230–3236.
- [240] J. Polchinski, “String theory, vol. 1, 2,” *Cambridge, UK: Univ. Pr* (1998) .
- [241] V. S. Dotsenko and S. N. Vergeles, “Renormalizability of Phase Factors in the Nonabelian Gauge Theory,” *Nucl. Phys.* **B169** (1980) 527–546.
- [242] S. P. Gavrilov and D. M. Gitman, “One-loop energy-momentum tensor in QED with electriclike background,” *Physical Review D* **78** no. 4, (2008) 045017.
- [243] A. D. Linde, “Fate of the false vacuum at finite temperature: theory and applications,” *Physics Letters B* **100** no. 1, (1981) 37–40.
- [244] A. D. Linde, “Decay of the false vacuum at finite temperature,” *Nuclear Physics B* **216** no. 2, (1983) 421–445.
- [245] J. S. Langer, “Statistical theory of the decay of metastable states,” *Annals Phys.* **54** (1969) 258–275.
- [246] I. Affleck, “Quantum-statistical metastability,” *Physical Review Letters* **46** no. 6, (1981) 388.
- [247] K. Selivanov, “Tunneling at finite temperature,” *Physics Letters A* **121** no. 3, (1987) 111–112.
- [248] S. Y. Khlebnikov, V. A. Rubakov, and P. G. Tinyakov, “Periodic instantons and scattering amplitudes,” *Nuclear Physics B* **367** no. 2, (1991) 334–358.

- [249] P. H. Cox, W. S. Hellman, and A. Yildiz, “Finite Temperature Corrections to Field Theory: Electron Mass and Magnetic Moment, and Vacuum Energy,” *Annals Phys.* **154** (1984) 211.
- [250] P. Elmfors and B.-S. Skagerstam, “Electromagnetic fields in a thermal background,” *Phys. Lett.* **B348** (1995) 141–148, [arXiv:hep-th/9404106 \[hep-th\]](#). [Erratum: *Phys. Lett.*B376,330(1996)].
- [251] P. Elmfors and B.-S. Skagerstam, “Thermally induced photon splitting,” *Phys. Lett.* **B427** (1998) 197–205, [arXiv:hep-ph/9802397 \[hep-ph\]](#).
- [252] H. Gies, “QED effective action at finite temperature,” *Physical Review D* **60** no. 10, (1999) 105002.
- [253] V. I. Ritus, “The Lagrange Function of an Intensive Electromagnetic Field and Quantum Electrodynamics at Small Distances,” *Sov. Phys. JETP* **42** (1975) 774. [Pisma Zh. Eksp. Teor. Fiz.69,1517(1975)].
- [254] V. I. Ritus, “Connection between strong-field quantum electrodynamics with short-distance quantum electrodynamics,” *JETP* **46** (1977) 423.
- [255] V. I. Ritus, “Effective Lagrange Function of Intense Electromagnetic Field in QED,” in *Frontier Tests of QED and Physics of the Vacuum*, vol. 1, p. 11. 1998.
- [256] H. Gies, “QED effective action at finite temperature: Two-loop dominance,” *Physical Review D* **61** no. 8, (2000) 085021.
- [257] H. Gies, J. Sanchez-Guillen, and R. A. Vázquez, “Quantum effective actions from nonperturbative worldline dynamics,” *Journal of High Energy Physics* **2005** no. 08, (2005) 067.
- [258] H. Ursell, “The evaluation of Gibbs’ phase-integral for imperfect gases,” in *Mathematical Proceedings of the Cambridge Philosophical Society*, vol. 23, pp. 685–697, Cambridge Univ Press. 1927.
- [259] J. E. Mayer, “Statistical mechanics of condensing systems,” *J. chem. Phys* **5** (1937) 67.
- [260] R. Pathria and P. Beale, “Statistical Mechanics. Butterworth,” 2009.
- [261] J. C. G. Callan, R. F. Dashen, and D. J. Gross, “Toward a Theory of the Strong Interactions,” *Phys. Rev.* **D17** (1978) 2717.

- [262] C. G. Callan Jr, R. F. Dashen, and D. J. Gross, “A theory of hadronic structure,” *Physical Review D* **19** no. 6, (1979) 1826.
- [263] H. Levine and L. G. Yaffe, “Higher order instanton effects,” *Phys. Rev.* **D19** (1979) 1225.
- [264] A. Jevicki, “Statistical Mechanics of Instantons in Quantum Chromodynamics,” *Phys. Rev.* **D21** (1980) 992–1005.
- [265] E.-M. Ilgenfritz, D. I. Kazakov, and M. Muller-Preussker, “On the Phase Transition in the Yang-Mills Instanton Gas,” *Phys. Lett.* **87B** (1979) 242–246.
- [266] E. Bogomolny, “Calculation of instanton-anti-instanton contributions in quantum mechanics,” *Physics Letters B* **91** no. 3-4, (1980) 431–435.
- [267] I. Affleck, “On constrained instantons,” *Nuclear Physics B* **191** no. 2, (1981) 429–444.
- [268] J. S. Langer, “Theory of the condensation point,” *Annals Phys.* **41** (1967) 108–157. [Annals Phys.281,941(2000)].
- [269] S. R. Coleman, “The Fate of the False Vacuum. 1. Semiclassical Theory,” *Phys. Rev.* **D15** (1977) 2929–2936. [Erratum: Phys. Rev.D16,1248(1977)].
- [270] J. C. G. Callan and S. R. Coleman, “The Fate of the False Vacuum. 2. First Quantum Corrections,” *Phys. Rev.* **D16** (1977) 1762–1768.
- [271] R. A. Brandt, F. Neri, and M.-a. Sato, “Renormalization of Loop Functions for All Loops,” *Phys. Rev.* **D24** (1981) 879.
- [272] A. I. Karanikas, C. N. Ktorides, and N. G. Stefanis, “On the infrared structure of the one fermion Green’s function in QED,” *Phys. Lett.* **B289** (1992) 176–183.
- [273] A. S. Goldhaber, “Monopoles and Gauge Theories,” in *Magnetic Monopoles. Proceedings, NATO Advanced Study Institute, Wingspread, USA, October 14-17, 1982*, R. A. Carrigan and W. P. Trower, eds., vol. 102, pp. pp.1–16. 1983.
- [274] G. P. Korchemsky and A. V. Radyushkin, “Loop Space Formalism and Renormalization Group for the Infrared Asymptotics of QCD,” *Phys. Lett.* **B171** (1986) 459–467.

- [275] G. C. Gellas, A. I. Karanikas, and C. N. Ktorides, “Green’s function approach to infrared factorization and finite eikonal corrections,” *Annals Phys.* **255** (1997) 228–249.
- [276] A. Monin and M. Voloshin, “Photon-stimulated production of electron-positron pairs in an electric field,” *Physical Review D* **81** no. 2, (2010) 025001.
- [277] I. K. Affleck and F. De Luccia, “Induced vacuum decay,” *Phys. Rev.* **D20** (1979) 3168.
- [278] M. Voloshin, “An illustrative model for non-perturbative scattering in theories with weak coupling,” *Nuclear Physics B* **363** no. 2-3, (1991) 425–450.
- [279] K. B. Selivanov and M. B. Voloshin, “Destruction of False Vacuum by Massive Particles,” *JETP Lett.* **42** (1985) 422.
- [280] B. I. Ivlev and V. I. Mel’nikov, “Tunneling and activated motion of a string across a potential barrier,” *Phys. Rev.* **B36** (1987) 6889–6903.
- [281] A. R. Brown, “Schwinger pair production at nonzero temperatures or in compact directions,” *arXiv preprint arXiv:1512.05716* (2015) .
- [282] L. Medina and M. C. Ogilvie, “Schwinger Pair Production at Finite Temperature,” *Phys. Rev.* **D95** no. 5, (2017) 056006, [arXiv:1511.09459 \[hep-th\]](#) .
- [283] G. Torgrimsson, C. Schneider, J. Oertel, and R. Schützhold, “Dynamically assisted Sauter-Schwinger effect — non-perturbative versus perturbative aspects,” *JHEP* **06** (2017) 043, [arXiv:1703.09203 \[hep-th\]](#) .
- [284] V. A. Rubakov, D. T. Son, and P. G. Tinyakov, “Initial state independence of nonperturbative scattering through thin wall bubbles in (1+1)-dimensions,” *Phys. Lett.* **B278** (1992) 279–283.
- [285] V. G. Kiselev, “The False vacuum decay induced by a two particle collision in two-dimensions,” *Phys. Rev.* **D45** (1992) 2929–2932.
- [286] J. Plateau, “Experimental and theoretical statics of liquids subject to molecular forces only,”.
- [287] J. W. Strutt and L. Rayleigh, “On the instability of jets,” *Proc. London Math. Soc* **10** no. 4, (1878) .

- [288] R. Gregory and R. Laflamme, “Black strings and p-branes are unstable,” *Physical review letters* **70** no. 19, (1993) 2837.
- [289] U. Brosa, S. Grossmann, and A. Müller, “Nuclear scission,” *Physics Reports* **197** no. 4, (1990) 167–262.
- [290] P. A. M. Dirac, “Classical theory of radiating electrons,” *Proc. Roy. Soc. Lond.* **A167** (1938) 148–169.
- [291] J. A. Wheeler and R. P. Feynman, “Interaction with the absorber as the mechanism of radiation,” *Rev. Mod. Phys.* **17** (1945) 157–181.
- [292] S. E. Gralla, A. I. Harte, and R. M. Wald, “A Rigorous Derivation of Electromagnetic Self-force,” *Phys. Rev.* **D80** (2009) 024031, [arXiv:0905.2391 \[gr-qc\]](#).
- [293] J. Garriga, “Instantons for vacuum decay at finite temperature in the thin wall limit,” *Phys. Rev.* **D49** (1994) 5497–5506, [arXiv:hep-th/9401020 \[hep-th\]](#).
- [294] J. Gordon and G. W. Semenoff, “World-line instantons and the Schwinger effect as a Wentzel–Kramers–Brillouin exact path integral,” *J. Math. Phys.* **56** (2015) 022111, [arXiv:1407.0987 \[hep-th\]](#).
- [295] C. Englert and J. Jaeckel, “Getting stuck! Using monosignatures to test highly ionizing particles,” *Phys. Lett.* **B769** (2017) 513–519, [arXiv:1610.06753 \[hep-ph\]](#).
- [296] P. B. Arnold and L. D. McLerran, “The Sphaleron Strikes Back,” *Phys. Rev.* **D37** (1988) 1020.
- [297] D. E. Kharzeev, L. D. McLerran, and H. J. Warringa, “The Effects of topological charge change in heavy ion collisions: ‘Event by event P and CP violation’,” *Nucl. Phys.* **A803** (2008) 227–253, [arXiv:0711.0950 \[hep-ph\]](#).
- [298] V. Skokov, A. Yu. Illarionov, and V. Toneev, “Estimate of the magnetic field strength in heavy-ion collisions,” *Int. J. Mod. Phys.* **A24** (2009) 5925–5932, [arXiv:0907.1396 \[nucl-th\]](#).
- [299] V. Voronyuk, V. D. Toneev, W. Cassing, E. L. Bratkovskaya, V. P. Konchakovski, and S. A. Voloshin, “(Electro-)Magnetic field evolution in relativistic heavy-ion collisions,” *Phys. Rev.* **C83** (2011) 054911, [arXiv:1103.4239 \[nucl-th\]](#).

- [300] A. Bzdak and V. Skokov, “Event-by-event fluctuations of magnetic and electric fields in heavy ion collisions,” *Phys. Lett.* **B710** (2012) 171–174, [arXiv:1111.1949 \[hep-ph\]](#).
- [301] W.-T. Deng and X.-G. Huang, “Event-by-event generation of electromagnetic fields in heavy-ion collisions,” *Phys. Rev.* **C85** (2012) 044907, [arXiv:1201.5108 \[nucl-th\]](#).
- [302] L. McLerran and V. Skokov, “Comments About the Electromagnetic Field in Heavy-Ion Collisions,” *Nucl. Phys.* **A929** (2014) 184–190, [arXiv:1305.0774 \[hep-ph\]](#).
- [303] A. De Roeck, H. P. Hächler, A. M. Hirt, M. D. Joergensen, A. Katre, P. Mermoud, D. Milstead, and T. Sloan, “Development of a magnetometer-based search strategy for stopped monopoles at the Large Hadron Collider,” *Eur. Phys. J.* **C72** (2012) 2212.
- [304] M. D. Joergensen, A. De Roeck, H. P. Hachler, A. Hirt, A. Katre, P. Mermoud, D. Milstead, and T. Sloan, “Searching for magnetic monopoles trapped in accelerator material at the Large Hadron Collider,” [arXiv:1206.6793 \[physics.ins-det\]](#).
- [305] **WA98** Collaboration, H. Schlagheck, “Thermalization and flow in 158-GeV/A Pb + Pb collisions,” *Nucl. Phys.* **A663** (2000) 725–728, [arXiv:nucl-ex/9909005 \[nucl-ex\]](#).
- [306] **WA98** Collaboration, M. M. Aggarwal *et al.*, “Observation of direct photons in central 158-A-GeV Pb-208 + Pb-208 collisions,” *Phys. Rev. Lett.* **85** (2000) 3595–3599, [arXiv:nucl-ex/0006008 \[nucl-ex\]](#).
- [307] K. Tuchin, “Synchrotron radiation by fast fermions in heavy-ion collisions,” *Phys. Rev.* **C82** (2010) 034904, [arXiv:1006.3051 \[nucl-th\]](#). [Erratum: *Phys. Rev.*C83,039903(2011)].
- [308] K. Tuchin, “Particle production in strong electromagnetic fields in relativistic heavy-ion collisions,” *Adv. High Energy Phys.* **2013** (2013) 490495, [arXiv:1301.0099 \[hep-ph\]](#).
- [309] K. Tuchin, “Time and space dependence of the electromagnetic field in relativistic heavy-ion collisions,” *Phys. Rev.* **C88** no. 2, (2013) 024911, [arXiv:1305.5806 \[hep-ph\]](#).



- [310] R. Baier, A. H. Mueller, D. Schiff, and D. T. Son, “‘Bottom up’ thermalization in heavy ion collisions,” *Phys. Lett.* **B502** (2001) 51–58, [arXiv:hep-ph/0009237 \[hep-ph\]](#).
- [311] E. Brezin and C. Itzykson, “Pair production in vacuum by an alternating field,” *Physical Review D* **2** no. 7, (1970) 1191.
- [312] G. V. Dunne and C. Schubert, “Worldline instantons and pair production in inhomogenous fields,” *Physical Review D* **72** no. 10, (2005) 105004.
- [313] A. Ilderton, G. Torgrimsson, and J. Wårdh, “Nonperturbative pair production in interpolating fields,” *Phys. Rev.* **D92** no. 6, (2015) 065001, [arXiv:1506.09186 \[hep-th\]](#).
- [314] C. Kohlfürst, *Electron-positron pair production in inhomogeneous electromagnetic fields*. PhD thesis, U. Graz (main), 2015. [arXiv:1512.06082 \[hep-ph\]](#).  
<http://inspirehep.net/record/1410605/files/arXiv:1512.06082.pdf>.
- [315] **LHCb** Collaboration, L. Massacrier, “First LHCb results from pA and Pb-Pb collisions,” in *4th Large Hadron Collider Physics Conference (LHCP 2016) Lund, Sweden, June 13-18, 2016*. 2016. [arXiv:1609.06477 \[nucl-ex\]](#).  
<http://inspirehep.net/record/1487542/files/arXiv:1609.06477.pdf>.
- [316] **ALICE** Collaboration, M. Wilde, “Measurement of Direct Photons in pp and Pb-Pb Collisions with ALICE,” *Nucl. Phys.* **A904-905** (2013) 573c–576c, [arXiv:1210.5958 \[hep-ex\]](#).
- [317] **ALICE** Collaboration, B. Abelev *et al.*, “Centrality determination of Pb-Pb collisions at  $\sqrt{s_{NN}} = 2.76$  TeV with ALICE,” *Phys. Rev.* **C88** no. 4, (2013) 044909, [arXiv:1301.4361 \[nucl-ex\]](#).
- [318] L. E. Roberts, “Dirac Magnetic Monopole Pair Production in Relativistic Nucleus Nucleus Collisions,” *Nuovo Cim.* **A92** (1986) 247–272.
- [319] T. Dobbins and L. E. Roberts, “Updated estimate of limits on the production rates of ’t Hooft-Polyakov magnetic monopoles,” *Nuovo Cim.* **A106** (1993) 1295–1307.
- [320] A. Reisenegger, “Origin and evolution of neutron star magnetic fields,” in *Proceedings, International Workshop on Strong Magnetic Fields and Neutron*

- Star: Havana, Cuba, April 6-13, 2003*, pp. 33–49. 2003.  
arXiv:astro-ph/0307133 [astro-ph].  
<http://www.if.ufrgs.br/hadrons/reisenegger1.pdf>.
- [321] J. A. Pons, J. A. Miralles, and U. Geppert, “Magneto–thermal evolution of neutron stars,” *Astron. Astrophys.* **496** (2009) 207–216, arXiv:0812.3018 [astro-ph].
- [322] A. Y. Potekhin, “The physics of neutron stars,” *Phys. Usp.* **53** (2010) 1235–1256, arXiv:1102.5735 [astro-ph.SR]. [Usp. Fiz. Nauk180,1279(2010)].
- [323] J. A. Harvey, M. A. Ruderman, and J. Shaham, “Effects of Neutron Star Superconductivity on Magnetic Monopoles and Core Field Decay,” *Phys. Rev. D* **33** (1986) 2084.
- [324] R. Turolla, S. Zane, and A. Watts, “Magnetars: the physics behind observations. A review,” *Rept. Prog. Phys.* **78** no. 11, (2015) 116901, arXiv:1507.02924 [astro-ph.HE].
- [325] S. P. Ahlen, “Stopping Power Formula for Magnetic Monopoles,” *Phys. Rev. D* **17** (1978) 229–233.
- [326] S. p. Ahlen and K. Kinoshita, “Calculation of the Stopping Power of Very Low Velocity Magnetic Monopoles,” *Phys. Rev. D* **26** (1982) 2347–2363.
- [327] L. Bracci and G. Fiorentini, “Binding of Magnetic Monopoles and Atomic Nuclei,” *Phys. Lett.* **124B** (1983) 493–496.
- [328] L. Bracci and G. Fiorentini, “Interactions of Magnetic Monopoles With Nuclei and Atoms: Formation of Bound States and Phenomenological Consequences,” *Nucl. Phys.* **B232** (1984) 236–262.
- [329] J. Derkaoui, G. Giacomelli, T. Lari, A. Margiotta, M. Ouchrif, L. Patrizii, V. Popa, and V. Togo, “Energy losses of magnetic monopoles and of dyons in the earth,” *Astropart. Phys.* **9** (1998) 173–183.
- [330] C. Thompson and R. C. Duncan, “Neutron star dynamos and the origins of pulsar magnetism,” *Astrophys. J.* **408** (1993) 194.
- [331] A. Hook and J. Huang, “Bounding milli-magnetically charged particles with magnetars,” arXiv:1705.01107 [hep-ph].

- [332] S. P. Kim, H. K. Lee, and Y. Yoon, “Nonperturbative QED effective action at finite temperature,” *Physical Review D* **82** no. 2, (2010) 025016.
- [333] A. K. Monin and A. Zayakin, “Semiclassical treatment of induced schwinger processes at a finite temperature,” *JETP letters* **87** no. 11, (2008) 611–617.
- [334] B. King, H. Gies, and A. Di Piazza, “Pair production in a plane wave by thermal background photons,” *Phys. Rev.* **D86** (2012) 125007, [arXiv:1204.2442 \[hep-ph\]](#). [Erratum: *Phys. Rev.*D87,no.6,069905(2013)].
- [335] L. Landau, “On the " Radius" of the Elementary Particles,” *Physical Review* **58** no. 11, (1940) 1006.
- [336] E. J. Moniz and D. H. Sharp, “Absence of runaways and divergent self-mass in nonrelativistic quantum electrodynamics,” *Phys. Rev.* **D10** (1974) 1133–1136.
- [337] E. J. Moniz and D. H. Sharp, “Radiation Reaction in Nonrelativistic Quantum Electrodynamics,” *Phys. Rev.* **D15** (1977) 2850.
- [338] F. E. Low, “Runaway solutions in relativistic spin 1/2 quantum electrodynamics,” *Annals Phys.* **266** (1998) 274–292, [arXiv:hep-th/9702151 \[hep-th\]](#).
- [339] R. Rosenfelder and A. W. Schreiber, “An Abraham-Lorentz-like equation for the electron from the worldline variational approach to QED,” *Eur. Phys. J.* **C37** (2004) 161–171, [arXiv:hep-th/0406062 \[hep-th\]](#).
- [340] C. R. Galley, B. L. Hu, and S.-Y. Lin, “Electromagnetic and gravitational self-force on a relativistic particle from quantum fields in curved space,” *Phys. Rev.* **D74** (2006) 024017, [arXiv:gr-qc/0603099 \[gr-qc\]](#).
- [341] S. Coleman and R. E. Norton, “Runaway modes in model field theories,” *Physical Review* **125** no. 4, (1962) 1422.
- [342] J. Fröhlich, “On the infrared problem in a model of scalar electrons and massless, scalar bosons,” *Ann. Inst. Henri Poincaré* **19** no. 1, (1973) 1–103.
- [343] E. H. Lieb and R. Seiringer, *The stability of matter in quantum mechanics*. Cambridge Univ. Press, Cambridge, 2010.
- [344] G. Calucci and R. Jengo, “On the Renormalization of the Quantum Field Theory of Point-like Monopoles and Charges,” *Nucl. Phys.* **B223** (1983) 501–524.

- [345] C. J. Goebel and M. T. Thomaz, “Antishielding of Magnetic Charge,” *Phys. Rev.* **D30** (1984) 823.
- [346] L. D. Faddeev and V. N. Popov, “Feynman Diagrams for the Yang-Mills Field,” *Phys. Lett.* **25B** (1967) 29–30.
- [347] A. I. Vainshtein, V. I. Zakharov, V. A. Novikov, and M. A. Shifman, “ABC’s of Instantons,” *Sov. Phys. Usp.* **25** (1982) 195. [Usp. Fiz. Nauk136,553(1982)].
- [348] V. B. Berestetskii, E. M. Lifshitz, and L. P. Pitaevskii, *Quantum Electrodynamics*, vol. 4 of *Course of Theoretical Physics*. Pergamon Press, Oxford, 1982.  
<http://www-spines.fnal.gov/spines/find/books/www?cl=QC680.B42>.
- [349] F. A. Berezin, *The Method of Second Quantization*. Academic Press, 1966.
- [350] M. Laine and A. Vuorinen, “Basics of Thermal Field Theory,” *Lect. Notes Phys.* **925** (2016) pp.1–281, [arXiv:1701.01554](https://arxiv.org/abs/1701.01554) [hep-ph].
- [351] O. Corradini and C. Schubert, “Spinning Particles in Quantum Mechanics and Quantum Field Theory,” 2015. [arXiv:1512.08694](https://arxiv.org/abs/1512.08694) [hep-th]. <https://inspirehep.net/record/1411712/files/arXiv:1512.08694.pdf>.
- [352] N. S. Manton, “The Force Between ’t Hooft-Polyakov Monopoles,” *Nucl. Phys.* **B126** (1977) 525–541.
- [353] C. W. Misner, K. S. Thorne, and J. A. Wheeler, *Gravitation*. Macmillan, 1973.